

Washington University in St. Louis

## Washington University Open Scholarship

---

All Theses and Dissertations (ETDs)

---

1-1-2011

### Enzymology of DHHC-mediated Protein S-Acylation

Benjamin Jennings

*Washington University in St. Louis*

Follow this and additional works at: <https://openscholarship.wustl.edu/etd>

---

#### Recommended Citation

Jennings, Benjamin, "Enzymology of DHHC-mediated Protein S-Acylation" (2011). *All Theses and Dissertations (ETDs)*. 593.

<https://openscholarship.wustl.edu/etd/593>

This Dissertation is brought to you for free and open access by Washington University Open Scholarship. It has been accepted for inclusion in All Theses and Dissertations (ETDs) by an authorized administrator of Washington University Open Scholarship. For more information, please contact [digital@wumail.wustl.edu](mailto:digital@wumail.wustl.edu).

WASHINGTON UNIVERSITY IN ST. LOUIS

Division of Biology and Biomedical Sciences

Program in Biochemistry

Dissertation Committee:

Maurine E. Linder, Chair

Kendall J. Blumer

Robert P. Mecham

Robert W. Mercer

Linda J. Pike

Paul H. Schlesinger

ENZYMOLOGY OF DHHC-MEDIATED PROTEIN *S*-ACYLATION

by

Benjamin C. Jennings

A dissertation presented to the  
Graduate School of Arts and Sciences  
of Washington University in St. Louis  
in partial fulfillment of the  
requirements for the degree  
of Doctor of Philosophy

August 2011

Saint Louis, Missouri

## ABSTRACT OF THE DISSERTATION

Enzymology of DHHC-mediated Protein *S*-Acylation

By

Benjamin C. Jennings

Doctor of Philosophy in Biology and Biomedical Sciences

(Biochemistry)

Washington University in St. Louis, 2011

Professor Maurine E. Linder, Chair

Protein *S*-acylation is the post-translational modification of proteins with long-chain fatty acids at cysteine residues via a thioester linkage. The most commonly attached lipid is 16-carbon palmitate, thus the process is often called palmitoylation. Unlike other lipid modifications, protein *S*-acylation is reversible. Consequently, cells use acylation/deacylation cycles to regulate protein localization, stability, and activity. A family of integral membrane enzymes called DHHC proteins because of a conserved Asp-His-His-Cys motif, catalyze protein *S*-acylation within cells. DHHC proteins have been associated with human diseases including cancers, Huntington's disease, and mental retardation. However little is known about their function or regulation. This work focuses on developing a better mechanistic understanding of mammalian DHHC proteins.

To facilitate biochemical characterization, a protocol was developed to express and purify recombinant DHHC proteins from insect cells using recombinant baculovirus. Protein *S*-acyltransferase (PAT) activity was measured by *in vitro* assays using

radiolabeled palmitoyl-coenzyme A and purified protein substrates. Assay conditions were optimized to maximize PAT activity.

In vitro, both protein substrate and DHHC protein incorporated palmitate. This latter process is termed enzyme autoacylation and lead to the hypothesis that DHHC proteins use a two-step ping-pong mechanism with an acyl-enzyme transfer intermediate. A fluorescent peptide, high performance liquid chromatography-based PAT assay was developed for classic steady-state kinetic experiments. Single turnover assays supported the hypothesis with radiolabeled fatty acid transferring from acyl-DHHC to protein substrate. Unexpectedly, these investigations also revealed that DHHC proteins display different acyl-CoA chain length preferences. A mechanism for this difference is proposed and tested.

Inhibitors of DHHC proteins will be useful tools for studying protein *S*-acylation within cells and as potential pharmaceutical agents. Others in the field have identified classes of compounds that reduce cellular *S*-acylation. Four representative compounds and the known palmitoylation inhibitor 2-bromopalmitate (2BP) were tested for inhibition of DHHC-mediated *S*-acylation with four DHHC proteins and their cognate substrates in vitro. Two compounds, 2BP and 2-(2-Hydroxy-5-nitro-benzylidene)-benzo[b]thiophen-3-one (compound V), inhibited autoacylation and acyl-transfer of all DHHCs tested. These compounds were further characterized for reversibility and time-dependence. Given their modest potency and lack of specificity, new screens for inhibitors of DHHC proteins are needed.

## **Acknowledgements**

Throughout this thesis work and my entire graduate career I have had the support and encouragement of many people, to whom I am truly grateful. I will mention a few here, but my apologies in advance to anyone I may inadvertently miss.

First, I must thank my advisor, Dr. Maurine Linder, for her mentorship over the years. She has taught me many things, the most important of which is how to be a good scientist. Her patience and investment in me are much appreciated, in addition to her proofreading skill. She is also credited with introducing me to the protein lipidation field, from which I would like to particularly acknowledge Dr. Robert Deschenes for contributing reagents and ideas. Thank you to my thesis committee for their support and recommendations during these investigations. Special thanks to Tom Broekelmann from Dr. Mecham's lab for assistance quantifying peptides and teaching me to run an HPLC.

I would also like to thank the members of the Linder Lab, past and present, for their support, helpful discussions, constructive feedback, and reagents—including those I took without their knowledge! While in the lab, I am thankful to have had the opportunity to mentor a handful of undergraduate students among others. Extra thanks to Wendy Greentree for teaching me my first PAT assay along with many other things, keeping the lab supplied and running, and synthesizing most of the radiolabeled palmitoyl-CoA used in these studies. I do not think the lab could have moved to Cornell University without you. I would like to especially thank Marissa Nadolski for sharing her purified proteins and ideas on the mechanism of DHHC proteins. A better colleague in sharing in the difficulties of studying integral membranes enzymes could not have

been had. To the current and future members of the lab, I wish you the best of luck with your experiments.

I must acknowledge and am grateful for contributions from the National Institute of General Medical Science (NIH) and a pre-doctoral fellowship from the Midwest Affiliate of the American Heart Association. Without their financial support, this project would literally not have been possible.

My graduate career has been a great journey and I have had the pleasure of meeting many wonderful people along the way. In St. Louis, I want to especially thank the latter four-fifths of BAKED (Andrew, Keri, Esther, and Danny) for sharing excellent weekend dinners, numerous adventures in the St. Louis area, and an atmosphere of non-science socializing. For providing additional relaxation and fellowship, I am indebted to my crews at More Than Carpentry, the local swing society, the Darrs and Taylors, and of course, my fellow classmates. While in Ithaca, I have been grateful for the support and camaraderie from Tobias Fuhrmann, Matt McConnell, and the McInnis brothers among others.

To my parents, Melvin and Janet Jennings, thank you for being supportive of me during this stage of my life and all those leading up to it. To my brothers, Chris and Josh, thank you for not letting me become too much of a science nerd and calling me out when I do. Lastly, to Meg, thank you for your patience, support, and companionship during this adventure; looking forward to many more.

## Table of Contents

Abstract of the Dissertation	ii
Acknowledgements	iv
List of Figures and Tables	vii
Abbreviations	ix
<b>Chapter 1: Introduction</b>	<b>1</b>
<b>Chapter 2: Development of Assays to Monitor DHHC-mediated Protein <i>S</i>-acylation.</b>	<b>24</b>
<b>Chapter 3: DHHC Protein <i>S</i>-Acyltransferases Use A Similar Ping-Pong Kinetic Mechanism But Display Different Acyl-CoA Specificities.</b>	<b>44</b>
<b>Chapter 4: 2-Bromopalmitate and 2-(2-Hydroxy-5-nitro-benzylidene)-benzo[b]thiophen-3-one Inhibit DHHC-Mediated Palmitoylation In Vitro</b>	<b>70</b>
<b>Chapter 5. Implications and Future Directions</b>	<b>100</b>
<b>Appendix: Characterization of DHHC9 in Ras Signaling and X-linked Mental Retardation.</b>	<b>111</b>
<b>References</b>	<b>121</b>
<b>Curriculum Vitae</b>	<b>137</b>

## List of Tables and Figures

### Chapter 1.

<i>Table 1.1</i>	Lipid modifications found on proteins.	20
<i>Table 1.2</i>	Proteins modified by <i>S</i> -acylation with acyl length other than 16-carbon palmitate.	21
<i>Table 1.3</i>	DHHC proteins associated with disease.	22
<i>Figure 1.1</i>	Predicted topology of DHHC proteins.	23

### Chapter 2.

<i>Table 2.1</i>	Standard radiolabel-based PAT assay.	39
<i>Table 2.2</i>	Effect of various compounds on PAT activity.	40
<i>Figure 2.1</i>	Detergent and buffer effects on in vitro DHHC PAT activity.	41
<i>Figure 2.2</i>	Reducing agents affect in vitro DHHC autoacylation and PAT activity.	42

### Chapter 3.

<i>Table 3.1</i>	Kinetic parameters for DHHC3 analyzed with the fluorescent peptide, HPLC-based PAT assay.	64
<i>Table 3.2</i>	Hydrolysis rates of different acyl-CoAs with DHHC3 and DHHC2.	64
<i>Figure 3.1</i>	Fluorescent peptide, HPLC-based kinetic characterization of DHHC3.	65
<i>Figure 3.2</i>	Autoacylated DHHC proteins transfer their acyl chain to protein substrate.	66
<i>Figure 3.3</i>	Acyl-CoA chain-length specificity of DHHC enzyme autoacylation parallels substrate specificity.	67
<i>Figure 3.4</i>	DHHC2 displays broader lipid substrate specificity than DHHC3.	68

<i>Figure 3.5</i>	Hydrolysis, enzyme autoacylation, and direct transfer of DHHC2 and DHHC3 with C18 stearate and C16 palmitate.	69
<b>Chapter 4.</b>		
<i>Figure 4.1</i>	Structure and names of inhibitor compounds used in this study.	93
<i>Figure 4.2</i>	Purification of human DHHC2 and catalytically inactive DHHS2.	94
<i>Figure 4.3</i>	DHHC2 palmitoylates myrLck <sub>NT</sub> at cysteines 3 and 5.	95
<i>Figure 4.4</i>	Inhibitor profiles for DHHC proteins.	96
<i>Figure 4.5</i>	Inhibitor effect on enzyme autoacylation.	97
<i>Figure 4.6</i>	Reversibility and time-dependent inhibition.	98
<i>Figure 4.S1</i>	Recombinant WT and C3,5S Lck <sub>NT</sub> are myristoylated.	99
<b>Appendix.</b>		
<i>Figure A.1</i>	Palmitoylation of GST-H-ras 30aa tail in vitro using purified DHHC9/GCP16 and [ <sup>3</sup> H]-palmitoyl-CoA in the presence or absence of FK506 or recombinant FKBP12.	118
<i>Figure A.2</i>	DHHC9 R148W displays reduced interaction with GCP16.	119
<i>Figure A.3</i>	DHHC9 R148W displays reduced protein S-acyltransferase activity for H-ras.	120

## Abbreviations

[ <sup>3</sup> H]palmCoA	[ <sup>3</sup> H] <sup>9,10</sup> -palmitoyl-coenzyme A
16-12-NBD-PC	1-palmitoyl-2-{12-[(7-nitro-2-1,3-benzoxadiazol-4-yl)amino]dodecanoyl}-sn-glycero-3-phosphocholine
2-BP	2-bromopalmitate, 2-bromohexadecanoic acid
ACBP	acyl-coenzyme A binding protein
APT	acyl-protein thioesterase
β-ME	β-mercaptoethanol
CMC	critical micelle concentration
CoA	coenzyme A
Compound V	2-(2-Hydroxy-5-nitro-benzylidene)-benzo[b]thiophen-3-one
CV	compound V, 2-(2-Hydroxy-5-nitro-benzylidene)-benzo[b]thiophen-3-one
DDM	<i>n</i> -dodecyl-β-D-maltoside detergent
DHHC	Asp-His-His-Cys
DHHC-CRD	Asp-His-His-Cys cysteine rich domain
DMSO	dimethylsulfoxide
DTT	1,4-dithiothreitol
ER	endoplasmic reticulum
FABP	fatty acid binding protein
GST	glutathione S-transferase
HPLC	high performance liquid chromatography
htt	huntingtin
IPTG	isopropyl β-D-1-thiogalactopyranoside

LCAs	Long-chain acyl-CoAs
MBOAT	membrane-bound O-acyltransferase
myr	<i>N</i> -myristoylation
myrG <sub>αi1</sub>	<i>N</i> -myristoylated G-protein α-subunit i1
myrGCG	<i>N</i> -myristoylated tripeptide Gly-Cys-Gly ethylenediamine linked to fluorescent nitro-benzoxadiazole (NBD)
myrLck <sub>NT</sub>	<i>N</i> -myristoylated lymphocyte specific kinase, N-terminal residues 1-226
palmCoA	palmitoyl-coenzyme A
PATs	protein <i>S</i> -acyltransferases
PM	plasma membrane
PMSF	phenylmethanesulphonyl fluoride
TCEP	<i>tris</i> (2-carboxyethyl)phosphine
TLC	thin layer chromatography
TMD	transmembrane domain
WT	wildtype

# Chapter 1

## Introduction

Cells typically use one of three mechanisms to anchor proteins at membranes: insertion with transmembrane domains, interaction with other membrane components, or covalent modification with lipids. This last process, called protein lipidation, occurs through multiple mechanisms and involves a variety of lipids including fatty acids, isoprenoids, and cholesterol (Table 1.1). Lipid modifications can be divided into two broad categories: those that occur in the cytoplasm or on the cytoplasmic face of membranes, and those that occur in the lumen of the secretory pathway (1). Lipid modifications on secreted proteins include glycosylphosphatidyl-inositol (GPI) anchors and fatty acylation including *O*-acylation and *N*-palmitoylation; however they are beyond the scope of this discussion and one is referred to reviews elsewhere (2-7). Lipid modifications occurring in the cytoplasm include protein *S*-acylation, *N*-myristoylation, and prenylation. While *S*-acylation is the main focus of these studies, it often occurs adjacent to *N*-myristoylation and prenylation sites; therefore, they will also be briefly discussed.

## Protein *S*-acylation

Protein *S*-acylation is the post-translational modification of proteins with long-chain fatty acids at cysteine residues via a thioester linkage. The most common fatty acid donor is 16-carbon palmitoyl-coenzyme A (palmCoA), so the process is often called protein palmitoylation. However, a second type of palmitoylation, *N*-palmitoylation,

exists so the term *S*-acylation will be used. *N*-palmitoylation occurs on secreted proteins and this modification is mediated by a separate group of enzymes, membrane-bound *O*-acylation transferases (MBOATS), which are structurally distinct from protein *S*-acyltransferases (PATs, (8)). The only known *N*-palmitoylated protein that is not secreted is  $G\alpha_s$ , which is *N*-palmitoylated on Gly<sup>2</sup> by an unknown mechanism and *S*-palmitoylated on Cys<sup>3</sup> (9).

Protein modification with fatty acids was the first covalent lipid modification described in eukaryotic cells (10). In 1971, two groups reported that highly purified brain myelin proteolipid protein contained covalently attached fatty acids (11, 12). Stoffyn and Folch-Pi further characterized the lipids as attached via an ester linkage (either oxy- or thio-ester) and a mixture of palmitate, stearate, and oleate (11). These properties are consistent with our current understanding of protein *S*-acylation. However, their work was largely forgotten and in 1979 *S*-acylation was rediscovered for viral membrane glycoproteins (13) and soon thereafter as a widespread modification of eukaryotic proteins (14). Today, thanks in particular to advances in chemical biology and mass spectrometry, palmitoyl-proteomes have been analyzed for a number of cell lines. Revealing both novel and known *S*-acylated proteins, these techniques detect hundreds of modified proteins and in some cases, identify the site(s) of modification (15-20).

Although protein *S*-acylation was discovered first, the molecular identity of the enzymes responsible remained unknown until the last ten years. Traditional biochemical approaches at determining the molecular identity of PATs were unsuccessful. Gutierrez and Magee detected a membrane localized PAT activity from mouse fibroblasts that co-

fractionated with Golgi markers and *S*-acylated N-ras, then called p21<sup>N-ras</sup> (21). Similarly, Berthiaume and Resh partially purified PAT activity from bovine brain that in vitro acylated *N*-myristoylated Fyn and behaved as a membrane-bound enzyme (22). Liu and coworkers also partially purified a palmitoyltransferase activity from rat liver that in vitro acylated H-ras using palmCoA as a substrate (23). However, subsequent sequencing and immunoblotting determined that Liu and coworkers had purified peroxisomal 3-oxoacyl-CoA thiolase A (24), an enzyme involved in  $\beta$ -oxidation of fatty acids, and unlikely a *bona fide* PAT. The ability of thiolase A to catalyze *S*-acylation was dependent on imidazole in the PAT assay, which was present in the buffer of the His-tagged Ras substrate. Since then, a number of thiolases have been shown to catalyze acylation in the presence of imidazole (25). Dunphy and coworkers from our group also partially purified detergent-solubilized PAT activity from bovine brain membranes. This activity was not contaminated with thiolase, was enriched in plasma membranes, and was capable of acylating G-protein  $\alpha$ -subunits (26). However, none of these groups could obtain highly purified preparations of detergent-solubilized PAT to permit molecular identification. Labile activity, poor recovery from conventional chromatographic steps, and sensitivity to freeze/thaw cycles limited further purification (10, 22). Of note, the N-ras PAT in Golgi membranes and the G $\alpha$ -subunit PAT in plasma membranes suggested multiple enzymes with different subcellular localizations, which is consistent with our present understanding of DHHC proteins (27).

Prior to the determination that DHHC proteins account for the majority of PAT activity in cells (16), some questioned whether *S*-acylation was enzyme catalyzed.

Nonenzymatic *S*-acylation, also called autoacylation, can occur by incubating a thiol-containing peptide or protein with long-chain acyl-CoAs in the context of a hydrophobic surface. Known *S*-acylated proteins that demonstrate autoacylation *in vitro* include G-protein  $\alpha$  subunits (28), myelin proteolipid proteins lipophilin (29) and P<sub>0</sub> (30), rhodopsin (31), and Bet3 (32). Supporting this nonenzymatic mechanism, *in vitro* acylation of these proteins displayed similar properties to acylation observed *in vivo*, including fatty acid attachment at similar cysteine residues, enhancement of acylation on *N*-myristoylated versus non-myristoylated proteins, and reactions occurring at physiological pH and temperature. While G $\alpha_s$  was shown to nonenzymatically *S*-acylate *in vitro* (33), subsequent work showed that this occurred at Cys<sup>160</sup> and not the physiological Cys<sup>3</sup> site (34). For lipophilin, rhodopsin, and G $\alpha$  subunits, the authors determined that autoacylation kinetics fit the Michaelis-Menten equation, saturating at high palmCoA concentrations, and reported  $K_m$  values of 50, 40, and 450  $\mu$ M palmCoA, respectively (28, 29, 31). However, these  $K_m$  values more likely reflected the concentration of detergent micelles in the assay (50, 50, and 400  $\mu$ M, respectively) and thus call into question the relevance of these observations for the following reasons. *In vitro* in aqueous buffer palmCoA forms micelles around 4  $\mu$ M (CMC = 3-4  $\mu$ M at 10 mM KCl, no detergent; (35)) and the *in vivo* predictions of free long-chain acyl-CoA concentrations are around 0.2  $\mu$ M after factoring in sequestration by acyl-CoA binding protein (ACBP) and fatty acid binding protein (FABP) (36). The abundant cytosolic protein ACBP binds long-chain acyl-CoAs with high nanomolar affinity and greatly increases the half-times for spontaneous *S*-acylation of proteins to tens of hours (37)

whereas in cells, acylation half-times are a few minutes (6 min H-ras, 1 min N-ras (38)). In contrast, partially purified G $\alpha$  PAT activity (26) remains active in the presence of physiological concentrations of ACBP and acyl-CoA and likely represents the predominant mechanism of *S*-acylation in vivo (39). Nonenzymatic autoacylation requires the cysteine residue and palmCoA present at an aqueous-hydrophobic interface (40, 41); thus the saturation observed in the kinetics may be more a measure of the amount of this reactive surface than of the binding interaction between palmCoA and protein substrate. It is possible that nonenzymatic acylation of some proteins is physiologically relevant (e.g. Bet3 (32)), although DHHC proteins account for most cellular *S*-acylation (16). When assaying in vitro DHHC-catalyzed acylation of substrates, and especially for proteins similar to G $\alpha$  subunits or at high acyl-CoA concentrations, nonenzymatic substrate autoacylation must be controlled for.

### **Dual Lipidation**

Although protein *S*-acylation can occur on otherwise completely cytoplasmic proteins, it often occurs in the context of other membrane association signals and in some cases, even on integral membrane proteins. To date, no well-defined amino acid recognition sequences are known for protein *S*-acylation sites except the presence of a free cysteine sulfhydryl. Nevertheless, software programs for the prediction of *S*-acylation sites have been developed and work with varying success (42-47). However, validation by biochemical experimental methods is recommended. These programs are in part based on the fact that protein *S*-acylation sites are frequently adjacent to other

membrane anchoring signals. The two-hit model, which has other names including the two-signal hypothesis and the kinetic trapping model, attempts to explain this occurrence of adjacent membrane anchoring signals. This model states that one membrane anchoring signal, such as *N*-myristoylation, prenylation, or a polybasic sequence, allows a protein to sample different cellular membranes because of a reasonably fast off rate from the membrane. Supporting this part of the model, peptides that were either *N*-myristoylated (48) or prenylated (49, 50) lacked sufficient binding energy to stably anchor them to the membrane. The model goes on to state that when a protein acquires a second hit, the dually anchored protein is trapped at the membrane due to a very slow off rate (1, 49, 51). Reversible protein *S*-acylation is often the ‘second hit’ allowing cycles of acylation/deacylation to dynamic regulation membrane association (38). While several ‘first hit’ anchoring signals exist, I want to highlight two: *N*-myristoylation and prenylation. In addition, I will describe the kinetic mechanism for the enzymes that mediate these lipid modifications so that they can be compared with the proposed catalytic mechanism for DHHC proteins.

### **Myristoylation**

Protein *N*-myristoylation is the covalent attachment of 14-carbon myristate to *N*-terminal glycine residues via an amide linkage (Table 1.1). In 1982, myristoylation was originally described as an unusual blocking group on *N*-terminal residues that was resistant to Edman degradation and that required high acetonitrile concentrations to elute from HPLC columns (52, 53). Following removal of the initiator methionine residue by

methionine aminopeptidase, myristoyl-CoA:protein *N*-myristoyltransferase (NMT) catalyzes the irreversible attachment of myristate. *S. cerevisiae* (54) and *Drosophila* (55) each contain one *NMT* gene, which is essential for survival, whereas vertebrates have two *NMT* genes, *NMT1* and *NMT2*. NMT is a soluble, monomeric enzyme recognizing a substrate consensus sequence of Gly<sup>2</sup>-X-X-X-Ser/Thr<sup>6</sup>- at the extreme N-terminus. Relevant examples include a subset of G-protein  $\alpha$  subunits (i, o, z, t, and g) and the Src family of tyrosine kinases (Lck, Fyn, Src, Lyn, etc) (56). These and most known examples of myristoylation occur co-translationally, however, a growing number of post-translational myristoylation events have been described. In apoptotic cells, activated caspases cleave proteins exposing internal “cryptic” myristoylation consensus sequences (57). Examples include BID (58),  $\beta$ -actin (59), gelsolin (60), and p21-activated kinase 2 (PAK2) (61). In the case of BID, myristoylated caspase-truncated BID was more effective than non-myristoylated at releasing cytochrome c from mitochondria (58).

Although NMT uses acyl-CoAs and protein substrates similar to DHHC proteins, its kinetic mechanism is likely different. Initially a ping-pong mechanism was suggested for yeast NMT because incubation of purified NMT with [<sup>14</sup>C]-myristoyl-CoA and hydroxylamine treatment demonstrated a covalent ester-linked acyl-enzyme (62, 63). However, subsequent Lineweaver-Bruke analysis (64, 65) and crystal structures with and without bound substrates (66-68) support a sequential ordered Bi Bi mechanism. Myristoyl-CoA binds first followed by protein substrate for a direct nucleophilic addition-elimination reaction, which is followed by the release of CoA and subsequent release of the *N*-myristoylated protein. Crystal structures also revealed that specificity

for 14-carbon acyl-CoAs is achieved by measuring the fatty acid length between an oxyanion hole binding the carbonyl and the floor of the hydrophobic pocket. In addition, a hydrophobic groove induces bends in myristate that further restrict acyl-chain saturation and branching (69).

## **Prenylation**

Protein prenylation is the covalent attachment of an isoprenoid lipid to C-terminal cysteine residues via a thioether linkage (Table 1.1). Three prenyltransferases are known: farnesyltransferase (FTase) and geranylgeranyltransferase type I (GGTase-I), together termed the CaaX prenyltransferases, and protein GGTase-II (or RabGGTase). FTase transfers the 15-carbon farnesyl-group using farnesyl diphosphate (FPP) as a lipid source whereas GGTases utilize geranylgeranyl diphosphate. FTase and GGTase-I have a consensus recognition sequences of -CaaX where C is the modified cysteine residue, 'a' are typically small aliphatic residues, and X is the terminal residue that helps specify which enzyme recognizes the site. After lipidation, most prenylated proteins undergo removal of the aaX tripeptide by the protease Rce1 and are then carboxymethylated on the prenylated cysteine residue by isoprenylcysteine carboxyl methyltransferase (Icmt). Farnesylation was first identified in 1978 on a fungal mating factor (70). In 1989, oncogenic Ras proteins were first described as farnesylated (71) and the next year, FTase was identified by multiple groups as the enzyme responsible for this modification (72, 73). FTase is a heterodimer composed of two subunits encoded by *RAM1* and *RAM2*, an essential gene in yeast (74, 75).

The kinetic mechanism of FTase is well characterized with all rate constants known, in part because it is a stable, soluble enzyme and crystallographic studies have produced structures of all major steps along the reaction pathway (76). FTase uses a sequential ordered Bi Bi reaction mechanism. FPP binds first followed by the CaaX substrate to form a ternary complex. A required  $Zn^{2+}$  ion helps orient and stabilize the cysteine thiolate ion for a direct  $S_N2$  reaction with the C1 carbon on the farnesyl group. This results in formation of a nascent thioether bond to the protein and loss of the oxyether bond to the pyrophosphate leaving group, which is stabilized by a  $Mg^{2+}$  ion. Pyrophosphate readily leaves the complex first, whereas release of the prenylated protein, the rate-limiting step, requires displacement by a new farnesyl diphosphate molecule (76-78).

### **DHHC proteins are protein *S*-acyltransferases**

DHHC proteins were determined to be the enzymes responsible for cellular *S*-acylation through the phenomenal power of yeast genetics. In 1999, a genetic screen in the yeast *Saccharomyces cerevisiae* using a palmitoylation-dependent RAS2 allele revealed the first PAT, effector of ras function, Erf2, and a second protein, Erf4 (79). Subsequent studies showed Erf2 function required binding partner Efr4, and they formed an endoplasmic reticulum-associated complex (80). In 2002, the Erf2/Erf4 complex was purified and shown to catalyze the transfer of radiolabeled palmitate from CoA to a Ras2-like substrate, demonstrating it was a *bona fide* PAT (81). Concurrently, a second yeast protein, Akr1, was also demonstrated to have PAT activity for the substrate Yck2 (82).

Analyzing amino acid sequences of these first two PATs lead to the discovery of a larger family of proteins called DHHC proteins with a conserved Asp-His-His-Cys cysteine-rich domain (DHHC-CRD) (83).

DHHC proteins make up a family of enzymes conserved in eukaryotes. Searching translated genome databases reveals 7 DHHC proteins in *S. cerevisiae*, 5 in *Schizosaccharomyces pombe*, 16 in *Caenorhabditis elegans*, 22 in *Drosophila melanogaster* (84), 23 in *Arabidopsis thaliana* (85), and 24 in *Homo sapiens* (86). In mammalian genomes, DHHC genes are designated *ZDHHC1- ZDHHC2- ZDHHC3* and so on, with the exception that there is no *ZDHHC10*. The “Z” reflects the fact that these proteins were originally predicted to be zinc-finger proteins involved in protein-protein or protein-DNA interactions (87); however, neither the metal nor DNA binding ability of these proteins has been characterized.

DHHC proteins have several conserved elements, with the function of some elements known. DHHC proteins are named for a highly conserved Asp-His-His-Cys motif within a larger cysteine-rich domain of approximately 51 amino acid residues (Figure 1.1) (83). Hydrophathy analysis of most DHHC proteins predicts four transmembrane domains (TMDs) with the DHHC motif on the cytoplasmic loop between TMD2 and TMD3 (27, 88). Yeast Ark1 and Akr2 and mammalian DHHC17 (HIP14) and DHHC13 (HIP14L) are part of a subset of DHHCs predicted to have N-terminal ankyrin repeats within the cytoplasm and two additional TMDs. Indeed, this topology was experimentally confirmed for Akr1 (88). Additionally, homology and phylogenetic analysis revealed a conserved DPG (aspartate-proline-glycine) motif N-terminal to the

DHHC sequence but within the same cytoplasmic loop and a TTxE (threonine-threonine-variable-glutamate) motif after the last TMD (Figure 1.1) (83). The function of these motifs is unknown.

The C-terminal cytoplasmic tails of DHHC protein vary greatly in sequence and length and have been assigned multiple functions. C-terminal to the TTxE motif, a 16 amino acid palmitoyltransferase conserved C-terminal (PaCCT) motif was described that is conserved in 70% of PATs from eukaryotic organisms (Figure 1.1). A conserved aromatic residue within this motif was essential for yeast DHHC proteins Swf1 and Pfa3 to *S*-acylate their protein substrates *in vivo* (89). Using mass spectrometry techniques to compare human *S*-acylated proteins in lipid raft versus non-raft membranes, Yang and coworkers identified DHHC5, DHHC6, and DHHC8 to be *S*-acylated on a novel three cysteine motif, CCX<sub>7-13</sub>C(S/T) (20). For DHHC6, this motif is about 50 residues downstream of the PaCCT motif. Interestingly, for DHHC5 and DHHC8 this tricysteine motif overlaps their PaCCT motifs. The functions of these motifs are largely unknown, however one possibility is that acylation-deacylation cycles of the tricysteine motif could regulate PaCCT motif accessibility and thus function. *In vivo* most long-chain acyl-CoAs are bound by ACBP (36, 90) and partially purified PAT activity can use ACBP-bound palmCoA (39). The PaCCT motif may be involved in recruiting ACBP:acyl-CoA complex to the DHHC protein and/or causing the release of acyl-CoA. It is unknown whether DHHC proteins can utilize ACBP-bound acyl-CoAs and the interaction between the two is an unexplored area in the field. The tricysteine and PaCCT motifs are present

on DHHCs with different subcellular localizations, arguing against them being localization signals.

DHHC proteins are localized to multiple membranes throughout the cell. Ohno and coworkers published the localization of ectopically expressed, epitope-tagged human and yeast DHHC proteins as well as the tissue expression patterns of human *ZDHHC* mRNAs (27). The majority of DHHC proteins displayed endoplasmic reticulum (ER) and/or Golgi localization. The exceptions were human DHHC-5, -20, and -21 and yeast Pfa5, which were localized to the plasma membrane (PM), and yeast Pfa3, which located to the yeast vacuole membrane (27, 91). However, a number of these results do not agree with work from others that looked at endogenous proteins or less highly expressed proteins. For example, Ohno *et al* described DHHC2 as having very restrictive tissue distribution and localizing to the ER and Golgi. In contrast, another group looking at DHHC2 found it was ubiquitously expressed in all tissues (92), and multiple groups have found DHHC2 localized to the PM and recycling endosomes (93-96). Interestingly, DHHC2 cycles between endosomes and the PM in PC12 cells and the PM localization is dependent on its C-terminal cytoplasmic tail (94). In neurons, DHHC2 also displays regulated localization, translocating from dendritic shaft vesicles to post-synaptic densities at the PM of dendritic spines and this translocation is enhanced in response to activity blockade (93). How the localization of most other DHHC proteins is determined or regulated remains unknown.

DHHC proteins may have other functions in addition to catalyzing protein *S*-acylation. Yeast Swf1, with its DHHC cysteine mutated to alanine, was still able to

mediate its functions of organizing the actin cytoskeleton and localizing Cdc42 (97). Similar, the *Drosophila* DHHC protein GABPI (CG17257) has a highly conserved DHHC-CRD with the important exception that the DHHC cysteine is a serine (84), which in all DHHC proteins tested blocks *S*-acyltransferase activity (83). GABPI shows high expression in neural tissue and uses its luminal loops, that are on the opposite side of the bilayer from the DHHC domain, to bind a Golgi localized glycosyltransferase (98). The mammalian orthologs of GABPI (DHHC-23, -11, and -1) have retained the canonical DHHC sequence whereas most insect orthologs have lost it (84, 98), suggesting this alternative DHHC function may be unique to insects.

DHHC proteins have been implicated in the transport of divalent metal ions. DHHC13 shares 69% sequence similarity with DHHC17 and is also referred to as HIP14-like protein or HIP14L. These two DHHC proteins have been associated with magnesium homeostasis. Low magnesium concentrations have been shown to increase endogenous DHHC-13 and -17 mRNA and protein levels. When expressed in *Xenopus oocytes*, both DHHC-13 and -17 mediated  $Mg^{2+}$  uptake that was dependent on the DHHC cysteine and sensitive to inhibition by 2-BP. The authors conclude that DHHC-13 and -17 are  $Mg^{2+}$  transport proteins and DHHC autoacylation regulates transport (99). Using similar techniques, this group also published that DHHC3 (GODZ) is a  $Ca^{2+}$  transport protein (100). While DHHC proteins may have dual functions as both acyltransferases and metal ion transporters, a more likely explanation is that DHHC-dependent acylation activates metal transporters or transport pathways within the cell. DHHC proteins have

not been directly tested for metal ion transport capabilities, however they are predicted to be zinc-binding proteins (87).

### **Functions and regulation of protein *S*-acylation**

Protein *S*-acylation can cause a variety of effects on the protein that is modified. From a technical standpoint, addition of a long-chain fatty acid to a protein increases its hydrophobicity, however this can have different functional consequences depending on the protein being modified.

Serving as a membrane anchor, *S*-acylation can influence protein localization and trafficking. A biologically important example of this is found on the proto-oncogene H-ras, which is part of the *ras* family of genes that are mutated in 30% of all human cancers. After prenylation and processing, H-ras is either mono- or dually acylated at cysteines 181 and 184. Monoacylation at Cys181 is required and sufficient for efficient trafficking to the plasma membrane. In contrast, monoacylation at Cys184 results in trafficking to the Golgi but not beyond (101, 102). A second example is the ATP-binding cassette transporter (ABC)A1 that is acylated on four cysteine residues, likely by DHHC8. Mutation of any one of these sites prevents ABCA1 trafficking to the plasma membrane (103).

The membrane microdomain distribution of a protein can also be influenced by *S*-acylation. A-Kinase anchoring protein 79 (AKAP79) is *S*-acylated on two N-terminal cysteine residues and is involved in the clustering of proteins for efficient cyclic AMP signaling. Mutation of AKAP79's acylation sites excludes it from lipid rafts and thus

prevents it from regulating adenylyl cyclase type 8 (AC8) activity (104). Acylation of the death receptor Fas on a cytoplasmic cysteine residue adjacent its single TMD targets it to cytoskeleton-linked lipid rafts. The Fas receptor ligand, FasL, is similarly acylated and localizes to rafts. Acylation of both receptor and ligand is necessary for Fas-FasL complex assembly in rafts and signaling to downstream caspases (105, 106). Acylation was shown to promote raft affinity for 35% of raft-associated transmembrane proteins (107). However, not all *S*-acylated transmembrane proteins associate with rafts, one example being transferrin receptor 1 (108). Other examples include the anthrax toxin receptors, TEM8 and CMG2. *S*-acylation of these transmembrane proteins prevents their association with lipid rafts, which in turn prevents premature ubiquitination by Cbl3, a necessary step in toxin internalization (109).

Protein *S*-acylation can regulate protein-protein interaction and facilitate complex formation. Two examples of this already mentioned are AKAP79-AC8 and Fas-FasL. A third example is  $G_{\alpha o}$ , which when lacking an acyl-group exists as a mixture of monomers and oligomers (dimers, trimers, tetramers, and pentamers) that disaggregate into monomers after  $GTP\gamma S$  stimulation. Acylated  $G_{\alpha o}$  however, exist only as oligomers and is resistant to  $GTP\gamma S$ -dependent disassembly (110). In the case of huntingtin (htt), *S*-acylation by DHHC17 (HIP14) reduces its ability to aggregate and form inclusion (111).

Finally, regulation of enzyme activity has been credited as a function of protein *S*-acylation. Acylation of G-protein-coupled receptor kinase GRK6 has dual roles in increasing its activity. Acylation promotes membrane association of GRK6, bringing it closer to its membrane-bound substrates and acylation also increases the kinase catalytic

activity of GRK6 (112). Within the epithelial Na<sup>+</sup> channel (ENaC), which has several transmembrane domains, *S*-acylation regulates channel gating (113).

Given the multiple functions of protein *S*-acylation and the fact that its thioester bond is reversible, it is likely that DHHC-mediated *S*-acylation is regulated in cells. To date the only process known to regulate DHHC protein activity is interaction with binding partners. Both yeast Erf2 and its human ortholog DHHC9 require interaction with accessory proteins Erf4 and GCP16, respectively, for transfer and autoacylation activities (81, 114) (Also see appendix). Perhaps serving a similar role, huntingin (htt) was shown to bind DHHC17 (HIP14) and stimulate both DHHC autoacylation and acylation of multiple substrates (115).

An alternative mechanism of regulating protein *S*-acylation is to control the access of DHHC proteins to cysteine thiols on protein substrates. Phosphodiesterase 10A (PDE10A) is phosphorylated in Thr16 and this prevents acylation of Cys11, which is otherwise acylated by DHHC7 and/or DHHC19 (116). Recently, the reciprocal modification of cysteine residues 3 and 5 in postsynaptic density protein 95 (PSD-95) has been described (117). Protein *S*-nitrosylation at these sites reduced *S*-acylation and vice versa. An alternative way to control DHHC access to substrate thiols is to regulate DHHC protein localization. This is the case for DHHC2, which following activity blockade in neurons, translocates between intracellular vesicles and postsynaptic densities where it mediates acylation of PSD-95 (93, 94). To date, there are no known posttranslational modifications of DHHC proteins that regulate acyltransferase activity.

## **Biological importance of DHHC proteins in disease**

As our understanding of DHHC proteins increases, a growing number of human diseases are being associated with DHHC proteins and protein *S*-acylation. *ZDHHC* genes that have been associated with disease are summarized in Table 1.1. A table summarizing DHHC proteins and their known protein substrates has recently been published (86). Several of these mammalian *S*-acylated proteins also have disease connections. Finally, the *S*-acylation of a large number of viral and parasitic proteins has been reported and in many cases, protein *S*-acylation is necessary for efficient infection (118-120). A few diseases connections to DHHC proteins are highlighted below; one is referred to recent reviews for more examples (86).

As previously mentioned, the causative protein of Huntington disease (HD), huntingtin (htt) is an *S*-acylated protein. DHHC17, also called huntingtin interacting protein 14 (HIP14), has been implicated as the PAT for htt. Polyglutamine tract expansion of htt, which proportionally increases susceptibility to HD, reduces interaction with DHHC17 and consequently reduces htt acylation. Nonacylated htt forms inclusions faster and is more toxic than acylated htt (111, 121). DHHC17 is also a potential oncogene having the ability to induce colony formation and anchorage-independent growth in cell lines, and tumors in mice (122).

Several DHHC proteins have been associated with human cancer. *ZDHHC2* was originally identified as a gene on 8p21.3-22 that displayed reduced expression associated with metastasis (REAM), suggesting that *ZDHHC2* might be a tumor suppressor. Reduced expression was observed in more than half of the human colorectal cancers

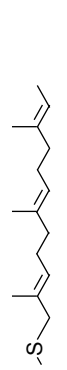
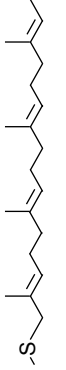
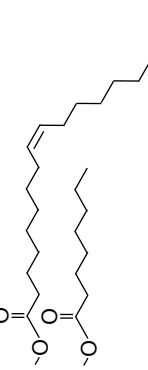
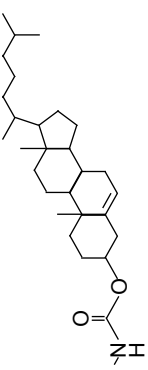
examined and somatic mutations of *ZDHHC2* were found in colorectal cancer (M356I, Figure 1.1), hepatocellular carcinoma (S306F), and a nonsmall lung cancer (R269stop) (92). Interestingly, two of these mutations (M356I and S306F) are found within a region of the C-terminal tail of DHHC2 (N299 to the C-terminus) that controls its dynamic translocation between recycling endosomes and the plasma membrane (94).

### **Concluding Remarks**

In my thesis work, I have focused on developing a better mechanistic understanding of how DHHC proteins catalyze protein *S*-acylation. Information on a protein's catalytic mechanism can provide insight into the function of residues within an active site and clarify structure-function relationships. Kinetic rate constants predict how enzyme activity will respond to cellular changes in substrate availability and provide insight into rate-limiting steps within pathways. Kinetic parameters can be used to quantify enzyme preferences among competing substrates or to quantify different enzymes preferences for the same substrate. Knowledge of substrate addition and product release can be beneficial in the development of enzyme inhibitors. Inhibitor sensitivities and mechanisms can reveal information about an enzyme's active site and catalytic mechanism. By initiating these types of studies on DHHC proteins, I sought to reveal new information about this biologically important family of enzymes.

In the following chapters I discuss the biochemical and enzymatic characterization of DHHC proteins and potential DHHC inhibitors. When these investigations began, partial purification and limited PAT activity assessment had only

been described for a few DHHC proteins (81, 82, 114, 123). In Chapter 2, I described the improvement of methods and assays to purified and characterize DHHC proteins. These procedures were used to determine that DHHC proteins use a two-step ping-pong catalytic mechanism. Additionally in Chapter 3 is the first reported evidence that DHHC proteins display acyl-CoA specificity. Assays that I developed were also used to characterize known and potential inhibitors of DHHC proteins. In the final chapter I discuss the implication of these studies and potential future studies based on these results.

Modification	Modifying Group	Attachment Site	Enzyme (substrate)	Linkage
S-Acylation (S-palmitoylation) <sup>1</sup>		Cysteine	DHHCs	Thioester to Cys
N-Myristoylation		(M)GXXXS/T--	NMT	Amide to N-Gly
Farnesylation		--CaaX	Fase	Thioether to Cys
Geranylgeranylation		--CaaL, --GXC, --CCX <sub>1-3</sub>	GGTaseI GGTaseII	Thioether to Cys
O-Acylation		--CKCHGXS <sub>2</sub> SGSCXXKTCW-- (--MAMA)GSS <sub>2</sub> FLSP--	Porcupine (Wnt-3a) GOAT (pro-ghrelin)	Oxyester
N-Palmitoylation		CGPGRGFGRRRHPKKL--	Rasp (Hh), Hhat (Shh) Unknown (Gαs)	Amide to N-Cys
Cholesterol		--G(CF--)	Non-enzymatic (Hh/Shh)	Cholesterol ester

**Table 1.1. Lipid modifications found on proteins.**

<sup>1</sup>Although C16:0 palmitate is the most common lipid attached through protein S-acylation, other acyl chain lengths ranging from C14 to C22 with various degrees of unsaturation have been observed on proteins isolated from cells.

**Table 1.2. Proteins modified by *S*-acylation with acyl length other than 16-carbon palmitate**

<b>Fatty Acid<sup>1</sup></b>	<b>Proteins</b>	<b>References</b>
14:0	band 3 (AE1), rhodopsin	(31, 124)
15:0	rhodopsin	(31)
16:1	band 3 (AE1), rhodopsin, unidentified proteins	(31, 124, 125)
18:0	P-selectin, HEF (influenza C virus), E1 (Semliki Forest virus), band 3 (AE1), rhodopsin	(31, 124, 126, 127)
18:1	band 3 (AE1), rhodopsin	(31, 124)
18:2	rhodopsin	(31)
20:4	G-protein $\alpha$ -subunits i, q, and z; rhodopsin, unidentified platelet proteins	(31, 128, 129)
20:5	unidentified platelet proteins	(129)
22:6	rhodopsin	(31)

Notes: <sup>1</sup>Number of carbons in acyl chain and number of desaturations.

**Table 1.3. DHHC proteins associated with disease**

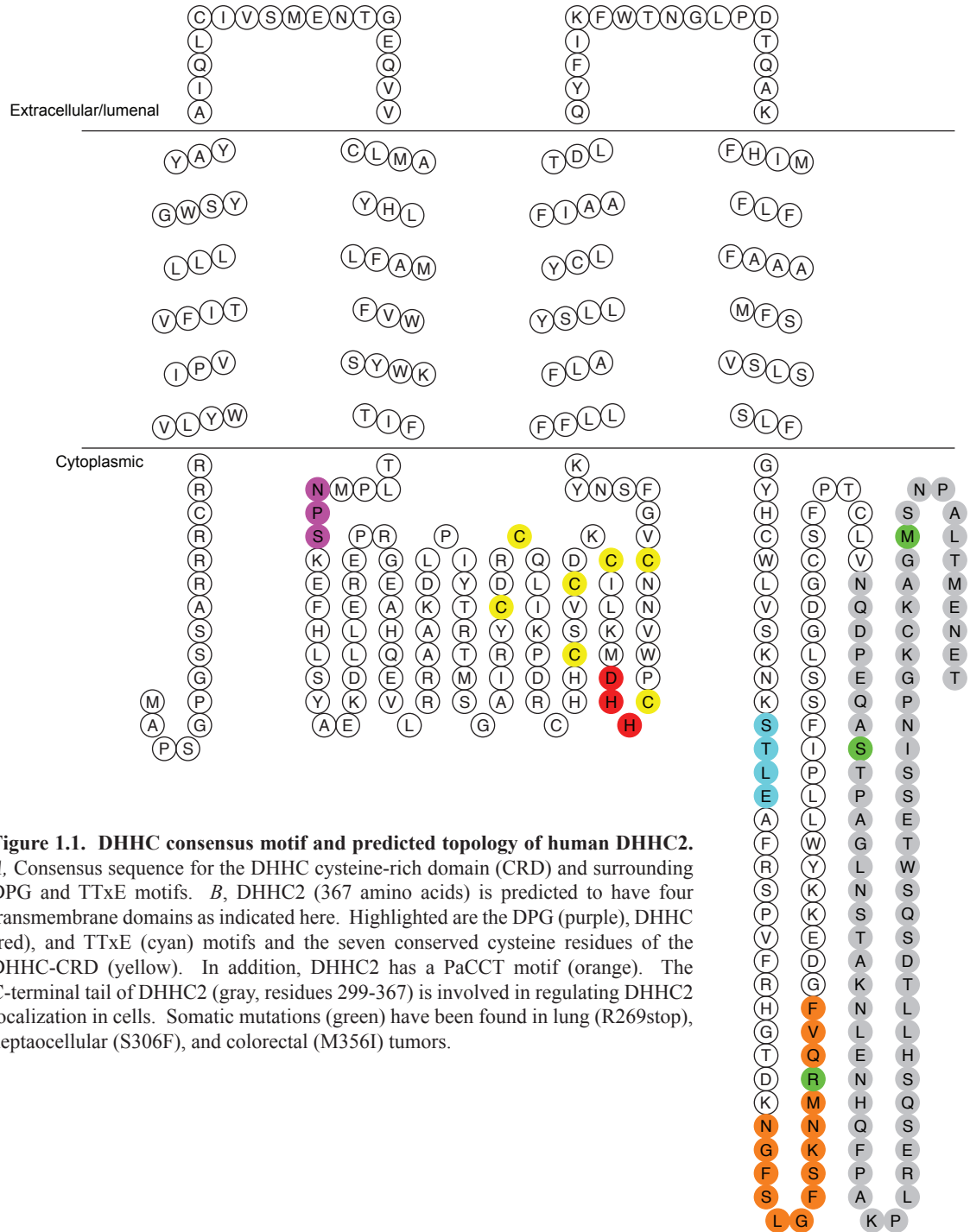
<b>DHHC<sup>1</sup></b>	<b>Disease</b>	<b>Ref.</b>
2 (REAM)	Cancer: colorectal, hepatocellular, and lung	(92)
3 (GODZ)	Squamous cell cervical carcinoma	(130)
5	Drip loss (in pigs)	(131)
7 (SERZ- $\beta$ )	Invasive breast cancer, oestrogen receptor-positive	(132)
8	Radiation susceptibility	(133)
8	Schizophrenia <sup>2</sup>	(134, 135)
8	Smooth pursuit eye movement (SPEM) abnormality	(136)
8	DiGeorge syndrome (22q11.2 deletion syndrome)	(137, 138)
9	X-linked mental retardation associated with Marfanoid habitus	(139)
9	Microsatellite stable and unstable colorectal cancer	(140)
9	Splay leg (in pigs)	(141)
9 (CGI-89)	Colorectal cancer	(142)
11	Bladder cancer progression	(143)
11	Cancer: non-small lung	(144)
13 (HIP14L)	Alopecia, osteoporosis, systemic amyloidosis	(145)
14	Post-transplant lymphoproliferative disorders Diffuse large B-cell lymphomas	(146)
14	Cancer: gastric	(147)
14	Acute biphenotypic leukemia Acute myeloid leukemia	(148)
15	X-linked mental retardation	(149)
17 (HIP14)	Huntington's Disease	(150)
17	Diabetes	(151)
17	Cancer: colon, stomach, breast, lung, and liver	(152)
19	Enterotoxigenic <i>E. coli</i> F4ab/ac susceptibility (in pigs)	(153)
20	Cancer: ovarian, breast, and prostate	(154)
21	Hair loss	(155)

Notes: <sup>1</sup>Alternative names for DHHC proteins are given in parenthesis. <sup>2</sup>Multiple reports have been published both supporting and refuting the association between *ZDHHC8* and schizophrenia.

A

--DPG-- ---C-C---KP-R--HC--C-C---DHHC-W--NC-G--N---F---- --TT-E--

B



# **Chapter 2**

## **Development of Assays to Monitor DHHC-mediated Protein *S*-acylation**

## **Abstract**

To facilitate our understanding of DHHC-mediated protein *S*-acylation, new and well-characterized experimental assays were needed. DHHC proteins are integral membrane enzymes and thus require detergent for membrane extraction and purification. However, detergents as well as other assay components can affect enzyme behavior. The conditions for an assay of protein *S*-acylation was modified from published protocols to optimize enzyme activity. The assay is referred to as the standard PAT assay, which measures the transfer of radiolabeled palmitate from palmitoyl-CoA to protein substrate. Improving this assay has revealed important aspects of DHHC function and enabled more detailed studies into the mechanism of DHHC proteins.

## Introduction

Developing purification protocols and robust and well-characterized assays for enzyme function are critical first steps to mechanistically studying an enzyme. Using the reductionist's approach to studying enzymes allows one to minimize the myriad of other simultaneous cellular processes and focus on the reaction of interest. Reconstitution of enzyme function with purified components allows measurement of activity with minimal side reactions and is a staple of the biochemist's toolbox. Here, I developed and improved assays for the reconstitution of DHHC PAT activity with purified components.

Earlier groups attempting to purify and identify PATs developed an assay for tracking PAT activity. These groups applied detergent extracts from liver or brain membranes to conventional chromatography columns. Column fractions were incubated with radiolabeled palmCoA and a protein substrate capable of being *S*-acylated. Reactions were stopped, resolved by SDS-PAGE, and analyzed by both fluorography, indicating which bands incorporated radiolabel palmitate, and scintillation counting, which provided a quantitative measure of PAT activity.

Once DHHC proteins were identified as catalyzing protein *S*-acylation, recombinant protein technologies could be used to enrich PAT activity. Affinity-tagged mammalian DHHC proteins were expressed with the Baculovirus system in Sf9 cells and purified over sequential nickel and FLAG affinity resins. When I joined the lab, the resulting purified DHHC proteins were tested with the same PAT assay used to monitor activity extracted from tissue even though this assay had not been optimized for DHHC

PAT activity. By carefully evaluating DHHC activity under various reaction conditions, I made several improvements to our standard radiolabel-based PAT assay.

## **Results and Discussion**

*Purification of DHHC proteins and PAT assay reagents*—My studies have focused primarily on DHHC2 and DHHC3, requiring protocols to express and purify both enzymes, as well as their protein substrates. Early studies with a His<sub>6</sub>-Express-DHHC2 (pML850) construct showed that the enzyme was undergoing C-terminal proteolysis, with enzyme autoacylation displaying two bands on films. Furthermore, one of the enzyme bands comigrated with the substrate myrG<sub>α1</sub>. Thus a construct was generated with affinity tags at both termini and the calmodulin binding peptide, His<sub>6</sub>-Express-CBP-DHHC2-FLAG-His<sub>6</sub> (pML943), to both limit proteolysis and increase the molecular weight. I first attempted to purify pML943 using sequential nickel and calmodulin resins. Unfortunately buffers used to elute from calmodulin resin are incompatible with binding to nickel resin and vice versa. This oversight was not unique (156) and a review now warns about using a His<sub>6</sub>-CBP tandem affinity tag (157). However, sequential chromatography using nickel and FLAG-peptide affinity columns resulted in relatively pure protein that immunoreacted with Express (Chapter 4, Figure 4.2) and Flag antibodies (not shown), suggesting that full-length protein was purified. Mouse DHHC3-FLAG-His<sub>6</sub> was purified in a similar way. Detailed methods for purification of DHHC2 and DHHC3 are found in chapters 4 and 3, respectively.

I used two *N*-myristoylated proteins as protein substrates for DHHC2 and DHHC3, *N*-myristoylated G<sub>α1</sub> (myrG<sub>α1</sub>) and *N*-myristoylated lymphocyte specific kinase, N-terminal residues 1-226 (myrLck<sub>NT</sub>). These were generated in *E. coli* coexpressing *N*-myristoyltransferase and were purified as described in Chapters 3 and 4. The lipid substrate in the PAT assay is [<sup>3</sup>H]palmCoA, I observed a spurious band in films of PAT assays that appeared at a position near DHHC2. This was identified as residual acyl-CoA ligase from the palmCoA preparations. To remove this contaminant, a chloroform-methanol extraction step was added to the palmCoA purification protocol.

*Radiolabel-based PAT assay optimization*—A protocol for assaying PAT activity from cell lines and tissues had previously been published by our group (Table 2.1, left side) (114), however reaction conditions had not been tested for their effect on DHHC activity. Detergents needed for the purification of integral membrane proteins can have unwanted effects on enzyme activity and behavior (158, 159). Initially our lab used Triton X-100 for enriching and assaying an unknown PAT activity (26). Because DHHC proteins were extracted from membranes and purified with nonionic *n*-dodecyl-β-D-maltoside (DDM), we sought to test DHHC PAT activity in the presence of DDM. As shown in Figure 2.1A, DHHC2 acylates myrG<sub>α1</sub> to a much higher extent when DDM detergent is used versus Triton X-100. This is consistent with other reports of integral membrane proteins showing highest activity in DDM when tested against a panel of detergents (160). Dose-response curves were performed at various DDM concentrations (Figure 2.1B). The highest activity was seen at 0.01% DDM, which is similar to DDM's critical micelle concentration (CMC) of 0.009% in water (ThermoScientific). Lower

DDM concentrations likely resulted in loss of micelles and DHHC aggregation, whereas high DDM concentrations likely resulted in more empty micelles, which could still bind substrates and sequestered them from micelles containing DHHC proteins.

Because DHHC proteins are predicted to be zinc-binding proteins, the buffer component EDTA was tested, however no effect was observed even at the highest concentration (Figure 2.1C). Interestingly when zinc ions were included in the assay, DHHC2 incorporated less palmitate into myrLck<sub>NT</sub> relative to either water or magnesium ion controls (Figure 2.1D). It is known that the N-terminal SH3 domain of Lck has a  $K_d$  for zinc of less than 100 nM and that zinc binding induces Lck homodimerization (161), but it is unknown whether zinc binding or dimerization alter Lck's ability to be acylated. Additionally, zinc also likely affected DHHC2 because enzyme autoacylation was observed on film in samples containing magnesium but not zinc (data not shown). Investigations with the yeast PAT Erf2/Efr4 suggest that zinc concentrations as low as 20  $\mu$ M are inhibitory (Robert Deschenes, personal communication). Whether DHHC proteins bind zinc as predicted remains unknown and warrants further investigation.

*Thiol-based reducing agents*—Protein S-acylation occurs through a thioester linkage that is reversible. While this property is beneficial to cells, using acylation/deacylation cycles to regulate protein behavior, it presents challenges to the researcher. The thioester bond is susceptible to cleavage by reducing agents and their concentration needs to be kept to a minimum. Conversely, formation of a thioester bond requires free cysteine residues that are prone to oxidation. Thus early PAT assays included low levels of dithiothreitol (DTT) in all buffers to maintain this balance (Table

2.1, left side). This practice was questioned when initial attempts to purify autoacylated enzyme for single turnover pulse-chase assays were unsuccessful. DHHC protein was pre-incubated with low concentrations of [<sup>3</sup>H]palmCoA, forming a radiolabeled acyl-DHHC. High concentrations of unlabeled palmCoA were added with or without a protein substrate and aliquots removed during a time course. It was predicted that [<sup>3</sup>H]-palmitate would only transfer off the DHHC when protein substrate was present. However, even in the absence of a protein substrate, DHHC proteins lost their radiolabeled palmitate on a rapid time scale (data not shown [PAT ID#525]). This suggested that DHHC proteins were rapidly acylating and deacylating during a standard PAT assay and thus hydrolyzing and depleting palmCoA pools.

The hypothesis that DHHC proteins were hydrolyzing palmCoA in the presence of thiol-based reducing agents was tested. DHHC3 was incubated with standard buffers containing 1 mM DTT for either 0.2 or 30 min. The reaction was stopped and analyzed by thin layer chromatography (TLC) for production of free [<sup>3</sup>H]-palmitate and by SDS-PAGE gels and fluorography for enzyme autoacylation (Figure 2.2A). As shown, after 30 min DHHC3 produced more free [<sup>3</sup>H]-palmitate than a catalytically inactive DHHS2 or buffer control. Also consistent with the hydrolysis model, DHHC3 at 30 min was radiolabeled less than at the earlier time point suggesting its palmitate was being released. To determine whether the hydrolysis of palmCoA was reducing-agent dependent, time courses for free [<sup>3</sup>H]-palmitate production were performed with or without DTT or β-mercaptoethanol (β-ME) and monitored by TLC. For both DHHC2 and DHHC3, reactions with reducing agent produced more [<sup>3</sup>H]-palmitate than those without (data not

shown [PAT ID#533, 547, 629]). DHHC enzyme autoacylation was also studied in the presence of reducing agents. As shown in Figure 2.2B, less acyl-DHHC3 was formed when DTT or  $\beta$ -ME were included in the assay. Additionally, the amount of autacylated DHHC3 rapidly decreased with time in the continued presence of reducing agent and palmCoA. A similar but less pronounced pattern was also seen with DHHC2 (Figure 2.2C). This rapid decrease in acyl-DHHC and the production of free [ $^3$ H]-palmitate suggest that DHHC proteins were autoacylating and then deacylating in a reducing agent-dependent process. Deacylation could occur by either an acyl-DHHC transferring its palmitate to a free thiol present on the reducing agent or by the reducing agent cleaving the acyl-enzyme thioester bond. Given the ratio of reducing equivalents to palmCoA of 2000 to 1, there is ample reducing agent present to greatly deplete the palmCoA pool. This is suggested by DHHC3 deacylating to a low steady state level (Figure 2.2B). The time frame required to reach this steady state level (under 10 min) was similar to the linear reaction range observed in substrate acylation time courses (not shown). One possibility is that the linear reaction ranges of substrate acylation were shortened because palmCoA pools were being rapidly depleted. Indeed, when reducing agent was omitted from a time course PAT assay with DHHC2 and myrLck<sub>NT</sub>, the linear range was extended to at least 30 min [PAT ID#553]. Measuring acylation within the linear reaction range was critical for the inhibitor and kinetics studies in subsequent chapters. The effect of DTT on substrate *S*-acylation was also measured (Figure 2.2D). As predicted, DHHC2 transferred less palmitate to myrLck<sub>NT</sub> in the presence of DTT.

Given the negative effect of thiol-based reducing agents on DHHC PAT activity, I sought to determine if reducing agents could be omitted. Reducing agents were originally included in PAT assays to maintain free thiols available for acylation. High pH accelerates non-enzymatic acylation and was used to evaluate the availability of thiols on myrLck<sub>NT</sub> in the presence of reducing agents. Figure 2.2E shows that treatment with reducing agents resulted in more myrLck<sub>NT</sub> being acylated at high pH. This suggests that reducing agents are needed for maintaining free thiols on protein substrates.

*Replacing thiol-based reducing agents with TCEP*—The non-thiol based reducing agent *tris*(2-carboxyethyl)phosphine (TCEP) was evaluated and determined to be less detrimental for PAT assays than DTT. TCEP is a phosphine-based reductant that unlike DTT is non-volatile, odorless, resistant to air oxidation, and compatible with immobilized nickel affinity capture resins (Thermo Scientific) (162). TCEP was tested in a DHHC2 autoacylation PAT and shown to increase incorporation of palmitate into DHHC2 but not the DHHS2 control (Figure 2.2 C). Analyzing reactions from the same assay by TLC also showed that inclusion of TCEP produced considerably less free [<sup>3</sup>H]-palmitate than inclusion of DTT (data not shown [PAT ID#629]). This suggests TCEP does not cause the DHHC-catalyzed acyl-CoA hydrolysis that was observed with DTT and β-ME. TCEP was also tested and shown to maintain free thiol availability on a protein substrate at similar levels to DTT (Figure 2.2E). Including TCEP in a PAT assay with DHHC2 and myrLck<sub>NT</sub> resulted in a 4-fold increase in palmitoyl-myrLck<sub>NT</sub> versus a reaction lacking reducing agent (Figure 2.2F). This indicated that TCEP could maintain free substrate thiols while not negatively affecting DHHC2 PAT activity. A titration of TCEP

into an assay with DHHC3 and myrG<sub>α1</sub> was carried out to determine the optimal TCEP concentration. Figure 2.2G indicates that for this enzyme-substrate pair, concentrations of TCEP greater than 1 mM were inhibitory to palmitate labeling of myrG<sub>α1</sub>. For this enzyme-substrate pair inclusion of TCEP into this assay did not increase substrate acylation over a reaction lacking reducing agent, which is unlike the DHHC2-myrLck<sub>NT</sub> pair in Figure 2.2F.

Together these results support the replacement of DTT with TCEP in PAT assays. Given that reductant is included to maintain substrate thiols (Figure 2.2E) and that high TCEP concentrations are inhibitory (Figure 2.2G), it is recommended that 1 mM TCEP only be included in the substrate buffer as shown in Table 2.1. This allows reduction of substrate thiols as well as dilution of the TCEP when the remaining assay components are added. Although unlikely, one possibility that was not investigated is that TCEP may break physiologically relevant disulfide bonds and the newly exposed thiols become sites of acylation. This could be tested by determining if TCEP causes acylation of a substrate that has the *in vivo* modified cysteine residues mutated (e.g. myrLck<sub>NT</sub> C3S C5S or myrG<sub>α1</sub> C3S). Finally, the difference in response to TCEP between DHHC2 and DHHC3 may suggest that DHHC proteins respond differently to reducing agents.

*Effect of various compounds on DHHC-mediated PAT activity*—Several other compounds were tested in the radiolabel-based PAT assay as summarized in Table 2.2 and are briefly discussed here. During the purification of DHHC proteins several protease inhibitors are used to limit protein degradation. These compounds were tested for their effect on DHHC activity and most were found to have no effect. Because

inhibitor compounds tend not be soluble in water at high concentrations and are instead dissolved in organic solvents, these solvents were tested. Of these, ethanol showed strong inhibition of PAT activity consistent with work by others in cells showing that ethanol inhibits palmitoylation of G-protein  $\alpha$ -subunits (163). Dimethylsulfoxide (DMSO) displayed the least inhibition of the solvents tested and was used as the vehicle for additives to the assay. Multiple reports have described the use of cerulenin, tunicamycin, and analogs of each to inhibit protein acylation within cells (164-167). Neither cerulenin nor tunicamycin inhibited DHHC2 PAT activity when tested, suggesting that in cells these compounds may have other targets such as acyl-CoA ligase or enzyme involved in fatty acid synthesis. Given the high conservation of cysteine residues within the DHHC cysteine rich domain and thus their likely importance to enzyme function, it was not surprising that the cysteine-specific alkylating reagent *N*-ethylmaleimide (NEM) strongly inhibited DHHC activity. Interestingly, the histidine-specific alkylating reagent diethylpyrocarbonate (DEPC) also inhibited DHHC activity. This may point to the histidine residues of the DHHC motif playing an important role in acyltransfer.

Finally, two compounds currently in clinical trials were tested for ability to alter DHHC PAT activity. Tecovirimat (ST-246) prevents the function of p37 (F13L), a palmitoylated protein necessary for poxvirus infections and has shown promise as an orally active drug (168, 169). When tested in our assay it showed no effect on PAT activity. Farnesyl thiosalicylic acid (FTS, Salirasib), which was originally identified as inhibiting carboxymethylation of CaaX motifs (170, 171), showed dose-dependent

inhibition of both DHHC2 and DHHC9. One possibility is that the long hydrophobic farnesyl-side chain of this inhibitor competes with the acyl-chain of palmCoA for binding to the DHHC. How DHHC proteins recognize and differentiate lipid substrates is unclear.

### **Concluding remarks and future experiments**

DHHC acyltransferase activity could be further improved by investigating other conditions. We used detergent to extract and purify DHHC proteins within detergent micelles, however in cells, DHHC proteins are found within a phospholipid bilayer. Thus, reconstitution of DHHC proteins into liposomes may better represent physiological conditions. For other integral membrane enzymes, profound effects on kinetics and specificity have been described following reconstitution into lipid vesicles. For example, the yeast polytopic integral membrane Ste14p, which acts on Ras, displays a ~15-fold enhancement upon reconstitution into *E.coli* liposomes (160). Another integral membrane enzyme MGAT (monoacylglycerol acyltransferase) displays 11-fold stimulation by reconstitution into phosphatidic acid containing micelles, but inhibition by oleate and sphingosine containing vesicles (172). One caveat of reconstitution into the liposomes is orientation of the DHHC protein within the lipid bilayer. It is likely that some DHHC proteins would incorporate with their active site to the lumen of the liposome and thus, inaccessible for interaction with either substrate during a PAT assay. When determining enzyme activity, these effectively inactive DHHC proteins could skew calculations of turnover and specific activity.

An alternative method of lipid reconstitution that gets around the orientation problem of liposomes is the use of high-density lipoprotein particles, also called Nanodiscs. Nanodiscs consist of a lipid bilayer approximately 7 nm in diameter surrounded by a self-assembling membrane scaffolding protein (MSP) ‘belt’ derived from human apolipoprotein A-1 (apo A1). Various lipids, including cholesterol, can be used to form the bilayer and MSP mutants of varying length can alter the bilayer diameter (173). Nanodisc components and a membrane protein of interest purified in detergent are mixed and as the detergent is removed, membrane proteins incorporate into the Nanodisc lipid bilayer. One advantage of this system is that both sides of the bilayer are solvent accessible, and thus, protein orientation within the bilayer is not an issue. The contribution of the surrounding lipid environment to DHHC activity is a largely unexplored area.

For my studies DHHC proteins were epitope tagged at the N-terminus (DHHC2 pML850), the C-terminus (DHHC3), or both (DHHC2 pML943) with multiple different tags. The yeast DHHC protein Erf2 displayed ~30% lower autoacylation and ~50% reduced transfer activity when FLAG-tagged at the C-terminus versus the N-terminus (83). Erf2-FLAG reduced activity could result from loss of interaction with its binding partner Erf4, however this was not tested. Nevertheless, given this precedent, the placement of affinity purification tags on DHHC proteins should be investigated.

As we learned more about DHHC proteins, differences are being found among family members. These include differences in acyl-CoA specificities (Figures 3.3-5), TCEP-induced activity enhancement (Figures 2.2F and G), binding partner requirements,

and protein substrate preferences. Thus, the idea that one set of assay conditions be optimal for all DHHC proteins seems unlikely and DHHC-specific protocol modifications may be needed. For other enzymes families that have been well characterized, assay conditions differ from one isoform to another. For example, within the PKC family of protein kinases, differences are noted in calcium, magnesium, diacylglycerol, and phospholipid requirements for maximal activity (174).

Given the data presented here regarding the use of thiol-based reducing agents in PAT assays, care should be taken in analyzing previously published results. One example is the inhibitor studies presented in Chapter 4 of this work. These studies were carried out before we knew about the detrimental effects of DTT on DHHC-mediated PAT activity. It is possible that those compounds that failed to inhibit DHHC proteins as expected did so because of the presence of DTT within reaction buffers. If inhibitors reacted with thiols within the DHHC protein, it is feasible the DTT could have removed these inhibitors and restored enzyme activity. To determine if DTT affected inhibitor action, DHHC9 was analyzed with the inhibitors in the absence of reducing agent. No change was observed in the inhibition profile (data not shown [PAT ID#561]).

A second example where DTT may have affected enzyme activity is the work presented by Mitchell and coworkers with the yeast DHHC protein Erf2 (175). They developed a continuous assay to monitor palmCoA use by coupling the release of CoA to the reduction of  $\text{NAD}^+$  to NADH by  $\alpha$ -ketoglutarate dehydrogenase and monitoring the change in NADH fluorescence. Using this assay they measured the rates of palmCoA hydrolysis by wildtype and several mutants of Erf2. The buffers for this assay were

reported to contain 1 mM DTT. If Erf2-catalyzed hydrolysis of palmCoA is DTT-dependent as shown here for other DHHC proteins, then their reported hydrolysis rates were likely dependent on reducing agent abundance and higher than rates had DTT been omitted or TCEP used. While this would not change the major findings of the paper, it complicates comparison of palmCoA hydrolysis rate to those determined by others.

Having robust, well-characterized assays of enzyme activity is one of the first steps in biochemically investigating an enzyme. Here I described the optimization and characterization of a number of properties for the radiolabel-based PAT assay. This characterization was necessary for subsequent inhibitor studies, which needed to be performed within the linear reaction range. Likewise, the single turnover assays used to determine the kinetic mechanism of DHHC proteins required purification of the acyl-DHHC transfer intermediate that was not possible until DTT was omitted from buffers. Together, these optimization experiments have improved the main assay used to study DHHC function and have opened the door for new investigations.

**Table 2.1 Standard radiolabel-based PAT assay**

<b>Fall 2005 (114)</b>	<b>Current Conditions</b>
<u>10 <math>\mu</math>L Enzyme in TEDT Buffer</u> 50 mM Tris pH 7.4 125 mM NaCl 1 mM EDTA 10% glycerol 0.1% Triton X-100 1 mM DTT	<u>10 <math>\mu</math>L Enzyme in Enzyme Dilution Buffer</u> 50 mM MES pH 6.4 100 mM NaCl 1 mM EDTA 10% glycerol 0.1% DDM
<u>10 <math>\mu</math>L Substrate in HED</u> 20 mM HEPES pH 8.0 1 mM EDTA 1 mM DTT	<u>10 <math>\mu</math>L Substrate in MET</u> 50 mM MES pH 6.4 1 mM EDTA 1 mM TCEP
<u>30 <math>\mu</math>L Reaction Hot Mix</u> 167 mM MES 6.4 1 mM DTT 1.7 $\mu$ M [ $^3$ H]-palmitoyl-CoA	<u>30 <math>\mu</math>L Reaction Hot Mix</u> 50 mM MES pH 6.4 1.7 $\mu$ M [ $^3$ H]-palmitoyl-CoA
Reaction at 30°C and stop with 5X Sample Buffer + 5 mM DTT final Heated 100°C for 60 sec	Reaction at 25°C and stop with 5X Sample Buffer + 2 mM TCEP final Heated 55°C for 60 sec

**Table 2.2 Effect of various compounds on PAT activity<sup>5</sup>**

PAT ID#	Compound	Conc.	Percent Inhibition	DHHC (pML)	Sub.
729	Zinc (Zn <sup>2+</sup> )	2 – 20 mM <sup>2</sup>	100	2 (943)	myrLck <sub>NT</sub>
729	Magnesium (Mg <sup>2+</sup> )	2 – 20 mM <sup>2</sup>	0	2 (943)	myrLck <sub>NT</sub>
179	3X FLAG ® peptide	3 – 333 ng/μL <sup>1</sup>	0	2 (943)	myrG <sub>ai1</sub>
263	Roche Complete® EDTA-free inhibitor tablets	1 tablet per 32 mL <sup>1</sup>	0	2 (943)	myrLck <sub>NT</sub>
263	Pepstatin A	5 μg/mL <sup>1</sup>	0	2 (943)	myrLck <sub>NT</sub>
123	<i>N</i> -α-Tosyl- <i>L</i> -lysiny-chloromethylketone (TLCK)	0.5 – 10 mM <sup>2</sup>	0 to 26	2 (850)	myrG <sub>ai1</sub>
123	<i>N</i> -tosyl- <i>L</i> -phenylalaniny-chloromethylketone (TPCK)	0.5 – 4 mM <sup>2</sup>	0	2 (850)	myrG <sub>ai1</sub>
123	Phenylmethanesulfonylfluoride (PMSF) in 2-Propanol	0.2 – 1 mM <sup>2</sup>	-22 <sup>6</sup>	2 (850)	myrG <sub>ai1</sub>
123	2-Propanol	2% <sup>2</sup>	-11 <sup>6</sup>	2 (850)	myrG <sub>ai1</sub>
181	Ethanol (EtOH)	10% <sup>1</sup>	87	2 (943)	myrG <sub>ai1</sub>
123	Methanol	2% <sup>2</sup>	0	2 (850)	myrG <sub>ai1</sub>
289	Dimethyl sulfoxide (DMSO)	0 – 50% <sup>1</sup>	Inhibits at >20%	2 (943)	myrG <sub>ai1</sub>
		0 – 50% <sup>1</sup>	Inhibits at >10%	2 (943)	myrLck <sub>NT</sub>
175	Tunicamycin	1 – 100 μM <sup>2</sup>	0	2 (943)	myrG <sub>ai1</sub>
181		5 – 500 μM <sup>1</sup>			
175	Ceruleinin	1 – 1000 μM <sup>2</sup>	0	2 (943)	myrG <sub>ai1</sub>
117	Palmitic Acid (PA)	50 –	0 to 14	2 (850)	myrG <sub>ai1</sub>
119		5000 μM <sup>1</sup>			
63	Diethylpyrocarbonate (DEPC)	5 mM <sup>1</sup>	59	2 (850)	myrG <sub>ai1</sub>
63	<i>N</i> -Ethylmaleimide (NEM)	5 mM <sup>1</sup>	88	2 (850)	myrG <sub>ai1</sub>
289	Tecovirimat (ST-246) <sup>3</sup>	0.5 – 500 μM <sup>2</sup>	0	2 (943)	myrG <sub>ai1</sub> myrLck <sub>NT</sub>
427	Farnesyl Thiosalicylic Acid (FTS, Salirasib) <sup>4</sup>	5 – 1580 μM <sup>1</sup>	0 – 100	2 (943)	myrLck <sub>NT</sub>
		1580 μM <sup>1</sup>	100	9 (418)	H-ras

Notes: <sup>1</sup>Concentration during pre-incubation with DHHC before addition of substrates.

<sup>2</sup>Final concentration in assay, no pre-incubation.

<sup>3</sup>Prevents function of p37 (F13L), a palmitoylated protein required by poxvirus (168, 169).

<sup>4</sup>Inhibits carboxymethylation of CaaX motifs (171).

<sup>5</sup>The concentrations of reaction components varied. Typical ranges were DHHC protein, 2 to 20 nM; protein substrates myrG<sub>ai1</sub>, myrLck<sub>NT</sub>, or H-ras 0.5 to 2 μM; and [<sup>3</sup>H]palmCoA, 0.5 to 1.3 μM. Reactions were incubated at 25°C for 4 to 12 min. <sup>6</sup>These compounds stimulated DHHC activity.

<sup>6</sup>These compounds stimulated DHHC activity.

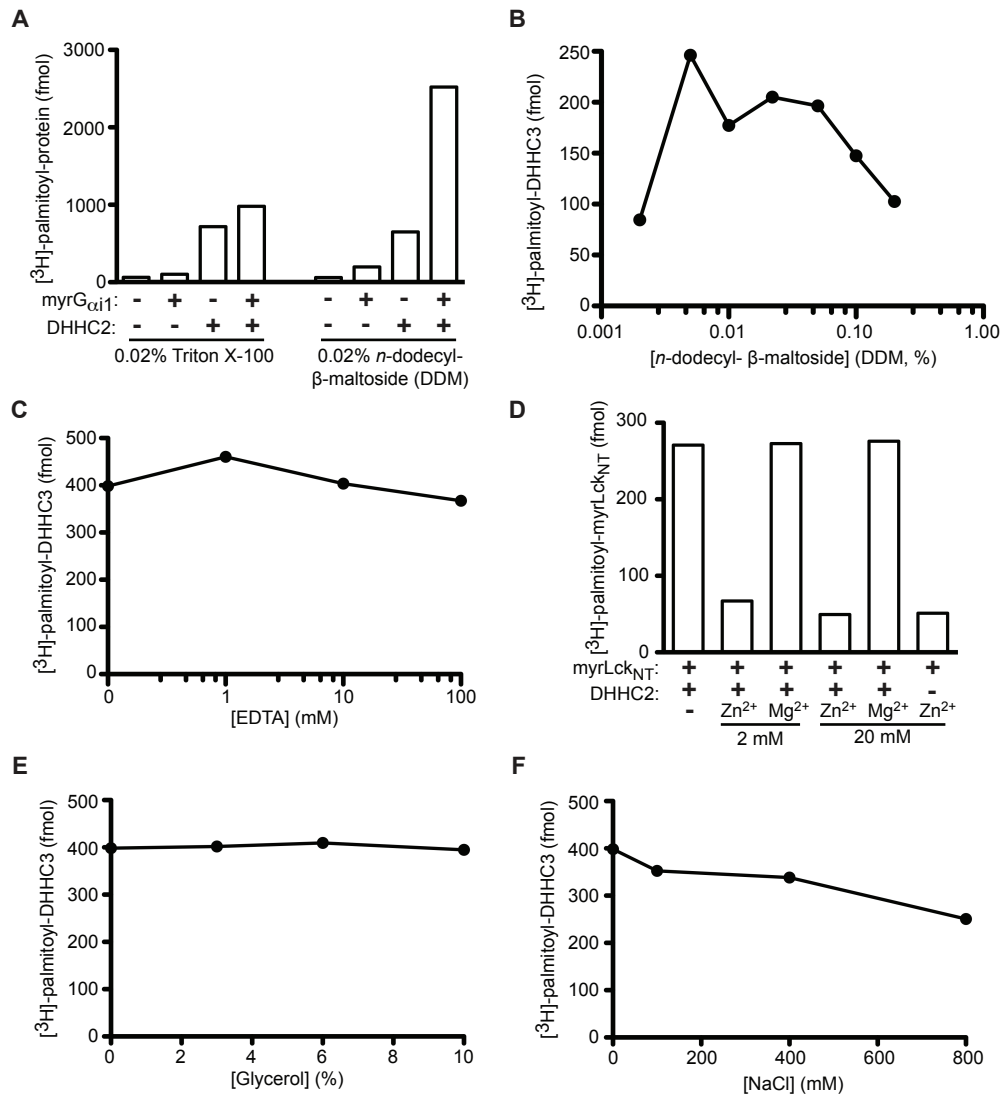


**Figure 2.1. Detergent and buffer effects on in vitro DHHC PAT activity.** *A*, DHHC2 (pML850) was assayed with myrG $\alpha$ i1 in the presence of either 0.02% Triton X-100 or 0.02% *n*-dodecyl- $\beta$ -maltoside (DDM) [PAT ID#107; n=1]. *B*, DHHC3 (1000 fmol) autoacylating in various amounts of DDM detergent for 2 min on ice in 1  $\mu$ M [<sup>3</sup>H]palmCoA [PAT ID#531; n=2]. *C*, *E*, and *F*, DHHC3 (500 fmol) autoacylating in EDTA, glycerol, or NaCl at the indicated concentrations for 4 min at 25°C in 1  $\mu$ M [<sup>3</sup>H]palmCoA [PAT ID#601; n=1]. *D*, DHHC2 (5 nM, pML943) was assayed for the ability to acylate myrLck<sub>NT</sub> (1  $\mu$ M) in the presence of either ZnCl<sub>2</sub> or MgCl<sub>2</sub> for 6 min at 25°C in 1.2  $\mu$ M [<sup>3</sup>H]palmCoA. The final concentration of metal ions in the 50  $\mu$ L reaction is listed [PAT ID#729; n=1].

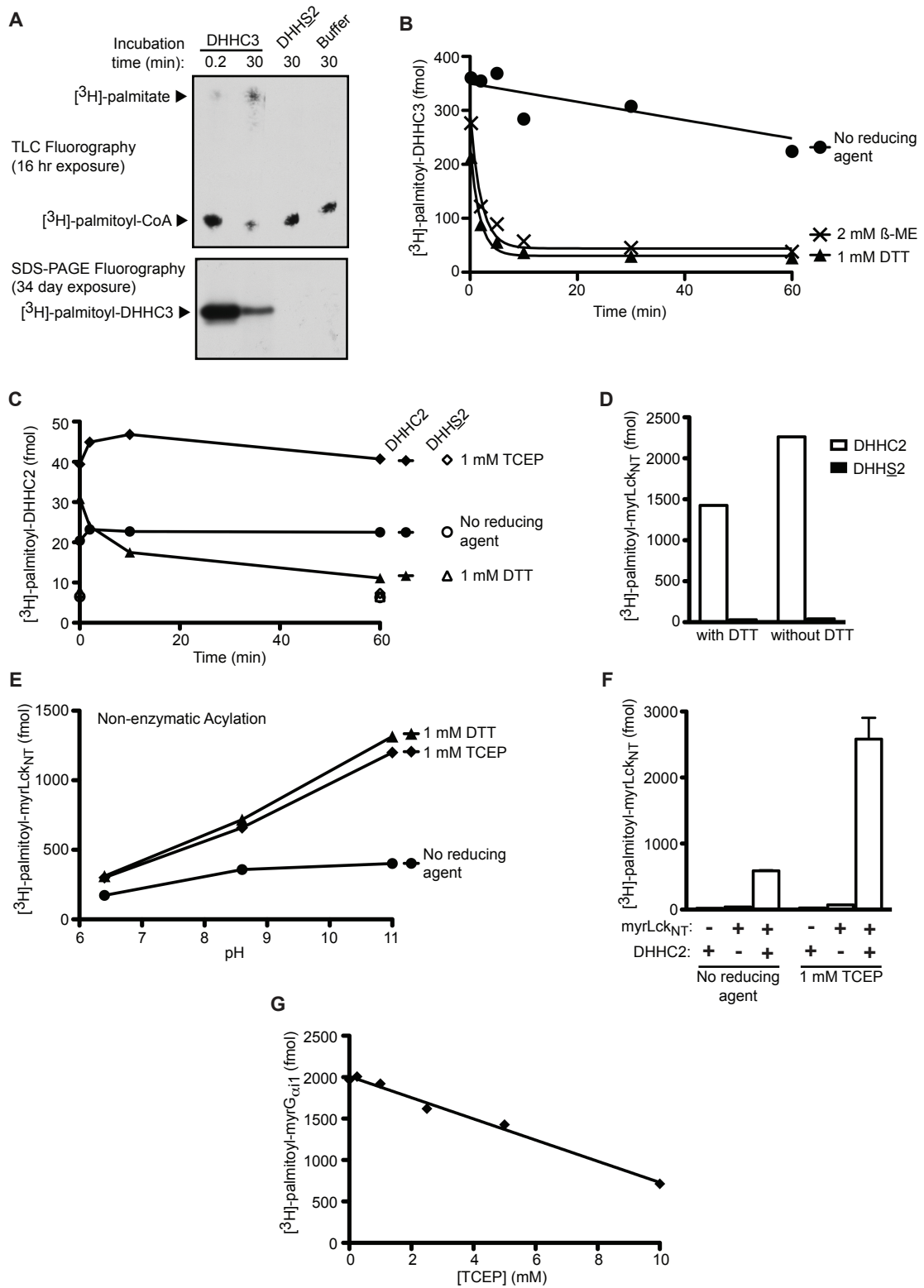


**FIGURE 2.2** Reducing agents affect in vitro DHHC autoacylation and PAT activity.

**FIGURE 2.2. Reducing agents affect DHHC autoacylation and PAT activity in vitro.**

*A*, DHHC3, DHHS2 (1 pmol), or enzyme buffer were incubated with 1.1  $\mu\text{M}$  [ $^3\text{H}$ ]palmCoA on ice for the indicated times. Reactions were stopped with SDS and an aliquot was spotted on thin layer chromatography plates that were then developed in 50% butanol/20% acetic acid/30% water for 5.5 hr. The plate was dried, sprayed twice with En<sup>3</sup>Hance solution, and exposed to film at  $-70^\circ\text{C}$ . The remaining reaction was resolved by SDS-PAGE gels and processed as described in Chapter 4 [PAT ID#529]. *B*, DHHC3 was autoacylated with [ $^3\text{H}$ ]palmCoA in buffer containing no reducing agent (●), 1 mM dithiothreitol (DTT, ▲), or 2 mM  $\beta$ -mercaptoethanol ( $\beta$ -ME, ✕). Aliquots representing 500 fmol DHHC were removed at various times and analyzed by SDS-PAGE and liquid scintillation counting [PAT ID#547; n=2]. *C*, DHHC2 (filled symbols) or DHHS2 (open symbols, 500 fmol each) was incubated with 1  $\mu\text{M}$  [ $^3\text{H}$ ]palmCoA in buffer containing no reducing agent (●), 1 mM DTT (▲), or 1 mM *tris*(2-carboxyethyl)phosphine (TCEP, ◆) for the indicated time on ice. DHHS2 was analyzed only at the 12 sec and 60 min time points. Reactions were processed as in B [PAT ID#629; n=2]. *D*, PAT assay of DHHC2 or DHHS2 (20 nM) with myrLck<sub>NT</sub> for 12 min in 0.9  $\mu\text{M}$  [ $^3\text{H}$ ]palmCoA with or without 1 mM DTT [PAT ID#541]. *E*, Non-enzymatic acylation of myrLck<sub>NT</sub> (100 pmol) in 1.7  $\mu\text{M}$  [ $^3\text{H}$ ]palmCoA with no reducing agent (●), 1 mM DTT (▲), or 1 mM TCEP (◆) for 35 min at the indicated pH [PAT ID#633]. *F*, DHHC2 (5 nM) and/or myrLck<sub>NT</sub> (1  $\mu\text{M}$ ) were incubated with 1  $\mu\text{M}$  [ $^3\text{H}$ ]palmCoA for 8 min at  $25^\circ\text{C}$  either with or without 1 mM TCEP [PAT ID#631]. *G*, DHHC3 (10 nM) was incubated with 2  $\mu\text{M}$  myrG <sub>$\alpha$ i1</sub> and 1  $\mu\text{M}$  [ $^3\text{H}$ ]palmCoA for 6 min at  $25^\circ\text{C}$  in buffer containing the indicated concentration of TCEP [PAT ID#779].

# Chapter 3

## **DHHC Protein *S*-Acyltransferases Use A Similar Ping-Pong Kinetic Mechanism But Display Different Acyl-CoA Specificities**

This chapter was reviewed for publication by the *Journal of Biological Chemistry*. Dr. Maurine Linder and I are coauthors. The manuscript is accepted pending revision and resubmission is anticipated in fall 2011.

## Abstract

DHHC proteins catalyze the reversible *S*-acylation of proteins at cysteine residues—a modification important for regulating protein localization, stability, and activity. However, little is known about the kinetic mechanism of DHHC proteins. A high performance liquid chromatography (HPLC), fluorescent peptide-based assay for protein *S*-acylation (PAT) activity was developed to characterize mammalian DHHC3. Time courses and substrate saturation curves allowed the determination of  $V_{max}$  and  $K_m$  values for both the peptide *N*-myristoylated-GCG and palmitoyl-coenzyme A. DHHC proteins acylate themselves upon incubation with palmitoyl-CoA, which is hypothesized to reflect a transient acyl-enzyme transfer intermediate. Single turnover assays with DHHC2 and DHHC3 demonstrated that a radiolabeled acyl group on the enzyme transferred to the protein substrate, consistent with a two-step ping-pong mechanism. Enzyme autoacylation and acyltransfer to substrate displayed the same acyl-CoA specificities, further supporting a two-step mechanism. Interestingly, DHHC2 efficiently transferred acyl-chains 14 carbons and longer, whereas DHHC3 activity was greatly reduced by acyl-CoAs with chain lengths longer than 16 carbons. The rate and extent of autoacylation of DHHC3, as well as the rate of acyl-chain transfer to protein substrate, were reduced with stearoyl-CoA compared to palmitoyl-CoA. This is the first observation of lipid substrate specificity among DHHC proteins and may account for the differential *S*-acylation of proteins observed in cells.

## Introduction

Protein *S*-acylation is the posttranslational addition of long-chain fatty acids to cysteine residues via a thioester linkage. Unlike other lipid modifications, *S*-acylation is reversible and thus regulated via acylation/deacylation cycles in cells. This regulation is important for the activity and localization of key signaling proteins including Ras isoforms (38, 176, 177), G-protein  $\alpha$ -subunits (178), huntingtin (111, 121), endothelial nitric oxide synthase (179), and ion channels (180). Protein acyltransferases (PATs) catalyze the addition of fatty acids to proteins whereas acyl-protein thioesterases (APTs) remove them. Despite the importance of protein *S*-acylation in these signaling pathways and in human diseases (86), little is known about the kinetic mechanism, regulation, and substrate specificities of PATs and APTs.

Genetic and biochemical studies in yeast have established that a family of integral membrane enzymes known as DHHC proteins catalyze protein *S*-acylation. While *S. cerevisiae* have seven DHHC PATs, mammalian genomes encode at least twenty-three. DHHC proteins are named for a highly conserved Asp-His-His-Cys sequence within a larger cysteine-rich domain (DHHC-CRD) that is situated on the cytoplasmic face of the membrane between four transmembrane domains (83). In vitro analyses with radiolabeled palmitoyl-CoA (palmCoA) have demonstrated that DHHC proteins are sufficient to catalyze the transfer of fatty acids from CoA to cysteine residues within target protein substrates. Additionally, DHHC proteins themselves become acylated upon incubation with palmCoA, a process called enzyme autoacylation. Mutational analysis has revealed that the cysteine residue within the DHHC motif is indispensable for both

palmitoyl-transfer and autoacylation activities (81, 82); however the site of autoacylation remains unknown as well as whether autoacylation occurs *in cis* or *trans*. It has been hypothesized that DHHC autoacylation reflects a transient acyl-enzyme intermediate with DHHC proteins using a two-step ping-pong mechanism to catalyze transfer (81, 82). Alternatively, DHHC autoacylation may reflect a modification of the enzyme that is not transferred to substrate but serves another function.

The fatty acid attached during *S*-acylation is most often the saturated 16-carbon fatty acid palmitate; thus, the process is frequently called *S*-palmitoylation or simply palmitoylation. However, *S*-acylation of other chain lengths has been reported. Incubation of platelets with [<sup>3</sup>H]-arachidonate acid (C20:4) resulted in the labeling of endogenous G-protein subunits  $\alpha_i$ ,  $\alpha_q$ ,  $\alpha_{13}$ , and  $\alpha_z$  via a thioester linkage (128). Mass spectrometry of fatty acids attached to native rhodopsin revealed that approximately 83% are C16 palmitate while the remaining are a mixture of 14:0, 15:0, 16:1, 18:0, 18:1, 18:2, 20:4, and 22:6 (31). Metabolic radiolabeling with palmitate versus either C20:4 arachidonate (129) or C18:0 stearate (127) demonstrated that some proteins are preferentially modified with chain lengths other than C16 palmitate. More recently, using click chemistry techniques and alkyl-fatty acids that mimic myristate, palmitate, or stearate to enrich for acylated proteins, Hang and coworkers identified proteins from Jurkat T cells that selectively labeled with different chain lengths (15). The mechanism responsible for these differences in acyl-chain length attachment remains unclear.

In the present study we characterize the kinetic mechanism and lipid substrate specificity of DHHC proteins. A high-performance liquid chromatography (HPLC)

fluorescent peptide-based PAT assay is developed to measure rate constants for a representative DHHC. Single turnover experiments directly address the question of whether DHHC autoacylation is a transient acyl-enzyme intermediate in a two-step ping-pong mechanism. One corollary of this predicted reaction scheme is that acyl-chain lengths capable of being transferred to protein substrates should also be capable of autoacylating the DHHC protein. This prediction is tested as well as the mechanism of DHHC lipid substrate specificity.

## **Experimental Procedures**

*Reagents.* The fluorescent peptide myrGCG was synthesized by AnaSpec, Inc (San Jose, CA) and consists of *N*-myristoylated glycine, cysteine protected by a disulfide link tert-butyl group, and glycine linked via ethylenediamine to nitro-benzoxadiazole (NBD). Aliquots dried under N<sub>2</sub> were stored at -80°C. [<sup>3</sup>H]<sup>9,10</sup>-palmitate (47.7 Ci/mmol) was purchased from PerkinElmer Life Science. [<sup>3</sup>H]<sup>9,10</sup>-stearic acid was purchased from Moravek Biochemicals, Brea, CA. The specific activity reported by the manufacturer for [<sup>3</sup>H]-stearic acid (75 Ci/mmol) exceeded the theoretical maximum specific activity of 57.6 Ci/mmol. The theoretical value was used for [<sup>3</sup>H]-stearic acid calculations. [<sup>3</sup>H]palmCoA for Figures 3.2 and 3.3 was synthesized and purified as described (181). For Figure 3.5, [<sup>3</sup>H]palmCoA and [<sup>3</sup>H]-stearoyl-CoA were synthesized as described except that the detergent *n*-dodecyl-β-D-maltoside (DDM) replaced Triton X-100. Radiolabeled acyl-CoA was separated from free fatty acid by chloroform/methanol extraction (28). Acetonitrile was purchased from Honeywell. Internal standard 16-12-

NBD-PC (1-palmitoyl-2-{12-[(7-nitro-2-1,3-benzoxadiazol-4-yl)amino]dodecanoyl}-sn-glycero-3-phosphocholine) and non-radiolabeled C6- and C10-CoAs were from Avanti Polar Lipids. CoA and the other unlabeled acyl-CoAs were from Sigma.

*HPLC-based fluorescent peptide PAT assay.* Peptide was deprotected by overnight incubation in 77% DMSO, 0.15% DDM, and 7.5 mM TCEP, under argon, protected from light at 25°C. Greater than 90% deprotection was achieved as assessed by HPLC before each experiment. Deprotected peptide was diluted with 50 mM MES pH 6.4 to 25% DMSO, 0.05% DDM, and 2.5 mM TCEP. PalmCoA (and later, other acyl-CoAs) and peptide were mixed in glass test tubes and warmed to 25°C. Partially purified DHHC protein warmed to 25°C was added to start the reaction. The final reaction was 50  $\mu$ L at 50 mM MES pH 6.4, 10% DMSO, 1 mM TCEP, and 0.028% DDM. Final concentrations of DHHC, acyl-CoA, and myrGCG are noted in the figure legends. Reactions were stopped with 500  $\mu$ L dichloromethane and held on ice until all reactions were complete. The reactions were spiked with 250  $\mu$ L of 0.02  $\mu$ M 16-12-NBD-PC dissolved in methanol as an internal standard and 250  $\mu$ L aqueous buffer (50 mM MES pH 6.4, 250 mM NaCl) to cause phase separation. This internal standard was chosen because it was tagged with NBD similar to the peptide, does not overlap with other peaks, and elutes in the same solvent as the palmitoylated peptide, minimizing NBD's high solvatochromic shift (182). The lower organic phase was collected and extracted twice more with 500  $\mu$ L dichloromethane. Pooled extracts were clarified with 300  $\mu$ L methanol, dried under N<sub>2</sub>, and stored at -20°C. For directly monitoring transfer of various acyl-CoA chain lengths, a similar assay was used with 10  $\mu$ M acyl-CoAs and 5

$\mu$ M deprotected myrGCG in a final 50  $\mu$ L reaction. Addition of DHHC (10 nM) or buffer was used to start the reaction, which was incubated at 25°C for 10 min. Reactions were stopped with 500  $\mu$ L dichloromethane and processed as described above.

Dried acylated peptides were dissolved in 100  $\mu$ L isopropanol and then, 100  $\mu$ L 0.5 mM TCEP added to reduce disulfide linked peptides. Samples were analyzed using a Beckman Coulter Gold HPLC system (508 autosampler, 126NM solvent module, 166NM detector) inline with a Jasco FP2020 fluorescence detector with buffer A (20% acetonitrile/80% water/0.1% trifluoroacetic acid) and buffer B (100% acetonitrile). For each reaction, an aliquot of 50  $\mu$ L was injected onto a reversed phase Vydac C4 (5  $\mu$ m, 300 Å, 4.6 x 250 mm) column equilibrated in 35% buffer B at 1 mL/min. After 1 min, a linear gradient over 5 min increased the mobile phase to 82.5% B, and it was held there for 10 min. The mobile phase was then returned to 35% B over 1.5 min and allowed to equilibrate for 3.5 min (Figure 3.1A, dashed line). UV absorbance was recorded at 254 nm and fluorescence excited at 465 nm and emission recorded at 531 nm with the gain set at 10-100x. This HPLC method was adapted from work by others (183). Version 8, 32 Karat software was used to record data and determine area under the curve for peptide and internal standard peaks. Areas were converted to pmol acylated myrGCG, fit to the Michaelis-Menten equation using nonlinear regression, and plotted with Prism 5 (GraphPad Software, Inc.).

*Constructs, expression, and protein purification.* Plasmids for murine myrLck<sub>NT</sub> and human DHHC2 were described previously (181). Mouse DHHC3 was amplified from the cDNA (Image Clone 3669723, NM\_026917.4) and subcloned into pBlueBac4.5

(Invitrogen; Carlsbad, CA) to encode a protein with a FLAG-His<sub>6</sub> sequence (GSELRVQAYVDYKDDDDKNSAEFH~~HHHHH~~(stop)) appended to the C-terminus of DHHC3. Called pML1117, this plasmid was used to generate catalytically inactive DHHC3-FLAG-His<sub>6</sub> (pML1354) by site-directed mutagenesis (Stratagene) of Cys157. Recombinant baculoviruses were generated as previously described (181). DHHC-2 and -3 WT and DHHC mutants were expressed in Sf9 cells and purified by Ni-NTA metal chelate chromatography as previously described except that TriEx™ Sf9 cells and media (EMD Chemicals) were used for cell culture. For peptide studies, direct transfer, and acyl-CoA competitions, Ni-NTA elutions were used, whereas for enzyme autoacylation studies (Figure 3.5) pooled FLAG affinity-resin elutions were used. *N*-myristoylated G-protein  $\alpha$ 1 (myrG <sub>$\alpha$ 1</sub>) and myrLck<sub>NT</sub> were co-expressed in *E. coli* with *N*-myristoyltransferase and purified as C-terminal His<sub>6</sub>-tagged proteins using established protocols (181, 184).

*Direct Transfer from DHHC to protein substrate.* For single turnover experiments (Figure 3.2), 350 pmol DHHC protein was incubated with 40  $\mu$ L FLAG affinity resin equilibrated in buffer C (50 mM Tris pH 7.4, 100 mM NaCl, 0.06% DDM, 5% glycerol, and 1 mM EDTA) at 4°C with end-over-end rotation for 60 min. Bound DHHC was washed three times with 500  $\mu$ L buffer C and twice with 650  $\mu$ L buffer D (50 mM MES pH 6.4, 20 mM NaCl, 0.06% DDM, 5% glycerol, and 1 mM EDTA). Bound DHHC was autoacylated by incubation with buffer D containing [<sup>3</sup>H]palmCoA (1400 pmol) for 7 min on ice. Free [<sup>3</sup>H]palmCoA was removed by washing with 850  $\mu$ L buffer D eleven times until the radioactive acyl-CoA content of the washes was <5nM.

Radiolabeled DHHC was eluted eight times with 50 mL buffer D containing 0.3  $\mu\text{g}/\mu\text{L}$  3X FLAG peptide (Sigma). Elutions 2-8 were pooled and the time course initiated by the addition of 1  $\mu\text{M}$  unlabeled palmCoA and either protein substrate or buffer at 25°C. Aliquots were removed at the indicated times and stopped with 5 $\times$  sample buffer with 2 mM tris(2-carboxyethyl)phosphine (TCEP) final. Reactions were divided between two SDS-PAGE gels with one set being processed for fluorography and the other for scintillation counting using established methods (181). For single turnover experiments with stearate (Figure 3.5C and D), an identical procedure was followed except [ $^3\text{H}$ ]-stearoyl-CoA was used.

*Acyl-CoA specificity of autoacylation and transfer.* For competition PAT assays, [ $^3\text{H}$ ]palmCoA and unlabeled acyl-CoA were pre-mixed on ice. Likewise, DHHC and protein substrate were pre-mixed before adding to the lipid substrate mixture and incubating 6 min at 25°C. Final assay concentrations were 20 nM DHHC, 1  $\mu\text{M}$  [ $^3\text{H}$ ]palmCoA, 10  $\mu\text{M}$  competing acyl-CoA, and either 1  $\mu\text{M}$  myrG<sub>oil</sub> or 0.5  $\mu\text{M}$  myrLck<sub>NT</sub> in a total of 25  $\mu\text{L}$ . Assays were stopped with 5 $\times$  sample buffer with 2 mM TCEP final and processed for scintillation counting.

Hydrolysis of acyl-CoAs (Table 3.2) was determined by incubating DHHC-2, -3 (45 nM), or buffer with either [ $^3\text{H}$ ]palmCoA or [ $^3\text{H}$ ]-stearoyl-CoA at 25°C and stopping with SDS. An aliquot of the reaction, equivalent to 5 pmol of the initial acyl-CoA in the reaction, was spotted on thin layer chromatography plates (LK6DF silica gel, Whatman) and resolved with 50% n-butanol/ 20% acetic acid/ 30% water for 5 hrs. The plate was dried, sprayed twice with EN3HANCE™ autoradiography enhancer spray (PerkinElmer),

and exposed to film at  $-70^{\circ}\text{C}$  for 42 hrs. The regions of the TLC plate containing free fatty acids were located by comparison with the film, scraped, and quantitated with scintillation counting. Background free fatty acid was determined from a control reaction lacking DHHC and subtracted before fitting the data by linear regression. To the remaining reaction,  $5\times$  sample buffer was added and an aliquot representing 1 pmol of DHHC protein was resolved on SDS-PAGE gels and processed for scintillation counting to monitor enzyme autoacylation. Analyzing a reaction without DHHC was set as the zero time point allowing the data to be fit to a single phase exponential by nonlinear regression.

## Results

*Determination of DHHC3 kinetic constants with fluorescent peptide, HPLC-based PAT assay.* To characterize DHHC proteins mechanistically, we determined steady state kinetic parameters with a modified high performance liquid chromatographic (HPLC) method initially described for the characterization of PAT activity in cell lysates (183). The advantages of the HPLC-based peptide assay were ease of achieving saturating substrate concentrations and elimination of the need for radioactive acyl-CoA compounds. For a palmitoylation site mimic, the three-residue peptide glycine-cysteine-glycine was synthesized with the N-terminus myristoylated and the C-terminus linked to the fluorescent group NBD (myrGCG; Figure 3.1A inset). A previous study showed that myrGCG is taken up by cells and efficiently palmitoylated in a manner that is time-

dependent and saturable (185), suggesting it is a good substrate for in vitro palmitoylation assays.

DHHC2, DHHC3, and DHHC9/GCP16 were individually tested for their ability to palmitoylate myrGCG. DHHC2 and DHHC3 showed similar levels of palmitate incorporation, approximately 2.5 times that of DHHC9/GCP16 (unpublished results). In vivo evidence suggests DHHC3 has broad protein substrate specificity (86), and it expresses well in insect cells infected with recombinant baculovirus. Therefore, it was chosen for further kinetic analysis. To determine the linear range of the reaction, a time course was performed. DHHC3, palmCoA, and myrGCG were incubated for various times, spiked with an internal standard, and separated on a C4 reversed phase HPLC column monitored with a fluorescence detector. A representative chromatogram is shown in Figure 3.1A. In addition to peaks of unreacted and palmitoylated peptide, a peak corresponding to a disulfide-linked myrGCG dimer appears, which results from the drying of unprotected myrGCG in the absence of reducing agent. The area of the palmitoylated peptide peak was compared to that of the internal standard and converted to pmol of palmitoylated peptide. At low concentrations of both substrates, the reaction was linear for at least the first 6 minutes (Figure 3.1B), however the standard assay was limited to 4 minutes before depletion of either substrate occurred. To determine  $K_m$  and  $V_{max}$  values, one substrate concentration was held at a constant saturating concentration while the other varied. Saturation with palmCoA and analysis with non-linear regression revealed a  $V_{max}$  of 10.0 pmol/min/pmol of DHHC3 and a  $K_m$  of 1.5  $\mu$ M myrGCG (Figure 3.1C, Table 3.1). At saturating myrGCG, a  $V_{max}$  of 10.7 pmol/min/pmol and a  $K_m$  of 1.2

$\mu\text{M}$  palmCoA were observed (Figure 3.1D). For both peptide and palmCoA titration curves,  $V_{max}$  values were approximately the same (Table 3.1) as expected under saturating conditions. Both substrate concentrations were varied around their  $K_m$  values to generate data for a double reciprocal, Lineweaver-Burke analysis. Unfortunately, these data were not adequate to distinguish a ternary complex from a ping-pong mechanism (186).

*Direct measurement of acyl-transfer from acyl-DHHC to protein substrate.* All DHHC proteins tested to date autoacylate, a process hypothesized to result from DHHC proteins using a ping-pong catalytic mechanism for substrate acylation. We directly tested whether DHHC enzyme autoacylation is a transfer intermediate. Because DHHC3 was identified as a PAT for G-protein  $\alpha$ -subunits (187), we first confirmed that DHHC3, but not the catalytically inactive mutant DHHS3 (DHHC3 C157S), could palmitoylate *N*-myristoylated  $G_{\alpha i1}$  (myr $G_{\alpha i1}$ ) above background levels. Also as expected, DHHC3, but not DHHS3, became autoacylated during the assay (Figure 3.2A).

Using this enzyme/substrate pair, we tracked the transfer of [ $^3\text{H}$ ]palmitate from [ $^3\text{H}$ ]palm-DHHC3 to myr $G_{\alpha i1}$ . Palmitoyl-DHHC3 was generated by binding partially purified DHHC3 to FLAG affinity resin and incubating with [ $^3\text{H}$ ]palmCoA to autoacylate. Unreacted [ $^3\text{H}$ ]palmCoA was washed out and [ $^3\text{H}$ ]palm-DHHC3 was eluted with FLAG peptide. Immunoblotting and fluorography indicated that elutions 2 through 7 contained [ $^3\text{H}$ ]palm-DHHC3 (Figure 3.2B). The absence of thiol-based reducing agents from the buffers was critical for purification of the acylated enzyme. Elutions were pooled and incubated with non-radiolabeled palmCoA and either myr $G_{\alpha i1}$  or buffer. Aliquots removed at various times were stopped, separated by SDS-PAGE, and analyzed

by both fluorography and scintillation counting. Figures 3.2C and 3.2D show that at early times most of the [<sup>3</sup>H]palmitate was attached to the DHHC3 but over time was lost from the enzyme and accumulated on myrG<sub>ci1</sub>. The rate of transfer of [<sup>3</sup>H]palmitate from DHHC3 inversely paralleled the rate of gain of [<sup>3</sup>H]palmitate on myrG<sub>ci1</sub> (Figure 3.2D). A comparable experiment was performed with DHHC2 and its substrate myrLck<sub>NT</sub> (181), and a similar pattern was observed both by fluorography (not shown) and scintillation counting (Figure 3.2E). A slower loss of [<sup>3</sup>H]palmitate from both DHHC proteins was observed when incubated without a protein substrate; this is likely due to hydrolysis of the thioester-attached lipid. Inclusion of an excess of non-radiolabeled palmCoA (1 μM) in the reaction was intended to compete with any residual [<sup>3</sup>H]palmCoA not removed during purification and to drive the reaction to completion. However, radiolabeled palmitate remained associated with DHHC2 and DHHC3 even at extended time courses up to 45 minutes. Spiking the reaction with additional protein substrate after 10 minutes did not cause the reaction to proceed further (data not shown).

*DHHC enzyme autoacylation acyl-CoA chain-length specificity parallels substrate acylation specificity.* If enzyme autoacylation is a transfer intermediate, then the protein substrate should only acylate with acyl-CoAs that also can acylate the DHHC protein. To test this prediction a competition assay was set up in which a ten-fold excess of non-radiolabeled acyl-CoAs of different chain lengths and saturations were used to compete with [<sup>3</sup>H]palmCoA (C16:0) for acylation of enzyme and substrate. For both DHHC2 and DHHC3, the level of enzyme autoacylation paralleled that of substrate acylation for each competing acyl-CoA tested (Figure 3.3A and B). Together with Figure

3.2 and work by others (175), these data strongly suggest that DHHC autoacylation represents a transient transfer intermediate and DHHC proteins use a two-step ping-pong mechanism for catalysis.

*DHHC2 and DHHC3 display different acyl-CoA specificities.* In Figure 3.3, a difference in lipid substrate profiles for DHHC2 and DHHC3 was observed. For DHHC2, acyl-CoAs of 14 carbons and longer inhibited [<sup>3</sup>H]palmCoA labeling of both substrate and enzyme. However, with DHHC3 only myristoyl-, palmitoyl-, and palmitoleoyl-CoA were effective and longer acyl-CoAs competed less well. The competition assays in Figure 3.3 suggested that DHHC2 transfers fatty acids longer than 16 carbons. However, the reduction in the [<sup>3</sup>H]palmitate labeling could be caused by these longer acyl-CoAs acting through a distinct mechanism, for example, by acting as inhibitors. The difference in acyl-CoA specificities between the DHHCs could also result from the different protein substrates used. To address both of these issues, DHHC-2 and -3 were tested in the HPLC-based PAT assay to directly monitor their ability to transfer various fatty acids to the same substrate, myrGCG. DHHC2 transferred fatty acids from all acyl-CoAs chain lengths tested (Figure 3.4) consistent with it having a broad specificity for long chain acyl-CoAs as seen in the competition assay (Figure 3.3B). In contrast, DHHC3 displayed a narrower lipid substrate profile, transferring only myristate (C14) and palmitate (C16) at significant levels. Thus, the difference in acyl-CoA specificity between DHHC2 and DHHC3 was independent of the protein or peptide substrate used.

## Discussion

In this study we examined the mechanism DHHC proteins use to catalyze acyl-transfer and their acyl-CoA specificity. An HPLC, peptide-based PAT assay enabled us to determine kinetic constants for each substrate. Single turnover assays confirmed the hypothesis that DHHC autoacylation represents the transient acyl-enzyme transfer intermediate of a two-step ping-pong mechanism. Acyl-CoA competition assays provided further evidence for this mechanism and revealed an unexpected difference in acyl-CoA preferences between DHHC2 and DHHC3. This difference was shown to result from DHHC3's reduced ability to autoacylate with and transfer acyl-chains longer than 16-carbon palmitate.

*Kinetic mechanism of DHHC-mediated protein acylation.* Others and we had previously hypothesized that DHHC proteins use a two-step mechanism based on their ability to autoacylate. Ungermann and coworkers used a “two-step reaction mechanism” to describe the activity of the yeast DHHC protein Pfa3p (188). However, their two steps referred to the binding of protein substrate by the DHHC and a second event encompassing the entire catalytic reaction. More recently, Mitchell *et al.* proposed a two-step reaction mechanism in the classical kinetic sense to differentiate steps within the catalytic reaction (175). Using TLC to monitor free palmitate production, they showed that Erf2p has palmCoA hydrolase activity that occurs with a rapid autoacylation step and a slower second step involving the transfer of palmitate to water. Addition of Ras2p, a palmitoylation substrate, increased Erf2p consumption of palmCoA but slowed production of free palmitate, suggesting the palmitate was now being transferred to

Ras2p in the second reaction step. Using single turnover assays, we isolated acylated-DHHC protein and confirmed that it can transfer its attached lipid group to a protein substrate. This confirmed DHHC autoacylation represents a transient transfer intermediate and thus supports the hypothesis that DHHC proteins use a two-step transfer mechanism.

To further characterize the mechanism of DHHC-mediated acylation, kinetic constants were determined for each substrate using an HPLC, peptide-based PAT assay. These constants were determined by fitting substrate titration data to the Michaelis-Menten equation. Michaelis-Menten assumes that enzyme and substrate(s) are freely diffusible in solution. However, DHHC proteins are integral membrane enzymes and were bound to detergent micelles in our assays. It is unclear whether DHHC proteins acquire their substrates from bulk solution or by horizontal diffusion within a lipid environment. Surface dilution kinetic models account for limited two-dimensional horizontal diffusion and offer an alternative model for fitting the data (189).

In single turnover assays, it is interesting to note that in no case did all the lipid transfer off the DHHC, even at later time points. Additionally at these later times, a similar amount of enzyme remained labeled regardless if the acyl-group was transferred to protein substrate or was hydrolyzed. It is unknown whether this reflects enzyme that is inactive with lipid still attached or whether there are secondary acylation sites that are not transferred and are less susceptible to hydrolysis. The stoichiometry of DHHC3 autoacylation was 0.5 palmitate per DHHC (Figure 3.5A), similar to a value of 0.65 reported for the yeast DHHC protein Erf2p (175). These data suggest that the

stoichiometry of autoacylation in vitro is one acyl chain per DHHC. The autoacylation site is predicted to be the conserved cysteine of the DHHC motif. Mutation of this canonical DHHC cysteine blocks autoacylation and transfer, but there is no direct evidence that this is the acylated cysteine. Proteomic analysis of DHHC proteins isolated from cells has revealed that a three-cysteine motif (CCX<sub>7-13</sub>C(S/T) in the cytoplasmic C-terminal domain of DHHC5, 6, and 8 is palmitoylated (20). This motif is not conserved among DHHC proteins, and it seems unlikely that palmitoylation of this domain represents the acyltransfer intermediate. However, it has been proposed that that intramolecular transfer of the acyl group from the catalytic cysteine to the distal palmitoylated cysteines could occur (20). Mapping of the sites of in vitro autoacylation is necessary to resolve this issue.

It is likely that the two-step transfer mechanism described here and elsewhere is common to all DHHC proteins. For DHHC2 and DHHC3, and for the yeast Ras PAT Erf2/Erf4 (175), the first step of autoacylation was rapid, suggesting that within cells, DHHC proteins in the presence of acyl-CoAs may persist in the acylated state poised for transfer. Regulation of protein acylation may depend on controlling the association between DHHC proteins and their substrates. Indeed, following activity blockade in neurons, DHHC2 was shown to translocate to postsynaptic densities, colocalize with one of its substrates, post-synaptic scaffolding protein PSD-95, and increase PSD-95 acylation (93). Alternatively, the acylation machinery may be constitutively active and deacylation is a regulated step. To date, no mechanism of post-translational modification has been described for the regulation of DHHC proteins or deacylating enzymes. While

we are beginning to develop a mechanistic understanding of DHHC proteins, more work is needed to understand their structure and regulation.

*Fatty Acyl-CoA Substrate Specificity.* Investigating the kinetic mechanism of DHHC proteins lead us to determine their acyl-CoA chain-length specificity. Surprisingly, a difference in acyl-CoA specificity was observed between DHHC3 and DHHC2. In the competition assay shown in Figure 3.3, the reduction of [<sup>3</sup>H]-palmitate incorporation into substrate by non-radiolabeled acyl-CoAs was presumed to be because unlabeled acyl-groups were transferred onto the substrate. Indeed, this was likely the case for DHHC2 and all acyl-CoAs tested in Figure 3.4 as they could be transferred. However, with DHHC3 and C18- or C20:4-CoA and to a lesser degree with C18:1, very little acyl-group was transferred to the peptide (Figure 3.4), yet all three caused about 70% reduction of [<sup>3</sup>H]-palmitate incorporation in the competition assay. Thus, it is likely acyl-CoAs longer than 16 carbons were interacting with DHHC3 in such a way as to slow acylation with palmitate. This was confirmed for DHHC3, in which the extent of autoacylation and the rate of transfer of stearate was slower than with palmCoA. The differential sensitivity of DHHC PAT activity to different acyl-CoAs suggests a possible mode of regulation in cells where changes in the availability of different species of acyl-CoA would impact which DHHC proteins were active and accordingly, which proteins are modified.

Hydrocarbon rulers for filtering different lipid lengths have been characterized for other enzymes. Protein *N*-myristoyltransferase (NMT) shows exquisite specificity for 14 carbon acyl-CoAs. Crystal structures of NMT bound to substrate analogs reveal that

specificity is achieved by measuring the fatty acid between an oxyanion hole binding the carbonyl and the floor of the hydrophobic pocket. Furthermore, a hydrophobic groove induces bends in myristate that further restrict acyl-chain saturation and branching (69). Fen1p and Sur4p subunits of the very-long chain fatty acid (VLCFA) synthase complex also display acyl-chain length specificity and, similar to DHHC proteins, are polytopic integral membrane enzymes (190). The sizing mechanism results from the distance between a cytoplasmic active site and a lysine residue extending from a transmembrane helix within the lipid bilayer. By shifting the lysine up and down turns of the helix, acyl-chain specificity was altered. While DHHC3 does not contain lysine residues within its predicted TMDs, it does contain charged residues that may behave similarly in restricting acyl-chain length. The structural basis for DHHC lipid substrate specificity provides a new area for investigation.

Inhibitors of DHHC proteins will be important tools for studying DHHC biology within cells, as well as having potential as therapeutic agents. An increasing number of DHHC proteins have been linked to different human diseases (86). We and others have attempted to find and characterize DHHC inhibitors with limited success (181). To date, 2-bromopalmitate (2-BP) remains the best DHHC inhibitor available, even though it lacks specificity among DHHC proteins as well as other cellular enzymes. Given the two-step mechanism of DHHC catalysis, it might be predicted that inhibitors of the autoacylation step would block acylation by all DHHC proteins. However, data presented here indicate that the autoacylation step displays acyl-CoA specificity. Thus it is likely that inhibitory compounds can be found that are selective for different DHHC

proteins, possibly through acyl-CoA analogs with different fatty acid chains. The success with developing potent and highly selective kinase inhibitors that occupy the ATP binding site encourages efforts to identify small molecules that target DHHC autoacylation.

### **Acknowledgements**

This work was supported by National Institutes of Health Grant GM51466. BCJ was supported by an American Heart Association pre-doctoral fellowship (Midwest Affiliate). We thank Wendy Greentree for technical support and Robert Deschenes for helpful discussions and comments on the manuscript.

**Table 3.1. Kinetic parameters for DHHC3 analyzed with fluorescent peptide, HPLC-based PAT assay**

	<b>K<sub>m</sub></b> ( $\mu\text{M}$ )	<b>V<sub>max</sub></b> (pmol/min/pmol)
MyrGCG titration at 10 $\mu\text{M}$ palmitoyl-CoA (n = 4)	1.5 $\pm$ 0.3	10.0 $\pm$ 1.2
Palmitoyl-CoA titration at 10 $\mu\text{M}$ myrGCG (n = 3)	1.2 $\pm$ 0.2	10.7 $\pm$ 1.7

**Table 3.2. Hydrolysis rates of different acyl-CoAs with DHHC3 and DHHC2**

	<b>C16:0 palmitoyl-CoA</b> (pmol/min/pmol)	<b>C18:0 Stearoyl-CoA</b> (pmol/min/pmol)
DHHC3 (n = 2)	0.027	0.008
DHHC2 (n = 2)	0.030	0.038

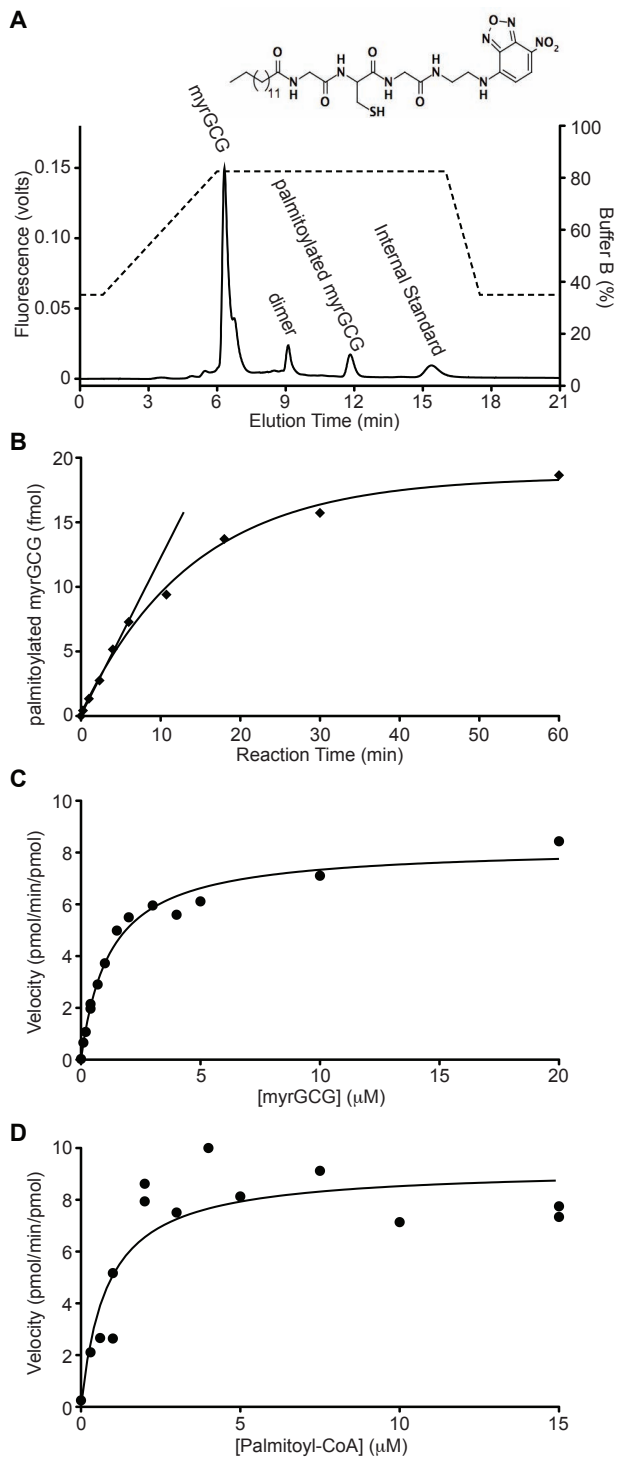


**Figure 3.1. Fluorescent peptide, HPLC-based kinetic characterization of DHHC3.**

*A*, Structure of the tripeptide substrate N-myristoylated Gly-Cys-Gly tagged via ethylenediamine with fluorescent NBD (myrGCG, inset). The elution profile of myrGCG following reversed-phase chromatography. After in vitro reaction with acyl-CoA and DHHC3, myrGCG was spiked with internal standard (16-12-NBD-PC), extracted, dried, and chromatographed using the gradients (dashed line) shown with Buffer A (20 % ACN/80% water/0.1% TFA) and Buffer B (100% ACN). Identity of peaks is indicated. *B*, Time course for the enzymatic palmitoylation of myrGCG (0.5  $\mu$ M) with palmCoA (0.5  $\mu$ M). Nonlinear regression fit the overall reaction to a single phase exponential, whereas values for 0 to 6 min were fit to a straight line ( $R^2 = 0.99$ ). *C*, Michaelis-Menton fit to myrGCG titration with DHHC3 (5 nM) and saturating palmCoA (10  $\mu$ M) reacting for 4 min. *D*, Michaelis-Menton fit to palmCoA titration with DHHC (5 nM) and saturating myrGCG (10  $\mu$ M) reacting for 4 min. A representative of three independent experiments is shown for each.

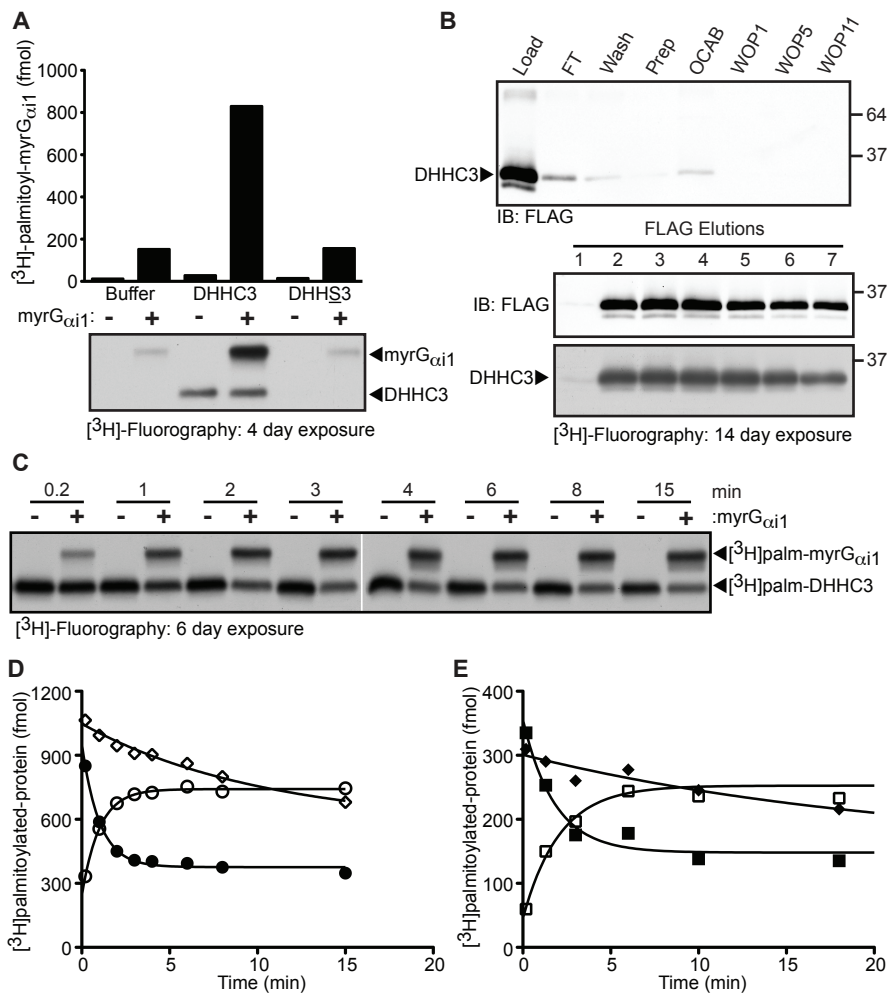


**Figure 3.2. Autoacylated DHHC proteins transfer their acyl chain to protein substrate.** *A*, DHHC3 palmitoylates *N*-myristoylated G $\alpha$ i1 (myrG $\alpha$ i1). DHHC3-FLAG-His<sub>6</sub> (20 nM), the catalytically inactive mutant DHHC3 C157S (DHHS3, 20 nM), or buffer were incubated with myrG $\alpha$ i1 (1  $\mu$ M) and [<sup>3</sup>H]palmCoA (1  $\mu$ M) for 6 min at 25°C. The reaction was stopped and [<sup>3</sup>H]palmitate incorporation was detected by fluorography (lower panel) or quantitated by scintillation spectrometry as described in Experimental Procedures. *B*, Partially purified DHHC3 (350 pmol, LOAD) was immobilized on FLAG affinity resin and the flow through (FT) collected. The column was washed (Wash) and prepped (Prep) for incubation with on-column acylation buffer (OCAB) containing [<sup>3</sup>H]palmCoA for 7 min on ice. Unbound [<sup>3</sup>H]palmCoA was washed out (WOP) with eleven column volumes. Radiolabeled DHHC3 was eluted and analyzed for DHHC3 by immunoblotting and [<sup>3</sup>H]palmitate incorporation. *C*, [<sup>3</sup>H]palm-DHHC3 was incubated either alone or with myrG $\alpha$ i1 in the presence of unlabeled palmCoA to monitor a single transfer event. After incubation at 25°C for the indicated times, reactions were stopped and analyzed as in *A* by film (*C*) or scintillation counting (*D*). *D*, Incubation of [<sup>3</sup>H]palm-DHHC3 (●) with myrG $\alpha$ i1 (○) or alone (◇) as in *C* were processed for scintillation counting. Data were fit to single phase exponential using nonlinear regression. *E*, Similar to *D*, [<sup>3</sup>H]palm-DHHC2 (■) was incubated with myrLck<sub>NT</sub> (□) or alone (◆). Exposures were at -70°C. Data are representative of one of three independent experiments.

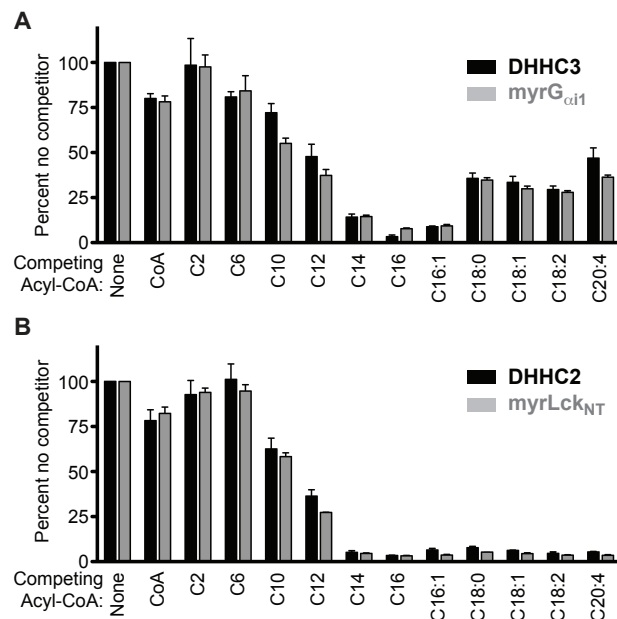


**Figure 3.3. Acyl-CoA chain-length specificity of DHHC enzyme autoacylation parallels substrate specificity.** *A*, Non-radiolabeled acyl-CoAs of the indicated chain length and saturation (10  $\mu$ M), coenzyme A (CoA), or buffer were added to reactions containing [ $^3$ H]palmCoA (1  $\mu$ M), DHHC3 (20 nM) and myrG $\alpha$ i1 (1  $\mu$ M). Reactions were incubated at 25°C for 6 min and processed for quantitation by scintillation spectroscopy. [ $^3$ H]-palmitate incorporation in the presence of each competitor was normalized to the average of two reactions lacking competitor. For DHHC3 without competitor, the average 100% values were 112, 114, and 65 fmol whereas for myrG $\alpha$ i1 they were 646, 630, and 585 fmol. Mean and standard error of the mean are shown for three independent experiments. *B*, Similar to *A*, except with DHHC2 (20 nM) and myrLck $\text{NT}$  (0.5  $\mu$ M). For DHHC2 without competitor, the average 100% values were 56, 46, and 30 fmol, whereas for myrLck $\text{NT}$  they were 1035, 914, and 886 fmol.

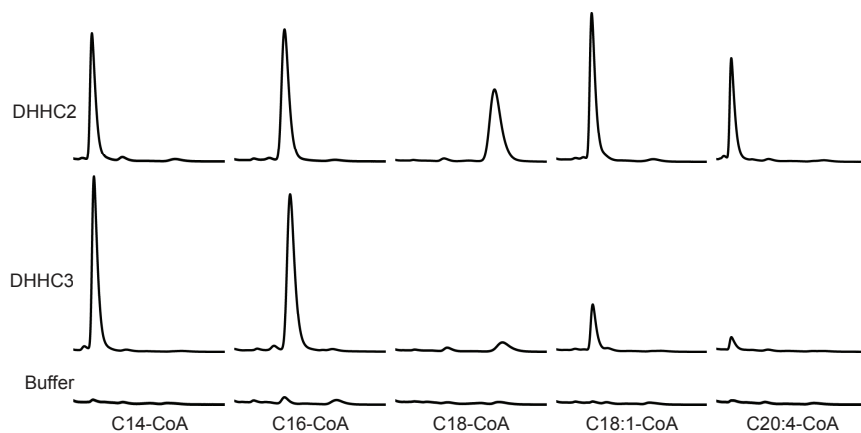


**Figure 3.4. DHHC2 displays broader lipid substrate specificity than DHHC3.** DHHC2, DHHC3 (10 nM), or enzyme buffer were incubated with myrGCG (5  $\mu$ M) and acyl-CoAs (10  $\mu$ M) of the indicated chain length for 10 min at 25°C. Reactions were stopped, extracted, and processed on an HPLC C4 column. For each reaction, the fluorescence chromatogram of myrGCG elution is shown between 9.5 and 15 min.

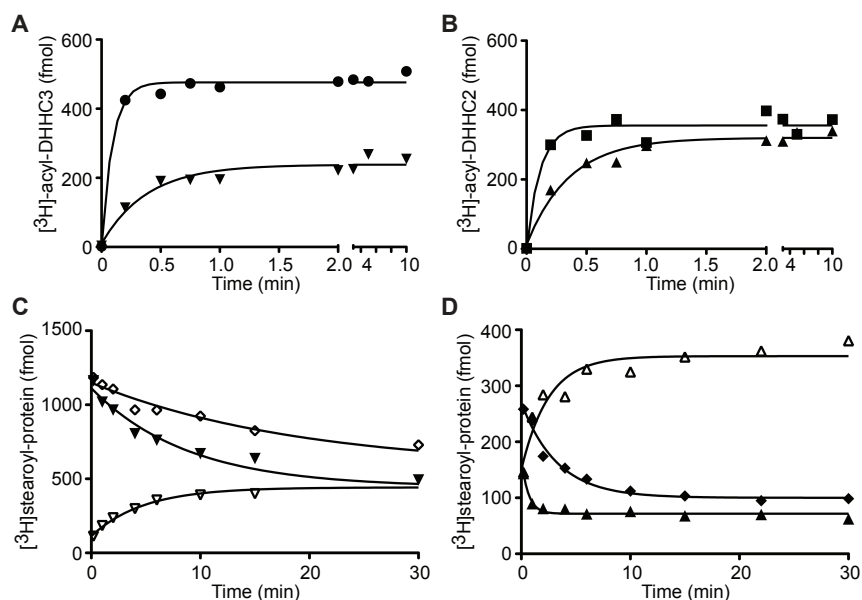


**Figure 3.5. Hydrolysis, enzyme autoacylation, and direct transfer of DHHC2 and DHHC3 with C18 stearate and C16 palmitate.** *A and B*, Enzyme autoacylation for DHHC3 (*A*) or DHHC2 (*B*) was determined by adding sample buffer to aliquots of the reactions described in Table 3.1 representing 1 pmol of DHHC and resolving it by SDS-PAGE. The DHHC band was excised and processed for scintillation counting. Analyzing a reaction lacking any DHHC was set as the zero time point allowing the data to be fit to a one phase exponential by nonlinear regression. Symbols are: ● DHHC3 with C16-CoA, ▼ DHHC3 with C18-CoA, ■ DHHC2 with C16-CoA, and ▲ DHHC2 with C18-CoA. *C and D*, Single turnover assays with [<sup>3</sup>H]stearoyl-DHHC. *C*, Incubation of [<sup>3</sup>H]stearoyl-DHHC3 (▼) with myrGai1 (▽) or [<sup>3</sup>H]stearoyl-DHHC3 alone (◇) for the indicated times and processed for scintillation counting. *D*, Similar to *C*, incubating [<sup>3</sup>H]stearoyl-DHHC2 (▲) with myrLck<sub>NT</sub> (△) or [<sup>3</sup>H]stearoyl-DHHC2 alone (◆) for the indicated times. Data were fit to a single exponential.

## Chapter 4

### **2-Bromopalmitate and 2-(2-Hydroxy-5-nitro-benzylidene)- benzo[*b*]thiophen-3-one Inhibit DHHC-Mediated Palmitoylation In Vitro**

This chapter was published in Jennings, B. C., Nadolski, M. J., Ling, Y., Baker, M. B., Harrison, M. L., Deschenes, R. J., and Linder, M. E. 2009. *Journal of Lipid Research*. **50**:233-242. Marissa Nadolski and Yiping Ling provided purified yeast proteins. Meredith Baker and Marietta Harrison provided plasmids to express wildtype and mutant Lck<sub>NT</sub>. I generated and purified the other constructs and conducted all of the experiments.

## Abstract

Pharmacologic approaches to studying palmitoylation are limited by the lack of specific inhibitors. Recently, screens have revealed five chemical classes of small molecules that inhibit cellular processes associated with palmitoylation (Ducker et al. (2006) *Mol Cancer Ther* 5:1647-1659). Compounds that selectively inhibited palmitoylation of *N*-myristoylated vs. farnesylated peptides were identified in assays of palmitoyltransferase activity using cell membranes. Palmitoylation is catalyzed by a family of enzymes that share a conserved DHHC cysteine-rich domain. In this study, we evaluated the ability of these inhibitors to reduce DHHC-mediated palmitoylation using purified enzymes and protein substrates. Human DHHC2 and yeast Pfa3 were assayed with their respective *N*-myristoylated substrates, Lck and Vac8. Human DHHC9/GCP16 and yeast Erf2/Erf4 were tested using farnesylated Ras proteins. Surprisingly, all four enzymes showed a similar profile of inhibition. Only one of the novel compounds, 2-(2-hydroxy-5-nitro-benzylidene)-benzo[*b*]thiophen-3-one (Compound V), and 2-bromopalmitate (2BP) inhibited the palmitoyltransferase activity of all DHHC proteins tested. Hence, the reported potency and selectivity of these compounds were not recapitulated with purified enzymes and their cognate lipidated substrates. Further characterization revealed both compounds blocked DHHC enzyme autoacylation and displayed slow, time-dependent inhibition but differed with respect to reversibility. Inhibition of palmitoyltransferase activity by Compound V was reversible, whereas 2BP inhibition was irreversible.

## Introduction

Protein palmitoylation is the post-translational attachment of palmitate or other long-chain fatty acids to cysteine residues in proteins via a thioester linkage (reviewed in (6, 191). The functional consequences of protein palmitoylation are diverse and include effects on protein localization, trafficking, and stability. In contrast to other lipid modifications, palmitoylation is reversible. Consequently several cellular processes use palmitoylation-depalmitoylation cycles to affect the localization and function of key proteins.

Protein acyltransferases (PATs) catalyze the addition of palmitate (83). Genetic and biochemical studies in yeast uncovered a family of integral membrane enzymes that mediate palmitate addition to proteins that are modified on the cytoplasmic face of cell membranes. The hallmark of this family of proteins is the DHHC (Asp-His-His-Cys) cysteine-rich domain. A family of seven DHHC proteins is present in *S. cerevisiae* and homology searches have identified at least 23 genes that encode DHHC proteins in mammals. PAT activity is dependent upon the DHHC domain and mutation of the cysteine of the DHHC motif abolishes catalytic activity of the enzyme.

Palmitoylated proteins are prominent in cell signaling pathways and are particularly abundant in the nervous system (192). Signal transducers, receptors, ion channels, and scaffolds are among the targets of palmitoyltransferases. Finding the enzymes responsible for palmitoylation has accelerated our understanding of the role of palmitoylation in both native and disease states. An example is HIP14 (DHHC17), a DHHC protein initially identified as huntingtin-interacting protein 14 (193). HIP14 has

been linked to palmitoylation of huntingtin, SNAP-25, cysteine string protein, and other neuronal substrates (121). Palmitoylation of htt by HIP14 influences htt localization and protects it from aggregation (111). In flies, HIP14 is essential for presynaptic function and plays a role in neurotransmitter release, likely through palmitoylation of SNAP-25 and cysteine string protein (194, 195).

Oncogenic Ras proteins are associated with numerous human tumors.

Palmitoylation of H- and N-Ras plays a key role in trafficking between the plasma membrane and Golgi apparatus (83), as well as facilitating the oncogenic potential of activating Ras mutations (196). Several DHHC proteins have been linked to cancer. Human HIP14 is oncogenic, promoting colony formation in soft agar and tumor formation in nude mice (122). HIP14 mRNA is upregulated in numerous tumors (152). DHHC9, a PAT for H- and N-Ras in vitro, is upregulated in microsatellite stable tumors (140), whereas DHHC2 is a putative tumor suppressor (92).

The importance of palmitoylation in physiology and pathophysiology suggest that palmitoylation inhibitors could be beneficial for the treatment of diseases, as well as tools for probing the role of palmitoylation in cellular processes. Inhibitors of palmitoylation have been limited to 2-bromopalmitate (2BP), cerulenin, and tunicamycin. The most commonly used, 2BP inhibits palmitoylation in cells (197) and PAT activity of DHHC proteins in vitro (123). However, 2BP also inhibits fatty acid CoA ligase (198) and other enzymes involved in lipid metabolism (199). Similarly, cerulenin and tunicamycin inhibit palmitoylation within cells but also inhibit other cellular process including fatty

acid synthesis (200) and *N*-glycosylation (165, 167), respectively. Consequently, there is a need to identify specific inhibitors of palmitoylation.

Smith and coworkers have developed high throughput screens for palmitoylation inhibitors (152). The screens yielded compounds that fell into five chemical classes and a representative compound from each class was further characterized. Cell membranes from MCF-7 cells were used as a source of PAT activity to evaluate the representative compounds' ability to inhibit palmitoylation in vitro. Fluorescently labeled peptides mimicking either *N*-myristoylated, palmitoylated proteins, such as G $\alpha$  subunits and Src-related tyrosine kinases, or mimicking C-terminally farnesylated, palmitoylated proteins, like N- and H-Ras, were used as substrates. Four of the representative compounds showed a preference for inhibiting palmitoylation of the Ras-like peptide (average of 76% inhibition) but not the myristoylated peptide (15% inhibited). Conversely, the fifth compound displayed the reverse, inhibiting palmitoylation of the myristoylated peptide (74%) but not the Ras-like peptide (17%). Thus, it appears these compounds not only inhibit palmitoylation but also display substrate specificity. Additionally, IC<sub>50</sub> values were reported in low to sub-micromolar range (11.8 to 0.5  $\mu$ M) (152).

We sought to further investigate the properties of these compounds. Because cell membranes were used as a source of PAT activity, it is unclear whether the inhibitors reduced palmitoylation by directly blocking DHHC proteins. Here we tested if these compounds inhibit DHHC-mediated palmitoylation of protein substrates. Additionally, by using DHHC proteins that display different substrate preferences, the ability of these inhibitor compounds to specifically inhibit palmitoylation of farnesylated substrates vs.

*N*-myristoylated substrates was examined. Compounds that inhibited DHHC-mediated palmitoylation were further characterized.

### **Experimental Procedures:**

*Inhibitor Compounds and Reagents.* Inhibitor compounds (Figure 4.1) were purchased from ChemBridge Corporation (San Diego, CA). [<sup>3</sup>H]palmitoyl-CoA was synthesized using [<sup>3</sup>H]palmitate (45 Ci/mmol, PerkinElmer Life Sciences), Coenzyme A (Sigma), and acyl CoA synthase (Sigma) as described (26) with the following modification. Following synthesis, [<sup>3</sup>H]palmitoyl-CoA was separated from palmitate by chloroform/methanol extraction (28) and subsequently purified on a C8 reversed phase cartridge (26).

*Plasmids.* Standard molecular biology techniques were used to manipulate DNA. All plasmid constructs were verified by DNA sequence analysis. DHHC2 was expressed using recombinant baculovirus. DHHC2 was prone to proteolysis and several constructs were made with affinity tags at both ends to generate a virus that would yield intact DHHC2 protein. Oligonucleotide sequences used to generate plasmids are available upon request. Human DHHC2 was amplified from Image Clone 4398300 (GenBank ID BF983682) and subcloned as a *KpnI* fragment into pBlueBacHis2B (Invitrogen; Carlsbad, CA). This yielded pML850, encoding His<sub>6</sub>Express-DHHC2. pML850 was digested with *HindIII* and *SalI* to permit ligation with a double stranded oligonucleotide linker that encodes a *HindIII* site, the FLAG epitope, an *EcoRI* site, a His<sub>6</sub> epitope, a stop codon, and a *SalI* site. This yielded pML892, encoding His<sub>6</sub>Express-DHHC2-FLAG-

His<sub>6</sub>. pML892 was cut with *Bgl*III and *Age*I, purified, and ligated with double stranded oligonucleotides encoding the calmodulin binding peptide (CBP) followed by an *Xba*I site to generate His<sub>6</sub>Express-CBP-DHHC2-FLAG-His<sub>6</sub> (pML943). Catalytically inactive DHHS2 (pML1023) was generated by site directed mutagenesis (Stratagene) of pML943.

Plasmids expressing the N-terminal 226 amino acids of Lck (Lck<sub>NT</sub>) and LckNT(C3,5S) were constructed as follows. The murine Lck cDNA encoding residues 1-226 was amplified as a *Nde*I-*Xho*I fragment and subcloned into the bacterial expression vector pET23a(+) yielding pML1008. This construct was used as template to generate the C3,5S mutant (pML1175) using a mutagenic primer to amplify the 5' end of the coding sequence.

Yeast *N*-myristoyltransferase (yNMT) was expressed using pBB131 (201). The plasmid pML1067 was constructed to express human *NMT1* by excising the yeast *NMT1* gene from pBB131 with *Bgl*III and *Eco*R1 and replacing it with human *NMT1* flanked by pBB131 vector sequences. Human *NMT1* was amplified from pBB218 and overlap extension PCR was used to generate flanking pBB131 vector sequences (202).

*Recombinant baculovirus and insect cell culture.* Sf9 insect cells were purchased from ATCC and grown in suspension culture medium (IPL-41 (Gibco) supplemented with 10% heat inactivated bovine growth serum, yeastolate, Pluronic F68, 50 mg/mL gentamycin, and 250 ng/mL fungizone) at 27°C with rotation at 110 rpm. Recombinant baculoviruses were generated using Invitrogen's Bac-n-Blue™ transfection kit with pML943 and pML1023 and plaque-purified.

*Purification of DHHC proteins.* For DHHC2, Sf9 insect cells were inoculated with baculovirus expressing human DHHC2 N-terminally tagged with His<sub>6</sub>-Express-CBP and C-terminally tagged with FLAG-His<sub>6</sub>. Infected cells were collected by centrifugation and washed with cold PBS 61 hr post infection. Cell pellets were stored at -80°C until purification. All purification steps were performed at 4°C and all buffers contained the protease inhibitors 1 mM PMSF, 1-5 µg/mL pepstatin A, 1.4 µg/mL aprotinin, 1.6 µg/mL leupeptin, and 1.6 µg/mL lima bean trypsin inhibitor. A cell pellet of ~5 mL (from 335 mL Sf9 culture) was quickly thawed at 37°C and suspended in 35 mL cavitation buffer (50 mM Tris pH 7.4, 150 mM NaCl, 10 mM β-ME, 1 mM EDTA). Cells were lysed by nitrogen cavitation (30 min at 700 psi). The lysate was centrifuged at 700g for 10 min to remove nuclei and unbroken cells. The postnuclear supernatant was centrifuged at 100,000g for 30 min to generate P100 and S100 fractions. P100 membranes were suspended in 9 mL extract buffer (50 mM Tris pH 7.4, 200 mM NaCl, 10 mM β-ME, and 10% glycerol) by sequential passage through 14, 18, and 25 gauge needles. Total protein concentration was determined using Bio-Rad's Bradford protein assay (Hercules, CA). Membranes were diluted with extract buffer and 10% *n*-dodecyl-β-D-maltoside detergent (DDM; Dojindo Laboratories, Japan) to give a final protein concentration of 2 mg/mL in 1% DDM. The extract was again passed through a 25G needle and incubated 80 min with end-over-end rotation. The extract was cleared at 100,000g for 30 min, diluted 1:1 with extract buffer (no DDM), and gravity-flowed twice through a column of 3.4 mL Ni<sup>2+</sup>-nitrilotriacetic acid-agarose resin (Ni-NTA; Qiagen) equilibrated in wash buffer (50 mM Tris pH 7.4, 100 mM NaCl, 3 mM β-ME, 10% glycerol, 0.1% DDM, and 20 mM

imidazole). The resin was washed with 60 mL wash buffer and eluted with wash buffer containing 200 mM imidazole ( $2 \times 3$  mL) and wash buffer containing 500 mM imidazole ( $3 \times 3$  mL). Ni elutions 1-4 were pooled, diluted 1:1 with buffer A (50 mM Tris pH 7.4, 100 mM NaCl, 10% glycerol, 0.1% DDM, 1 mM EDTA, and 0.2 mM  $\beta$ -ME), and passed thrice through a column of 300  $\mu$ L ANTI-FLAG® M2-agarose affinity gel (Sigma) equilibrated in buffer A. The resin was washed with 14 mL buffer A and eluted with  $5 \times 250$   $\mu$ L buffer A containing 0.23 mg/mL FLAG peptide (Sigma) with a 10 min incubation for each elution. The concentration of enzyme was determined by extrapolation from a linear curve with known concentrations of bovine serum albumin using Sypro Ruby protein gel stain (Molecular Probes) and quantitation with a Storm<sup>TM</sup> 860 (Amersham Biosciences).

DHHS2 purification paralleled that of DHHC2 through nickel affinity chromatography. The identity of purified DHHC2 or DHHS2 was confirmed by immunoblots using antibodies at the following dilutions: anti-FLAG 1:3000 (Stratagene), anti-Express 1:1500 (Invitrogen), and goat anti-mouse IgG secondary conjugated to HRP at 1:2000 (MP Biomedicals, OH).

For human DHHC9/GCP16, Sf9 cells were co-infected with baculoviruses expressing DHHC9-myc-His<sub>6</sub> and FLAG-GCP16 (114) and cultured for 73 h before harvesting. DHHC9/GCP16 was purified similarly to DHHC2.

The purification of Erf2/Erf4p was performed as previously described (203).

For partially purified yeast Pfa3, YPH499 was transformed with a Pfa3-His<sub>6</sub>-Flag pESC expression construct. Yeast were cultured and cell membranes prepared as

described (91). Pfa3-His<sub>6</sub>-Flag was extracted from cell membranes in 1% Triton X-100 at 5 mg/mL total protein in extraction buffer (50 mM Tris pH 8.0, 100 mM NaCl, 10% glycerol, 5 mM β-ME, and 0.1 mM PMSF) rotating for 1 hr at 4°C. Insoluble material was pelleted at 200,000g for 20 min. The detergent extract (7.5 mg total protein) was diluted 1:1 in extraction buffer and allowed to bind to 2 mL Ni-NTA resin for 1 hr at 4°C. The resin was reconstituted in a column and washed with 20 mL wash buffer (50 mM Tris pH 8.0, 100 mM NaCl, 10% glycerol, 5 mM β-ME, 0.1% Triton X-100, 0.1 mg/mL bovine liver lipids (Avanti Polar Lipids), and 0.1 mM PMSF). Bound proteins were eluted with elution buffer (50 mM Tris pH 8.0, 100 mM NaCl, 10% glycerol, 200 mM imidazole, 1 mM β-ME, 0.1 % Triton X-100, and 0.1 mg/ml bovine liver lipids) and four 2 mL fractions were collected. Fractions one and two were pooled, aliquoted, and stored at -80°C.

*Purification of PAT substrates.* Mouse *N*-myristoylated Lck<sub>NT</sub> (myrLck<sub>NT</sub>) was purified from ER2566 *E.coli* (New England Biolabs) harboring pBB131 (201) and pML1008. Cells were grown in Luria-Bertani broth containing 50 μg/mL kanamycin and 50 μg/mL ampicillin at 37°C with shaking at 250 rpm for 4 hr. IPTG was added to 0.6 mM final concentration and the temperature was reduced to 30°C for 5 hr. Cells were harvested by centrifugation at 3080g for 20 min at 4°C. Cell pellets were washed with cold PBS, collected by centrifugation at 3800g for 17 min at 4°C, flash frozen in liquid N<sub>2</sub>, and stored at -80°C until needed. Purification steps were performed on ice or in a 4°C cold room. Cell pellets representing 400 mL culture were quickly thawed at 30°C, suspended in 11 mL lysis buffer (50 mM Tris pH 7.4, 8 mM β-ME, 150 mM NaCl, 1

$\mu\text{g}/\text{mL}$  pepstatin A,  $1.6 \mu\text{g}/\text{mL}$  leupeptin,  $1.6 \mu\text{g}/\text{mL}$  lima bean trypsin inhibitor, and  $1.4 \mu\text{g}/\text{mL}$  aprotinin), and passed thrice through a French Press cell. The soluble fraction was collected by centrifugation at  $76,500g$  for 30 min. To enrich for myristoylated-Lck<sub>NT</sub>, this soluble fraction was extracted twice with 1.3 mL 10% Triton X-114 detergent (Sigma) essentially as described (204) except incubations were for 5 min at  $37^\circ\text{C}$ . The detergent phases were pooled, diluted to 0.2% Triton X-114 (135 mL total), and gravity loaded onto a 3 mL Ni-NTA column equilibrated in wash buffer (50 mM Tris pH 8.0, 300 mM NaCl, 10 mM imidazole, and 8 mM  $\beta$ -ME). The column was washed with 150 mL wash buffer and eluted  $5 \times 3$  mL with elution buffer (50 mM Tris pH 7.4, 100 mM NaCl, 300 mM imidazole, 8 mM  $\beta$ -ME, and 10% glycerol). Elution 2 was used for subsequent PAT assays. The concentration of myrLck<sub>NT</sub> was determined by extrapolation from a linear curve with known concentrations of bovine serum albumin using Coomassie Blue gel stain and quantitation with ImageJ software (NIH). C3,5S myrLck<sub>NT</sub> was expressed in BL21(DE3) *E.coli* transformed with pML1067 and pML1175 and purified as described for WT. The identity of purified protein was confirmed by immunoblotting with mouse monoclonal anti-Lck (3A5, sc-433) purchased from Santa Cruz Biotechnology (Santa Cruz, CA).

Yeast *N*-myristoylated Vac8 was purified by ion-exchange and hydroxylapatite chromatography as described (203). Prenylated Ras proteins were expressed in yeast from the galactose-inducible vector pEG(KG) and purified as described (81, 203). The GST-Ras2(HV) construct consists of the C-terminal 35 amino acid residues of yeast Ras2 fused to GFP. Full-length mammalian H-Ras was fused to GST.

*In vitro PAT assays.* Inhibitors were dissolved and serially diluted to 100X stocks in 100% DMSO. Stocks were diluted to 5X with TED (20 mM Tris pH 7.4, 1 mM EDTA, and 1 mM DTT). Equal volumes (5  $\mu$ L) of DHHC enzyme and 5X inhibitor solutions were pre-incubated for various times and temperatures as indicated in figure legends. Protein substrates diluted in TED (5  $\mu$ L) were pre-mixed with reaction hot mix (RHM; 10  $\mu$ L; 250 mM MES pH 6.4, 1 mM DTT, 1.2-3.4  $\mu$ M [ $^3$ H]palmCoA) and incubated at the same temperature as enzyme/inhibitor mix. This substrate mixture (15  $\mu$ L) was added to the enzyme/inhibitor mix to start the reaction and incubated as indicated for each figure. The reactions (25  $\mu$ L) were stopped by addition of 5X gel loading buffer with final 2 mM DTT (6.25  $\mu$ L). Except for assays of reversibility, all inhibitor concentrations shown are for the final 25  $\mu$ L reaction. Stopped reactions were heated for 60 sec at 95°C before resolution by SDS-PAGE. Gels were stained with Coomassie Blue, destained, and scanned. Protein substrate bands were excised from the gel, placed into scintillation vials, solubilized in 500  $\mu$ L Soluene 350 (PerkinElmer) at 50°C for at least 3 hr, and quantitated by liquid scintillation spectroscopy.

Enzyme autoacylation assays without inhibitors (Figure 4.2, right panel) were performed similar to inhibitor profile assays described above. Briefly, 500 fmol of enzyme was incubated in 0.82  $\mu$ M [ $^3$ H]palmCoA for 10 min at 25°C in RHM. Reactions were stopped with gel loading buffer and resolved by SDS-PAGE. Gels were stained, destained, soaked in 1 M sodium salicylate/15% methanol for 20 min, dried onto filter paper, and exposed to film at -80°C for 8 days. Enzyme autoacylation assays with inhibitors (Figure 4.5) were performed similar to inhibitor profile assay except without

protein substrate. Briefly, 250 fmol of DHHC2 was pre-incubated with inhibitor for 8 min at 25°C. Pre-warmed RHM was added to give a final concentration of 1.1 μM [<sup>3</sup>H]palmCoA in 25 μL and the reaction proceeded for 2 min before stopping with 5X gel loading buffer. Reactions were processed similar to those in Figure 4.2.

The assay for reversibility was similar to those above, except the initial reaction volume was 200 μL and 25 μL aliquots were removed at the indicated times. DHHC2 was pre-incubated for 30 min at 25°C with inhibitor at the first concentration indicated. Equilibrated substrates in RHM with either DMSO or inhibitor were used to dilute the enzyme/inhibitor 40-fold to the second concentration indicated and to start the reaction, which was maintained at 25°C. At the indicated times, aliquots (25 μL) were removed from the reaction, stopped with gel loading buffer, and processed as above. In experiments to measure time-dependent inhibition, DHHC2 (100 fmol) was pre-incubated 30 min at 25°C with inhibitor or a DMSO control. Reactions were started by addition of either both substrates in RHM to enzyme/inhibitor mix (pre-incubation) or both substrates and inhibitor to enzyme/DMSO mix (no pre-incubation). Reactions (25 μL, 2% DMSO final) were incubated 7 min at 25°C before stopping and processing as above. Data were graphed and analyzed using Microsoft Excel and GraphPad Prism 5.0.

## **Results**

*Purification of active DHHC2.* The predicted targets of the palmitoylation inhibitors identified by Ducker et al. are the DHHC proteins. Furthermore, the pattern of specificity shown by the inhibitors in assays using cell membranes as a source of

palmitoyltransferase activity suggests that some of the inhibitors would more potently inhibit DHHC proteins that modify farnesylated substrates, whereas others would be more effective inhibitors of PATs for *N*-myristoylated substrates. To test these predictions, we purified mammalian and yeast DHHC PATs that display the appropriate substrate specificity. Yeast Erf2/Erf4 is a PAT for yeast Ras (81), but displays little activity toward Vac8, an *N*-myristoylated protein (203). Conversely, yeast Pfa3 palmitoylates Vac8 (91) but not Ras2 (203). Mammalian DHHC9/GCP16 palmitoylates H-Ras in vitro, but has little or no activity for *N*-myristoylated G<sub>ia1</sub> (114).

We sought to identify a mammalian DHHC protein that has robust activity for an *N*-myristoylated substrate. Preliminary experiments revealed that the nonreceptor tyrosine kinase Lck, a protein palmitoylated at cysteine residues near the myristoylated N-terminus, was a good substrate for DHHC2 (data not shown). To further characterize this interaction, we expressed human DHHC2 with epitope tags at both the N- and C-termini to aid in the purification of full-length enzyme. Detergent extracts from membranes were passed sequentially over nickel and FLAG affinity resins to generate purified enzyme (Figure 4.2, left). Immunoblotting revealed full-length protein was isolated (Figure 4.2, center).

In all DHHC proteins characterized to date, PAT activity has been coupled with incorporation of palmitate into the DHHC protein itself, a process termed enzyme autoacylation (83). Although it is uncertain whether this process represents an acyl-enzyme transfer intermediate, autoacylation serves as a read out for functional enzyme. Purified DHHC2 incorporated [<sup>3</sup>H]palmitate derived from [<sup>3</sup>H]palmitoyl CoA. This

reaction was specific as neither heat-treated DHHC2 nor DHHS2, a mutant predicted by homology to be catalytically inactive (83), showed radiolabeling (Figure 4.2, right). Thus, we have purified DHHC2 and shown it to be functionally active as monitored by autoacylation.

*DHHC2 palmitoylates myrLck<sub>NT</sub> at cysteines 3 and 5.* To test Lck as a substrate for DHHC2, we used a model substrate consisting of the N-terminal myristoylation, palmitoylation motif (SH4 domain) and the SH3 and SH2 domains (Lck<sub>NT</sub>). This fragment is more easily purified than the full-length protein that includes the kinase domain. To confirm that in vitro palmitoylation of Lck<sub>NT</sub> was occurring at cysteine residues palmitoylated in vivo, we also expressed and purified C3,5S myrLck<sub>NT</sub>. Lck is palmitoylated in vivo at Cys3 and Cys5, which may differentially regulate Lck localization (205). Lck has two additional cysteines near the amino terminus (Cys20 and Cys23) that are required for binding coreceptors CD4 and CD8 (206). Because myristoylation facilitates subsequent palmitoylation both in vivo and in vitro (26, 207), we purified wild type and mutant Lck<sub>NT</sub> from *E. coli* coexpressing human *N*-myristoyltransferase (NMT) to produce *N*-myristoylated substrates. Metabolic labeling with [<sup>3</sup>H]myristic acid indicated that both proteins were myristoylated in this system and that mutation of the palmitoylation sites did not affect myristoylation (see Supplemental Figure 4.S1).

Wildtype and C3,5S myrLck<sub>NT</sub> were purified and assayed for their ability to be acylated by DHHC2 in an in vitro PAT assay. Incubation of either form of myrLck<sub>NT</sub> with [<sup>3</sup>H]palmCoA and enzyme buffer did not result in incorporation of radiolabel in

myrLck<sub>NT</sub> as monitored by scintillation counting or fluorography (Figure 4.3, first 3 lanes). When 200 fmol of DHHC2 was included in the reaction, greater than 1500 fmol of [<sup>3</sup>H]palmitate was incorporated into wild type myrLck<sub>NT</sub>, indicating that transfer is catalytic. Less than 100 fmol of [<sup>3</sup>H]palmitate was incorporated into C3,5S myrLck<sub>NT</sub> by DHHC2. When autoacylation-defective DHHC2 was assayed, no radiolabel was incorporated into myrLck<sub>NT</sub> (Figure 4.3, last 3 lanes). The low levels of radiolabel in C3,5S myrLck<sub>NT</sub> may indicate that DHHC2 weakly palmitoylates myrLck<sub>NT</sub> at other cysteine residues nonspecifically.

*Evaluation of potential PAT inhibitors using enzyme-substrate pairs.* Using the three established enzyme-substrate pairs described above along with DHHC2 and myrLck<sub>NT</sub>, we sought to determine if the PAT inhibitors identified by Ducker et al. blocked DHHC-mediated palmitoylation and displayed the predicted substrate specificity. We obtained and tested four of the five compounds along with 2-bromopalmitate (2BP; Figure 4.1). Compound IV (CIV; 2-(2-fluoro-benzyl)-1-phenyl-1,2,3,4-tetrahydro-pyrrolo[1,2,-a]pyrazine) was not available from commercial sources and was not tested here. For inhibitor PAT assays, the inhibitor was pre-incubated with DHHC protein, followed by the addition of both protein substrate and [<sup>3</sup>H]palmCoA that had been pre-mixed and equilibrated at the assay temperature. To remain in the linear range for each reaction, concentrations, temperature, and lengths of incubations varied for each pair and are listed in the legend to Figure 4.4.

Overall, less potent and specific inhibition was observed than expected (Figure 4.4). For all pairs tested, 2BP was the best inhibitor displaying an average IC<sub>50</sub> of ~10

$\mu\text{M}$ . This result confirmed that 2BP inhibits DHHC-mediated palmitoylation in vitro as shown previously for DHHC15 (123). Compound V (CV) was initially described as a selective inhibitor of *N*-myristoylated, palmitoylated protein but not farnesylated, palmitoylated proteins, with an  $\text{IC}_{50}$  of  $0.5 \mu\text{M}$  for an *N*-myristoylated peptide (152). As shown here, CV inhibited all DHHCs tested but was less potent than 2BP, displaying a higher  $\text{IC}_{50}$  for three of the four enzyme-substrate pair. The remaining compounds (CI, CII, and CIII) were previously demonstrated to inhibit PAT activity toward a farnesylated peptide mimicking Ras, with  $\text{IC}_{50}$  values of 4 to  $12 \mu\text{M}$ . When tested against the DHHC Ras PATs, DHHC9/GCP16 and Erf2/Erf4, little or no inhibition was observed for any of the enzymes, even at the highest concentration tested ( $100 \mu\text{M}$ , Figure 4.4). Thus with the DHHC enzyme-substrate pairs tested, the predicted selectivity of these compounds was not observed.

*2-Bromopalmitate and Compound V inhibit enzyme autoacylation.* 2BP and CV reduced DHHC-mediated palmitoylation. Accordingly, we characterized these compounds further. Because 2BP and CV affected all four enzyme-substrates pairs equally, DHHC2 and myrLck<sub>NT</sub> were chosen as a representative pair for further experiments. To date all DHHC proteins that display PAT activity also autoacylate. Thus, we determined the effect of 2BP and CV on enzyme autoacylation. As seen in Figure 4.5, both compounds inhibited enzyme autoacylation, with 2BP being more potent at blocking enzyme radiolabeling than CV.

*Evaluation of reversibility and time-dependent inhibition.* We next wanted to assess whether the inhibition of PAT activity by 2BP and CV was reversible or

irreversible. DHHC2 was pre-incubated with either 2BP or CV at the first, pre-dilution concentration indicated in Figure 4.6A. This preformed enzyme-inhibitor complex was diluted 40-fold with buffer containing both protein and lipid substrates to give the second inhibitor concentration indicated. The lack of recovery of PAT activity following dilution of 2BP compared to the inhibited controls maintained at persistent concentrations of inhibitor indicates that 2BP is an irreversible inhibitor (Figure 4.6A, left side; square symbols relative to filled symbols). In contrast, when CV was similarly diluted, approximately 70 percent of PAT activity was recovered compared to the inhibited control maintained at the diluted concentration of CV (Figure 4.6A, right side). This indicates that the inhibitory effect of CV is reversible.

Finally, because inhibitor profiles for each enzyme-substrate pairs were done following pre-incubation with inhibitor, we wanted to assess whether 2BP and CV displayed time-dependent inhibition (also called slow-binding inhibition; Figure 4.6B). During one set of conditions (without inhibitor pre-incubation) substrates and 2BP or CV were premixed and the assay started by addition of DHHC2 pre-incubated with a DMSO control. Alternatively, under a second set of conditions (with inhibitor pre-incubation), DHHC2 and 2BP or CV were pre-incubated 30 minutes before addition of both substrates to initiate the reaction. For both compounds, an increase in inhibitor potency following pre-incubation was observed with the curves shifting to the left (Figure 4.6B). This suggests that both CV and 2BP are time-dependent inhibitors of DHHC2 PAT activity. Higher concentrations of CV were not tested because of limitations in the solubility of the compound.

## **Discussion**

As advances are made in the palmitoylation field it is becoming increasingly clear that DHHC proteins play an important role in both native and disease states. DHHC proteins have been identified that are responsible for palmitoylating proteins involved in cell growth (114, 122), maintaining vascular homeostasis (179), neurotransmitter receptor trafficking (123), and cell-cell adhesion (208). DHHC proteins have also been linked to several diseases including cancer (122, 140, 152), Huntington's disease (111), and mental retardation (139). Identification of potent and specific palmitoylation inhibitors that target DHHC proteins could lead to novel therapies, as well as provide tools to investigate palmitoylation's roles in cellular processes.

With that in mind, we sought to determine whether DHHC proteins were targets of the palmitoylation inhibitor compounds described by Ducker et al. (152). We found that one of the four compounds, CV, behaved similarly to 2BP, in that it inhibited all four of the DHHC proteins tested. Both 2BP and CV inhibited autoacylation of the enzyme, which is tightly correlated with the ability to transfer palmitate to substrate. It is unknown whether autoacylation represents an acyltransfer intermediate. However, the loss of autoacylation with inhibitors that also block transfer to substrate is consistent with such a mechanism. Furthermore, the ability of CV to inhibit autoacylation, a property common to all DHHC proteins, suggests that it will not be selective for different DHHC proteins.

Inhibition of DHHC2 PAT activity by 2BP was irreversible. This was not unexpected as 2BP has been shown to irreversibly inhibit fatty acid metabolism (209, 210), as have other halogenated fatty acid analogs (211). Additionally, others have previously hypothesized that 2BP forms an irreversible bond with PATs (212). In contrast the inhibition by CV was mostly reversible. This is perhaps not unexpected in that CV does not contain any highly reactive centers (Figure 4.1). Both 2BP and CV displayed time-dependent inhibition, albeit to different degrees. Time-dependent inhibition is considered an advantage in a pharmacological setting because the enzyme is inhibited for longer periods of time (213). This, plus the fact that 2BP inhibits other enzyme families (198, 199), suggest that CV may be a good candidate for future structure-activity relationship studies with substituent side-chain replacement focused on enhancing potency and specificity.

We were unable to detect significant inhibition of DHHC proteins by three of the compounds tested, nor did CV display selective inhibition of DHHC PAT activity for N-myristoylated substrates. Several possible explanations could account for the differences between the original report describing these compounds and those documented here. Ducker et al. (152) used MCF-7 cell membranes as a source of PAT activity. DHHC proteins have not been studied in these cells, but given the large family size, it is likely that multiple DHHC proteins are expressed. Reverse transcriptase-PCR has detected mRNA for both DHHC2 and DHHC9 in MCF-7 cells (unpublished observations). However, it is possible that DHHC proteins other than DHHC2 and DHHC9/GCP16 are possibly more sensitive to these compounds. Phylogenetic analysis of DHHC sequences

from humans and yeast place DHHC9 and Erf2 within a larger subfamily (DHHC5, 8, 9, 14, 18, 19, and Erf2). Similarly, DHHC2 and Pfa3 cluster with a different group of DHHC proteins (DHHC2, 3, 7, 15, 20, and Pfa3) (123). DHHC proteins less closely related to these two groups were not tested.

An important difference between the two studies is the substrates that were tested. Ducker et al. assayed short fluorescent, lipidated peptides (myristoyl-Gly-Cys and Cys-Leu-Cys-farnesyl,O-methyl). We assayed full-length (myristoyl-Vac8 and farnesyl-H-Ras) or larger protein fragments (HVRas2, the farnesylated hypervariable domain of Ras, and myristoyl-Lck<sub>NT</sub>). It remains to be determined whether Lck and H-Ras are *in vivo* substrates, as well as *in vitro* substrates of DHHC2 and DHHC9/GCP16. However, the yeast enzymes and their substrates have been validated both genetically and biochemically (81, 91, 214), and display strong preferences for their respective substrates relative to the other lipidated substrates (203). Accordingly, these yeast enzymes and their substrates represented an excellent system to test the inhibitors for substrate specificity.

Inhibition of PAT activity in MCF-7 membranes by the compounds may be dependent on a membrane environment. DHHC proteins are integral membrane proteins and the surrounding lipid environment can affect both rate and specificity of such enzymes (160). The hydrophobic compounds tested here may act indirectly, disrupting the membrane surrounding DHHC proteins rather than directly interacting with them. Alternatively, DHHC proteins within a lipid bilayer may adapt a conformation that makes them more susceptible to these compounds. Because the DHHC proteins tested here

were purified and assayed in detergent micelles, effects of the compounds on DHHC proteins that require a lipid membrane would have been missed. Initial attempts at reconstituting DHHC proteins into liposome were unsuccessful and more work is needed in this area.

Finally, it is possible that proteins other than DHHC proteins are targets of these compounds. A study of the palmitoylproteome in yeast suggests that DHHC PATs account for most cellular palmitoylation events (16). In mammals, secreted proteins such as the morphogens Hedgehog and Wnt, as well as the peptide hormone ghrelin, are posttranslationally modified with fatty acids through the action of membrane-bound O-acyltransferases (MBOAT) (6, 215). Modification of these secreted proteins occurs in the lumen of the secretory pathway. To date only one MBOAT protein has been characterized biochemically (8). It is unknown if these activities could account for palmitoylation of the peptides in the MCF-7 cell membranes.

The finding that CV is an inhibitor of DHHC PATs and the antitumor activity reported for all of the compounds makes them interesting reagents for further study. Future investigations into DHHC enzymology and mechanism will likely aid the search for specific and potent PAT inhibitors.

## **Acknowledgements**

The authors would like to thank Dr. Charles Smith for providing the compounds studied here and Wendy Greentree for technical support. B.C.J. and M.J.N. were supported by American Heart Association pre-doctoral fellowships (Midwest Affiliate). Work in the authors' laboratories is supported by NIH grants GM51466 (M.E.L.), CA050211 and GM073977 (R.J.D.), and GM48099 (M.L.H).

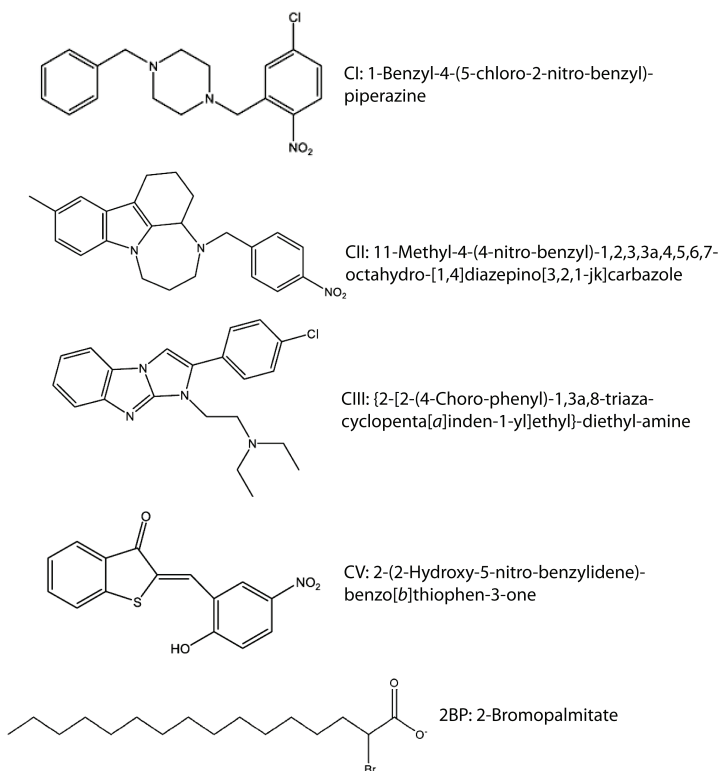


**Figure 4.1. Structure and names of inhibitor compounds used in this study.**

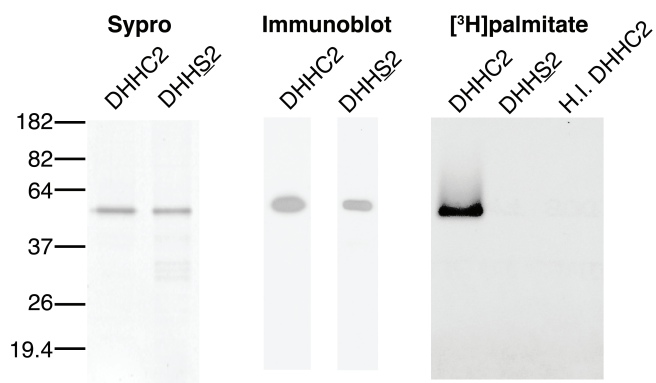


**Figure 4.2. Purification of human DHHC2 and catalytically inactive DHHS2.** DHHC2 was expressed in Sf9 cells and purified sequentially by nickel chelate and FLAG affinity chromatography. Catalytically inactive DHHS2 was purified by nickel affinity chromatography; the fifth elution is shown. Purified DHHC2 and DHHS2 were detected by Sypro staining (left) and immunoblotting with anti-Express antibody (center). DHHC2, but not DHHS2, autoacylates (right). DHHC2, DHHS2, or heat inactivated DHHC2 (500 fmol each) were incubated in 0.8  $\mu$ M [ $^3$ H]palmCoA at pH 6.4 for 10 min. The reactions were stopped with SDS sample buffer and processed for fluorography. The film was exposed for 8 days.

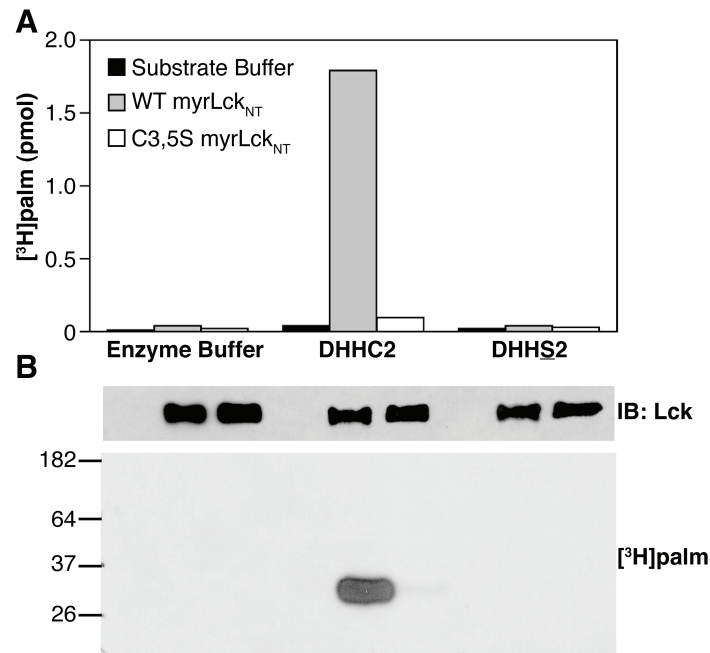


**Figure 4.3. DHHC2 palmitoylates myrLck<sub>NT</sub> at cysteines 3 and 5.** Purified DHHC2, DHHS2 (200 fmol), or enzyme buffer was mixed with purified myrLck<sub>NT</sub> (25 pmol) on ice. Reaction buffer was added to give a final concentration of 0.8  $\mu$ M [<sup>3</sup>H]palmCoA in 50  $\mu$ L and incubated at 25°C for 7 min. The reaction was stopped with SDS sample buffer and divided between two SDS-PAGE gels, which were stained and destained. *A*, The region containing myrLck<sub>NT</sub> was excised from one gel, solubilized with Soluene, and the amount of [<sup>3</sup>H]palmitate present determined by scintillation counting. *B*, The second gel was processed for fluorography and exposed to film at -80°C for 90 hr. MyrLck<sub>NT</sub> was detected by immunoblotting reactions run without radioactive palmCoA.

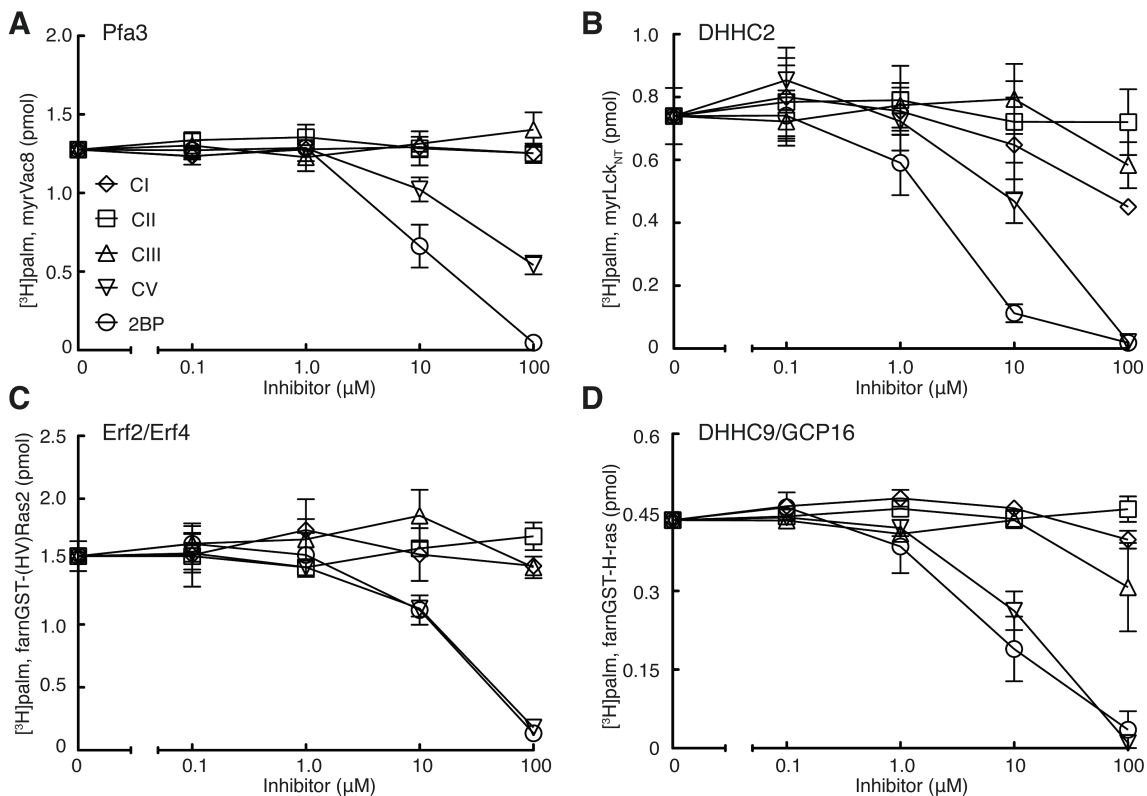


**Figure 4.4. Inhibitor profiles for DHHC proteins.** Inhibitor profiles for each enzyme-substrate pair were carried out as described in the text. *A*, Partially purified yeast Pfa3 (5  $\mu$ L) was pre-incubated with inhibitor for 8 min at 30°C. MyrVac8 and [ $^3$ H]palmCoA were mixed, warmed to 30°C, and added to the reaction at final concentrations of 0.5  $\mu$ M and 0.8  $\mu$ M, respectively. The reaction proceeded for 10 min at 30°C before stopping with SDS sample buffer. *B*, Purified human DHHC2 (100 fmol) was pre-incubated 8 min at 25°C with inhibitors. MyrLckNT and [ $^3$ H]palmCoA were added to give final concentrations of 0.5  $\mu$ M and 0.8  $\mu$ M, respectively, and the reaction proceeded for 7 min at 25°C before stopping. *C*, Purified yeast Erf2/Erf4 (100 fmol) was pre-incubated 8 min at 25°C with inhibitors. [ $^3$ H]palmCoA and the farnesylated hypervariable region of Ras2 fused to GST were added to give final concentrations of 0.9  $\mu$ M and 1.0  $\mu$ M, respectively, and the reaction proceeded for 10 min at 25°C before stopping. *D*, Purified human DHHC9/GCP16 (150 fmol) was pre-incubated 5 min on ice with inhibitors. [ $^3$ H]palmCoA and the farnesylated H-Ras fused to GST were added to give final concentrations of 0.9  $\mu$ M and 1.2  $\mu$ M, respectively, and the reaction proceeded for 7 min at 25°C before stopping. Values represent the means  $\pm$  the standard error of the mean determined from three independent experiments.

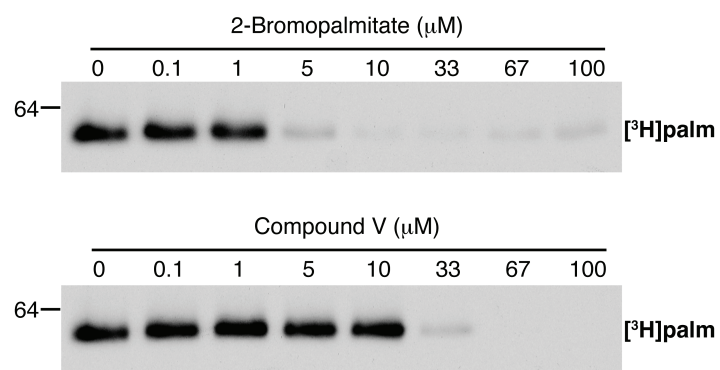


**Figure 4.5. Inhibitor effect on enzyme autoacylation.** DHHC2 (250 fmol) was pre-incubated with inhibitor and assayed as described in Experimental Procedures. The film was exposed for 8 days.

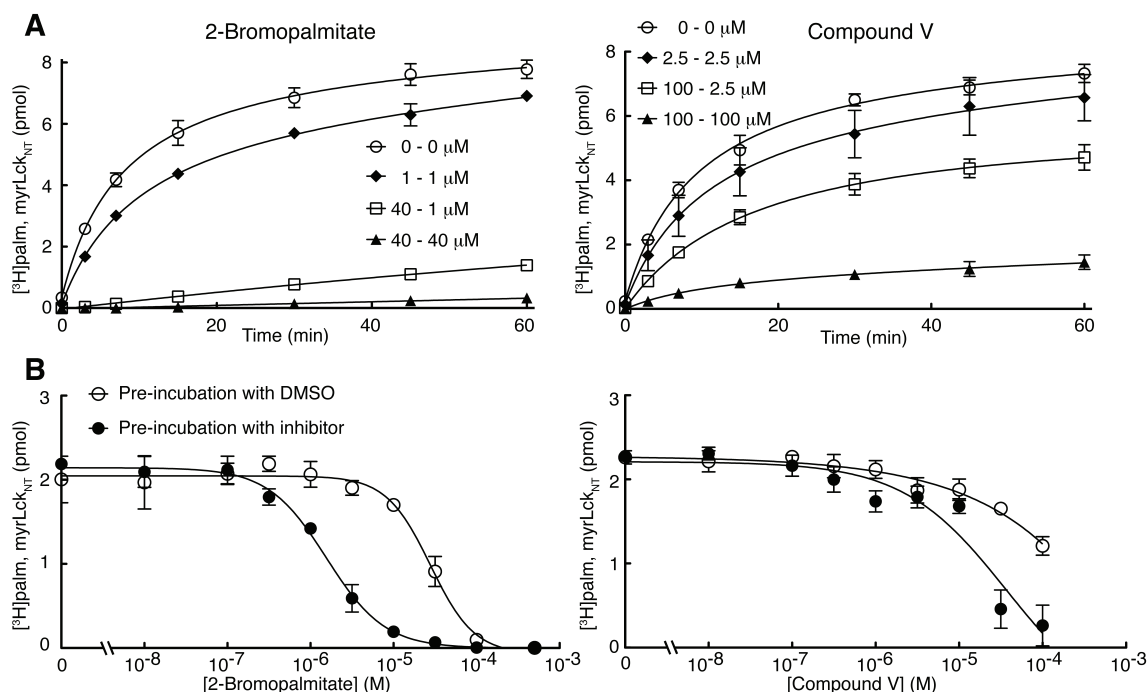
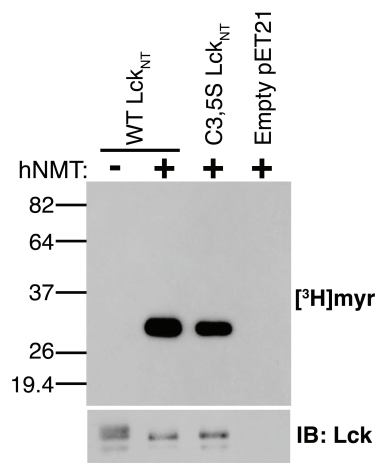


**Figure 4.6. Reversibility and time-dependent inhibition.** Experiments were performed as described in Experimental Procedures. *A*, Reversibility of 2BP and CV was tested by incubating DHHC2 (100 fmol) with the first concentration indicated for 30 min at 25°C. This mix was diluted 40-fold with both substrates to the post-dilution concentration indicated, incubated at 25°C, and aliquots removed at the indicated time points. *B*, Time-dependent inhibition was evaluated by pre-incubating enzyme with inhibitors at the indicated concentrations or DMSO for 30 min at 25°C. Both substrates without or with inhibitor were added to start the reaction, which was incubated at 25°C for 7 min before stopping. Values represent the means  $\pm$  the standard error of the mean determined from three independent experiments.



**Supplemental Figure 4.S1. Recombinant WT and C3,5S Lck<sub>NT</sub> are myristoylated.** *E. coli* BL21(DE3) were transformed with pML1008 (WT Lck<sub>NT</sub>-His<sub>6</sub>), pML1175 (C3,5S Lck<sub>NT</sub>-His<sub>6</sub>), or empty pET21 vector with or without pML1067 (human NMT1). Cultures were grown at 37°C to OD<sub>600</sub> = 0.7-0.8 and induced with 0.3 mM IPTG for 100 min at 30°C. A portion of the culture (1 mL) was incubated with 1.7 nmol [<sup>3</sup>H]myristic acid (50 μCi, PerkinElmer Life Sciences) for 4 hr at 30°C. Cells were collected by centrifugation and washed in cold PBS. Whole cell lysates were made by addition of 200 μL 1.5X sample buffer with 30 mM DTT and heating to 95°C for 4 min with vortexing. Samples were frozen overnight at -20°C. The next day thawed samples were spun at 10,000g for 2 min and 3 μL of each were separated by SDS-PAGE and processed for fluorography or immunoblotting with α-Lck (1:5000). The dried gel was exposed to film at -80°C for 16 hr. The dark bands present in lanes 2 and 3 indicate that both WT and C3,5S Lck<sub>NT</sub> are being myristoylated in *E. coli*.

# Chapter 5

## Implications and Future Directions

### Findings of the thesis

In this thesis, I have described the development and utilization of protein *S*-acyltransferase (PAT) assays to examine the mechanism of DHHC proteins. When this work began, the DHHC protein family had recently been identified as the group of enzymes responsible for catalyzing protein *S*-acylation. Of the DHHC proteins that had previously been isolated, all incorporated palmitate when incubated with radiolabeled palmCoA. Although this was hypothesized to reflect an acyl-enzyme intermediate (81, 82), it was possible that DHHC acylation represented a non-transferable modification consistent with other integral membrane proteins being stably acylated on cysteine residues adjacent to transmembrane domains. Thus, the hypothesis that DHHC autoacylation reflected a transfer intermediated needed to be tested. Assays initially used for the characterization of PAT activity in tissues and cell lines were optimized for

DHHC proteins. The detrimental effects of thiol-based reducing agents on DHHC activity were reported and assay conditions altered.

Using these new assay conditions, the predicted catalytic mechanism of DHHC proteins was determined. Single turnover assays provided evidence to support the hypothesis that autoacylated DHHC proteins represent a transient acyl-enzyme transfer intermediate. These results supporting a two-step ping-pong mechanism of transfer that agree well with results by others published recently (175). During this investigation it was discovered that DHHC proteins display different acyl-CoA specificities and the mechanism of this specificity was investigated. For DHHC3 the reduced ability to transfer longer chain fatty acids was not due to increased hydrolysis of the acyl-intermediate but rather reduced formation of acyl-enzyme and a significantly reduced rate of transfer to protein substrate. These differences in DHHC acyl-CoA specificity provide a mechanism to explain the differences in acyl-chain lengths observed on native *S*-acylated proteins isolated from cells and tissues.

Assays of PAT activity were also used to evaluate the specificity and potency of potential protein *S*-acylation inhibitors with DHHC proteins. At the initiation of these studies, previously described inhibitors of protein acylation were limited to 2-bromopalmitate (2BP), cerulenin, and tunicamycin. While capable of reducing *S*-acylation within cells, these compounds were also known to inhibit other enzymes and thus, lacked specificity. Nevertheless, tunicamycin and cerulenin were assayed for their ability to block DHHC-mediated acylation and found to have no effect on PAT activity (Table 2.2). This lack of specific *S*-acylation inhibitors motivated others to develop

screens for finding new inhibitors. Ducker *et al* published five representative compounds they found using cell-based screening methods and follow-up studies with assays of PAT activity in crude cell membranes (152). I directly tested whether these compounds and 2BP were capable of inhibiting DHHC-mediated protein acylation. My studies revealed that two compounds, 2BP and Compound V, were capable of inhibiting DHHC-mediated protein acylation, and their mechanism of inhibition was characterized. Given the importance of DHHC proteins in human diseases, my results stress the importance of testing lead compounds directly on intended targets and outline a methodology to do so.

### **Future Directions**

The following model is proposed for the catalytic mechanism of DHHC proteins based on my investigation and the published work of others. A DHHC protein initially binds a long-chain acyl-CoA and, in a reaction that is dependent on the cysteine residue of the DHHC motif, forms a thioester bond with the acyl group. This enzyme autoacylation step of the reaction is rapid and may display burst kinetics. A free thiol group on a protein substrate, which can bind before (188) or after autoacylation (Figure 3.2 and 3.5), then enters the active site. In the acyltransfer step, the acyl chain attached to the DHHC is transferred to the free thiol and a new thioester bond is formed in a reaction that is dependent on the first histidine of the DHHC motif (81, 175). Release of the newly *S*-acylated protein generates free enzyme that then becomes available for another round of catalysis. Given the hydrophobic character of the protein substrate, I speculate that the acylated protein product dissociates from the enzyme and diffuses within the

plane of the membrane. The mechanistic insight into DHHC catalysis provided by this thesis work represents a significant advance from knowledge available when these investigations began. However, the details of the DHHC catalytic mechanism remain to be determined.

*Acyl-CoA source.* How DHHC proteins acquire their acyl-CoAs in cells is unknown. Cytosolic free *long-chain acyl-CoA* (LCA) concentrations are calculated to be in the 2-10 nM range even though total cellular concentrations may be as high as 160  $\mu$ M (36). The difference reflects that fact that most LCAs are compartmentalized in the mitochondria or other organelles, membrane-bound, cleaved by hydrolases, or bound by acyl-CoA binding protein (ACBP) or fatty acid bind protein (FABP). Given that other enzymes utilize LCAs and the rapid kinetics observed for cellular acylation-deacylation cycles (38, 216), it is predicted that if DHHC proteins used free LCAs, the low cytosolic pool would rapidly become depleted. One possibility is that DHHC protein acquire their LCAs through lateral diffusion in the membrane. This could require the LCA to slide into a binding pocket, capable of determining chain-length preference, and may suggest membrane fluidity surrounding the DHHC could regulate substrate accessibility. An alternative is that DHHC proteins could use ACBP-bound LCAs. Supporting this substrate source, the integral membrane enzyme acyl-CoA:lysophospholipid acyltransferase (LAT) prefers ACBP-bound LCAs over free acyl-CoAs (217). Furthermore, previous work in our lab has shown that an unidentified PAT activity is capable of utilizing ACBP-bound acyl-CoAs (39). If DHHC proteins acquire LCAs from

ACBP in cells, then inclusion of ACBP in PAT assays may better represent physiological conditions.

*Kinetic rate constants.* Little quantitative information is available on the rates of individual steps within the reaction pathway. Based on the work here, it is known that the enzyme autoacylation step occurs rapidly reaching maximum incorporation of radiolabeled acyl group in less than ten seconds, relative to a slower transfer step. Measurements less than this time scale are not possible with the discontinuous radiolabel-based PAT assay. Combining the CoA production coupled-assay (175) and stop-flow spectroscopy could allow more accurate determination of autoacylation rates. Rates for different enzymes as well as with different acyl-CoAs could be used to quantify acyl-CoA and protein substrate preferences. Rates could also be used to quantitatively determine the contribution of other membrane anchoring signals such as *N*-myristoylation or prenylation to the reaction. Although the acyltransfer step is slower than autoacylation, it is unknown whether acyl group transfer or release of acyl-substrate is the rate-limiting step. Measuring rate constants could address this. Measuring reaction rates for DHHC proteins with mutations within the conserved DHHC cysteine rich domain (CRD) could help determine the role of individual residues within the reaction mechanism and provide insight into structure-function relationships.

*Mapping the acyl-DHHC attachment site.* The cysteine of the DHHC motif is required for enzyme autoacylation and is likely the site of acyl attachment, although this has not been shown. DHHC proteins have seven conserved cysteine residues within the DHHC cysteine rich domain (DHHC-CRD) and an additional 1 to 15 non-conserved

cysteine residues; the average DHHC has a total of 16 cysteine residues. It is likely that *S*-acylation occurs outside the DHHC motif. Indeed for DHHC-5, -6, and -8, a tricysteine motif in the C-terminal tail has been shown to be acylated (20). Mapping the modified residue(s) of the acyl-enzyme intermediate would provide a target residue for inhibitor design and would aid in determining the stoichiometry of autoacylation. Knowing the stoichiometry would allow enzyme concentrations to be based on functional enzyme concentrations rather than total enzyme, which is skewed by misfolded, aggregated, and inactivated protein. Our early attempts to identify the acylated peptide by mass spectrometry of trypsin-digested acyl-DHHC have been unsuccessful. Two improvements are suggested: enrichment of the acyl-peptide and removal or replacement of the fatty acid prior to mass spectrometry. Acyl resin-assisted capture (acyl-RAC) (18) or acyl-biotin exchange (ABE) (218) are newer, nonradiolabel-based methods of analyzing protein *S*-acylation and accomplish both improvements.

*Oligomerization of DHHC proteins.* It is unknown whether DHHC proteins function as multimers. Co-immunoprecipitation of epitope-tagged DHHC3 and DHHC7 expressed in cells suggests that these DHHC proteins can form homo- and heteromultimers (219). Further suggesting DHHC proteins may interact directly, ectopic expression of DHHS-15 or AAHC-15 in cells resulted in a dominant negative phenotype with reduced activity observed for cotransfected wildtype DHHC15 and DHHC2 (123). For DHHC9 and the yeast ortholog, Erf2, heterodimers are formed with cognate binding partners GCP16 and Erf4, respectively. Although the function of these binding partners is unknown, multimerization of other DHHC proteins may serve a similar function. If

DHHC proteins form oligomers, then cooperativity between subunits is possible and this would affect interpretation of kinetic data.

Oligomerization of DHHC proteins also allows a type of behavior called half-of-sites reactivity. This is a behavior in oligomeric enzymes in which the number of active subunits is less, typically one-half, than the total number of subunits. This can be caused, for example, by substrate binding to one subunit of a dimer and inducing a conformational change in the other subunit that blocks substrate binding, and thus is a type of negative cooperativity (220). The integral membrane protein phospholipase A (OMPLA) is an example of an enzyme displaying this behavior (221). In kinetic studies this mode of reactivity presents itself as the maximal stoichiometric yields of either an enzyme intermediate or the product of a single turnover assay as being only half the number of enzyme active sites. The maximal stoichiometries of DHHC autoacylation observed were 0.5 palmitate per DHHC3 (Figure 3.5A) and 0.65 palmitate per Erf2/Erf4 (175), consistent with a half-of-sites mechanism. However, other explanations, such as inactive enzyme, could also explain DHHC stoichiometries less than one. In single turnover assays we observed approximately half the acyl-enzyme transferring its acyl group to protein substrate. Again, this could be explained by either a half-of-sites model or by enzyme inactivated after autoacylating. Knowing if DHHC proteins form oligomers would be the first step in testing this mechanism.

*Structural basis for acyl-CoA specificity.* The structural basis for the observed differences in acyl-CoA specificity for DHHC proteins remains unclear. When tested by an in vitro competition PAT assay, DHHC15-mediated incorporation of radiolabeled

palmitate was reduced 90% by non-labeled palmCoA but only 57% by non-labeled C18 stearoyl-CoA (123). This may suggest that DHHC15, similar to DHHC3, is less able to transfer acyl chains longer than 16-carbon palmitate. A structural basis for these observed specificities may reside in the DHHC transmembrane domains (TMDs). It has been shown for the multienzyme complex fatty acid synthase (FAS) that a lysine residue regulates final acyl-CoA chain length by protruding from TMDs in Fen1 or alternative subunit Sur4 at different distances from the catalytic core. Examining their predicted membrane topology, three TMDs of DHHC3 contain charged residues at the midpoint of the bilayer that are not present in DHHC2, which has broader acyl-CoA specificity. Swapping TMDs between these DHHCs and site-directed mutagenesis could reveal whether this region controls acyl-CoA specificity. If this is found not to be the case, mutations at these sites may still be informative as these charged residues buried within DHHC3's TMDs likely serve some function, perhaps forming a salt bridge that stabilizes dimers.

*Zinc binding capability and other cofactors.* DHHC proteins were originally classified as zinc-finger proteins (87) and have been implicated in the transport of  $Mg^{2+}$  and  $Ca^{2+}$  ions (99, 100), however their ability to bind these metal ions has not been tested. Inductively coupled plasma mass spectrometry (ICP-MS) could be used to determine the number and species of metal ions bound to DHHC protein. It is probable that DHHC proteins contain at least one metal ion, likely binding residues with the DHHC-CRD domain, based on predictions and sequence conservation of residues known to bind metal-ions in other proteins. Given that mammalian DHHC22 and yeast Ark1,

Ark2, and Pfa5 lack a number of residues within the DHHC-CRD, it is possible they do not share this feature or bind a different metal species. Reports describing the  $Mg^{2+}$  and  $Ca^{2+}$  transport capabilities of DHHC proteins were based on indirect assays and these alternative functions should be tested directly. Reconstitution of DHHC proteins into liposomes and monitoring ion uptake by fluorescent chelators or radiolabeled ions is one method of testing ion transport.

*Discovering new inhibitors of DHHC-mediated protein S-acylation.* Inhibitors of protein S-acylation would be beneficial both as tools for studying DHHC proteins within cells and as potential pharmaceutical agents. Having inhibitors with characterized methods of inhibition can aid in determining the order of substrate binding and product release. For example, although the acyl chain is transferred from CoA to DHHC forming the acyl-intermediate, it is unknown whether the CoA leaves before protein substrate binding or after release of acylated protein. Given the role of protein S-acylation and DHHC proteins in human diseases (Table 1.3), inhibitors may be clinically useful.

Additional screens are needed to find inhibitors of DHHC proteins. The compounds tested in chapter 4 were representative of 4 chemical classes from the results of three inhibitor screens. An additional 87 compounds were identified that belonged to these classes as well as 65 unique compounds not belonging to any of the chemoclasses (152). Given that these compounds inhibited S-acylation in both a live cell-based screen and in PAT assays with crude cell membranes, they should be directly screened with purified proteins and in vitro PAT assays to determine their ability to inhibit DHHC proteins.

High-content screening (HCS) is one strategy to find DHHC inhibitors. A DHHC protein and/or one of its substrates fused to a monomeric fluorescent protein are expressed in cells. The assay is based on a substrate displaying a different localization in the acylated and non-acylated states. Following growth in a multi-well imaging plate, cells are treated with compounds and monitored for changes in fluorescence localization. Because of the complexities of cells and protein trafficking, compounds that altered localization would need to be validated with secondary screens. A more detailed explanation of this approach is available (222).

Cell-free screens for the direct inhibition of DHHC proteins are also possible. Using purified DHHC proteins and either a protein or peptide substrate, the production of the reaction by-product CoA can be monitored. One such assay has already been described and used to monitor the rates of palmCoA hydrolysis by Erf2 (175). This approach involves coupling the production CoA to the reduction of  $\text{NAD}^+$  with  $\alpha$ -ketoglutarate dehydrogenase ( $\alpha$ -KDH) and monitoring the reaction by NADH fluorescence emission. Lead compounds would need to be validated by secondary screen for a number of reasons, including the possibility of inhibiting  $\alpha$ -KDH. Another cell-free screen possible with purified DHHC protein could be based on the ultra-high throughput screen (uHTS) developed to find inhibitors of fatty acid synthase and acetyl-CoA carboxylase (223). The free thiol of CoA would react with 7-diethylamino-3-(4'-maleimidylphenyl)-4-methylcoumarin (CPM), a compound that becomes fluorescent upon reaction with thiols. It is unknown if CPM would react with thiols on the DHHC and protein substrate, however this was not the case for two enzymes previously tested.

Unlike the coupled-assay, this latter approach involves only one enzyme and may present fewer challenges. Compounds found through any screening assay will need further validation with secondary assays and subsequent characterization. Additionally, structure-activity relationship (SAR) studies and the synthesis of analogous compounds will likely be needed to develop potent and specific inhibitors. One feature of DHHC proteins to exploit to achieve inhibitor specificity is the acyl-chain length specificities demonstrated in this work.

### **Concluding Remarks**

With this work, I have shown that the currently available inhibitors for DHHC proteins are limited in potency and specificity and have further characterized the two most potent inhibitors available. Uncovering the mechanism of DHHC proteins will aid in our ability to find better inhibitors as well as improve our understanding of this biologically important family of enzymes. With that goal in mind, I have determined that DHHC proteins use a two-step ping-pong catalytic mechanism and display acyl-CoA specificity. I hope that I have highlighted the contributions this work has made to a mechanistic understanding of DHHC proteins and the future work that is needed to further advance the protein *S*-acylation field.

# Appendix

## Characterization of DHHC9 in Ras Signaling and X-linked Mental Retardation

The portion of this appendix related in FKBP12 and H-ras *S*-acylation was published in Ahearn, I. M., Tsai, F. D., Court, H., Zhou, M., Jennings, B. C., Ahmed, M., Fehrenbacher, N., Linder, M. E., and Philips, M. R. 2011. FKBP12 binds to acylated H-ras and promotes depalmitoylation. *Molecular Cell*. **41**:173-185. My contributions appear in Figure 2.

## **Introduction**

The yeast protein Erf2 and its mammalian ortholog DHHC9 are protein *S*-acyltransferases (PATs) for ras proteins. Effector of ras function 2 (Erf2) as well as Erf4 were identified in a genetic screen that required *S*-acylation of yeast Ras2 for survival (79). These proteins were later shown to form a complex localized in the endoplasmic reticulum (80) and catalyze the acylation of Ras2 in vitro (81). DHHC9 is the mammalian ortholog of Erf2, and along with its binding partner Golgi complex protein 16 (GCP16), can catalyze the acylation of N- and H-ras (114). Although the most likely candidate, to date no one has shown that DHHC9/GCP16 is responsible for acylating Ras in cells. The role of Erf4 and GCP16 is unknown, as no other DHHC proteins tested have required binding partners for activity. DHHC9 has been associated with a number of human diseases (Table 1.3) including colorectal cancer (140, 142) and X-linked mental retardation (139). This appendix highlights two projects related to DHHC9 mediated protein *S*-acylation.

### **FKBP12 binds to acylated H-ras and promotes depalmitoylation.**

Proline isomerization of H-ras affects its palmitoylation status. Workers within the laboratory of Mark Philips noted that green fluorescent protein (GFP) tagged with last 19 amino acids of H-ras recapitulated the full-length protein localization to both the Golgi and PM, but GFP tagged with the last 10 amino acids of H-ras localized only to the PM. The last ten amino acids of H-ras (-GCMSCKCVLS.) has two cysteine residues known to be acylated and a CaaX box cysteine residue known to be *prenylated*.

Acylation of these constructs was evaluated and the shorter GFP-10aa tail was shown to contain 2.5 times more radiolabeled palmitate than the GFP-19aa tail. The additional nine residues (-LNPPDESGP-) in the longer GFP tail was rich in proline residues and led researchers to hypothesize that proline isomerization may regulate H-ras acylation and thereby trafficking.

Inhibiting prolyl isomerization was used to test this hypothesis. Indeed, chemical inhibition of prolyl isomerization increased H-ras incorporation of radiolabeled palmitate up to 4-fold. FK506-binding proteins (FKBPs) are one family of prolyl isomerases with FKBP12 being the best characterized, and it is inhibited by FK506. Cells expressing the GFP-19aa tail of H-ras, when treated with FK506 or FKBP12 siRNA showed an increase in palmitate incorporation into GFP-19aa tail. This was not observed when constructs lacking the proline residues or the GFP-10aa tail were expressed. This increase in H-ras acylation when FKBP12 activity is suppressed could result from increased H-ras acylation, decreased H-ras deacylation, or both.

Directly testing whether FKBP12 altered H-ras acylation with purified components was my contribution to this work. In a radiolabel-based in vitro PAT assay, DHHC9/GCP16 was used to palmitoylate the last 30aa of H-ras fused to GST, and the effects of FKBP12 and FK506 on this reaction were monitored. The last 30aa rather than the last 19aa were used because purified preparations of farnesylated protein were available. As shown in Figure A.1, inclusion of FKBP and/or FK506 into the reaction did not significantly alter the palmitoylation of GST-H-ras 30aa tail [PAT ID#617]. Three similar experiments were performed to confirm the result: one with full-length N-

terminally tagged H-ras, His<sub>6</sub>-H-ras [PAT ID#621], and the remaining two with full-length N-terminally tagged N-ras, His<sub>6</sub>-N-ras, including a titration of FKBP12 [PAT ID#621 and 625]. In no case was FKBP12 or FK506 able to alter DHHC9-mediated acylation of H-ras or N-ras. While their effect could be through another DHHC protein in cells, it seemed more likely that FKBP12-mediated prolyl isomerization was decreasing deacylation of H-ras in cells.

Indeed, further experiments showed that FKBP12 affected the acylation level and localization of H-ras by increasing the deacylation of H-ras. Co-immunoprecipitation experiments showed that FKBP12 bound to H-ras and N-ras, but not K-ras. These interactions were blocked by FK506, 2-bromopalmitate, or mutation of the H-ras acylation sites (C181,184S), suggesting that acylation of H-ras was required for FKBP12 binding. Interestingly, FKBP12 did not require the C-terminal proline residues to co-IP with H-ras. Additional functional studies showed that FKBP12 affected H-ras localization and retrograde trafficking from the PM to the Golgi. Inhibition of FKBP12 also resulted in greater GTP-loading of endogenous H-ras following EGF stimulation, consistent with inhibition of FKBP12 preventing depalmitoylation of H-ras and confining it to the PM adjacent upstream activators.

The role of FKBP12 in modulating Ras deacylation adds a new level to complexity to the regulation of Ras signaling. It also raises several questions. For example, how does soluble FKBP12 bind the membrane anchored acylated tail of H-ras and does the deacylation involve recruitment of acyl-protein thioesterases (APTs)? Another issue raised in the Preview for this article (224) is that FK506 is currently in

use as an immunosuppressant and the work here may suggest FK506 has tumor promoting properties. Given the challenges in monitoring prolyl isomerization, it remains to be determined whether the interplay between these two modifications is unique to Ras signaling or if prolyl *cis-trans* isomerization is a broader regulator of protein *S*-acylation.

**DHHC9 X-linked mental retardation mutant R148W displays reduced association with binding partner GCP16 and protein *S*-acyltransferase activity.**

Genetic studies in humans have linked DHHC9 to X-linked mental retardation (XLMR) (139). In order to find genes that cause XLMR, researchers characterized a cohort of 250 families in which at least two males have clinically diagnosed mental retardation with no known molecular cause. Two truncations arising from a 4 bp insertion and a mutation causing alternative exon splicing, and two missense mutations were found in the *ZDHHC9* gene. The *ZDHHC9* missense mutations resulted in proteins in which arginine 148 was changed to tryptophan (R148W) and proline 150 to serine (P150S). These residues (R148 and P150) are conserved in DHHC9 orthologs from yeast to humans whereas overall sequence conservation is only 30%. Both mutations are upstream of the canonical DHHC motif but still within the 51aa cysteine-rich domain. Our laboratory has begun to investigate the protein product of these mutations for differences in localization, PAT activity, and protein stability.

Given my expertise in analyzing DHHC PAT activity, I set out to determine if either of these point mutants affects the ability of DHHC9 to palmitoylate H-ras.

Coworkers generated Baculoviruses to express R148W and P150S DHHC9-myc-His<sub>6</sub> proteins in Sf9 insect cells. The P150S virus had poor expression levels and was not analyzed further. The R148W DHHC9 was co-expressed with FLAG-GCP16 and purified over nickel resin (Figure A.2A). Interestingly, unlike similar purifications with WT DHHC9, the binding partner GCP16 did not co-purify with R148W DHHC9. Another purification was attempted and compared to identical purifications of WT DHHC9 and both with and without GCP16. As shown with nickel elutions in Figure A.2B, the R148W mutant displayed markedly reduced ability to co-purify GCP16 relative to WT DHHC9. Because the nickel elutions contained a number of contaminating proteins (not shown), we attempted to use myc-affinity resin to further purify all four samples. The yield from such purifications was insufficient to use in activity assay, however immunoblotting of elutions did confirm again that WT DHHC9 binds GCP16 whereas the R148W mutant does not (Figure A.2C). Collectively, these results demonstrate that R148W DHHC9 displays reduced affinity for GCP16.

Using samples normalized for equal amounts of DHHC9 protein (Figure A.3B), I determined the ability of WT and R148W to palmitoylate H-ras using the standard radiolabel-based PAT assay (Figure A.3A). WT DHHC9 with GCP16 robustly palmitoylated H-ras and autoacylated as previously described by our group (114). DHHC9 alone also autoacylated and palmitoylated H-ras but only at 30% of the levels observed when GCP16 was present. This is unlike the original characterization of DHHC9 that showed no activity in the absence of GCP16 (114). R148W alone and with GCP16 displayed a similar pattern to WT DHHC9 but with activities reduced by 50%.

These results suggest that R148W DHHC9 has reduced PAT activity because of its reduced association with GCP16.

While these results do not provide a clear connection to XLMR, they do raise several new questions. One difference between the original characterization of DHHC9 PAT activity and those here is that in the earlier studies PAT assay buffers contained thiol-based reducing agents. These reagents may have cleaved the acyl-enzyme thioester bonds present in the DHHC9 alone reactions here. This would point to a role for GCP16 in protecting the acyl-enzyme intermediate from hydrolysis. Measuring acyl-CoA hydrolysis by WT and R148W could test this hypothesis. R148W may display reduced PAT activity exclusively due to reduced GCP16 interaction or R148W may also be detrimental to catalysis. Titration of GCP16 into the PAT reaction may differentiate these possibilities. Interestingly, in the genetic screen in yeast that identified Erf2 as a Ras PAT, mutation of the R148 equivalent residue, R182, to alanine was not lethal. This may suggest that in cells R148W retains enough PAT activity to acylate Ras and that defects in the acylation of other substrates are responsible for the XLMR phenotype. Techniques have been described to find protein substrates of individual DHHC proteins in mammalian cells (225); such methods may be needed to draw a connection between DHHC9 and XLMR. Further, cell-based work examining protein localization and stability will also be important for characterizing these disease-associated mutations.

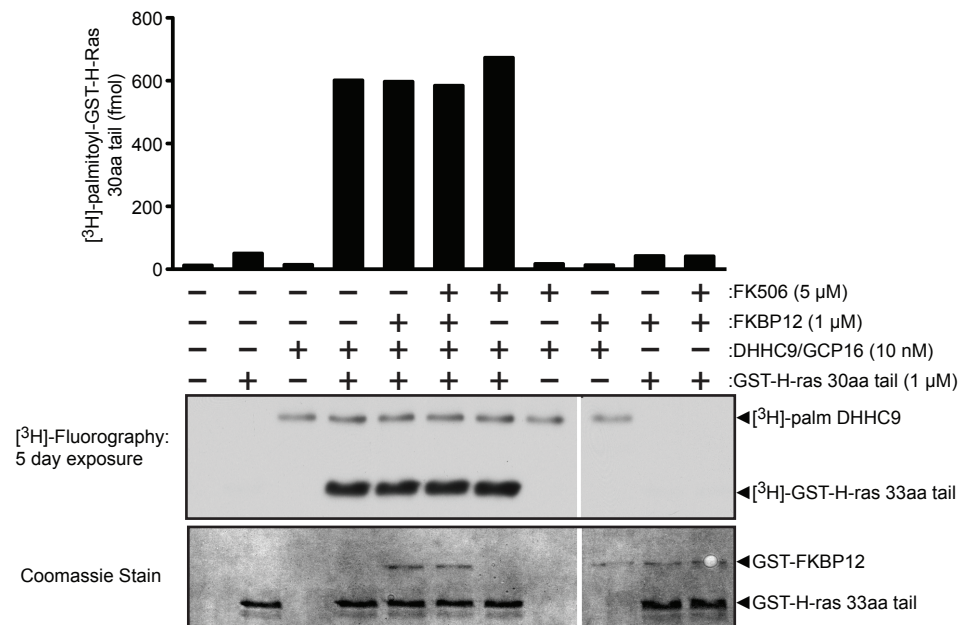


**Figure A.1. Palmitoylation of GST-H-ras 30aa tail in vitro using purified DHHC9/GCP16 and [3H]-palmitoyl-CoA in the presence or absence of FK506 or recombinant FKBP12.** The indicated concentrations of reaction components were incubated at 25°C for 7 min. Reactions were stopped with sample buffer and resolved by SDS-PAGE. GST-H-ras 30aa tail bands were excised from one set of gels and processed for scintillation counting, while the other set of gels was processed for fluorography and exposed to film at -80°C [PAT ID#617].

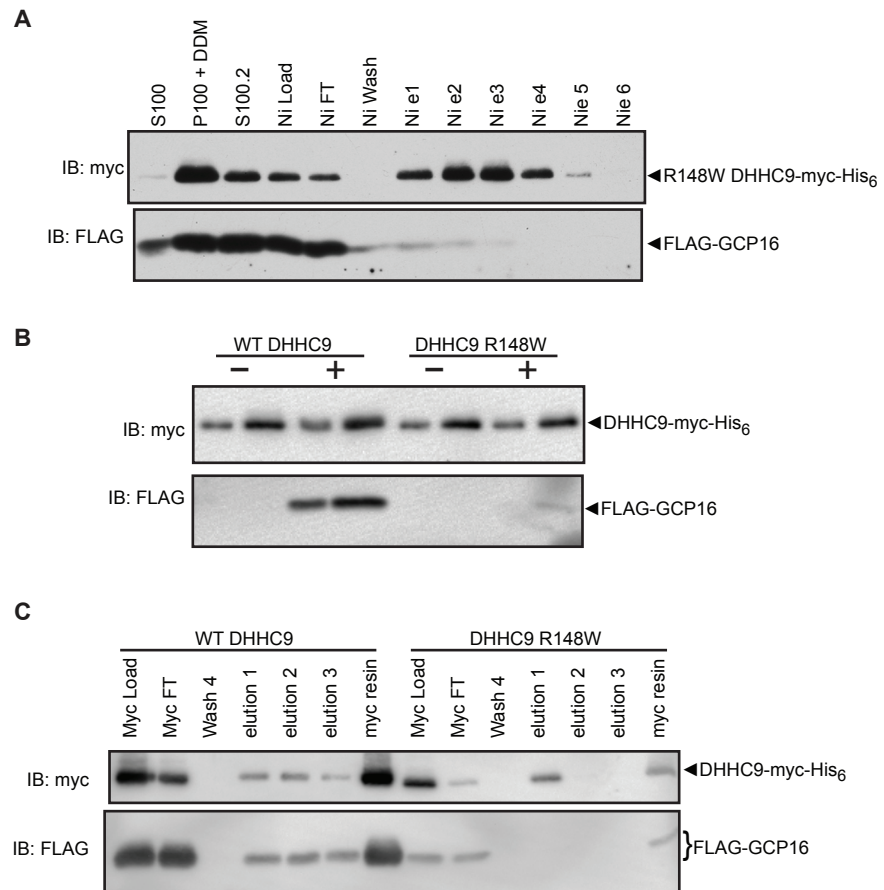


**Figure A.2. DHHC9 R148W displays reduced interaction with GCP16.** *A*, Purification of DHHC9-myc-His<sub>6</sub> R148W (pML1311) co-expressed with FLAG-GCP16 (pML756) over Ni-NTA resin. Sf9 cells were co-infected with viruses expressing both constructs, harvested, and lysed by nitrogen cavitation. The soluble (S100) and membrane (P100) fractions were separated by centrifugation. Detergent (DDM) was added to the membranes to extract DHHC9. This detergent extract (S100.2) was diluted and loaded onto Ni-NTA resin. The flow through (FT) was collected, the column was washed, and proteins were eluted with imidazole. Immunoblotting was used to detect proteins within each sample [PAT ID#725]. *B*, WT and R148W DHHC9-myc-His<sub>6</sub> were expressed with or without FLAG-GCP16 in Sf9 cells. Purification with Ni-NTA resin was performed as in *A*. Two volumes of a nickel elution were loaded for each sample [PAT ID#775]. *C*, Partially purified nickel elutions containing WT or R148W DHHC9-myc-His<sub>6</sub> co-expressed with FLAG-GCP16 were bound to myc-affinity resin. The flow through (FT) was collected, the column was washed, and proteins were eluted with myc peptide. A sample of myc-affinity resin after elution was also run on the gel [PAT ID#737]. Purification and immunoblotting procedures were similar to those described in Chapters 3 and 4.

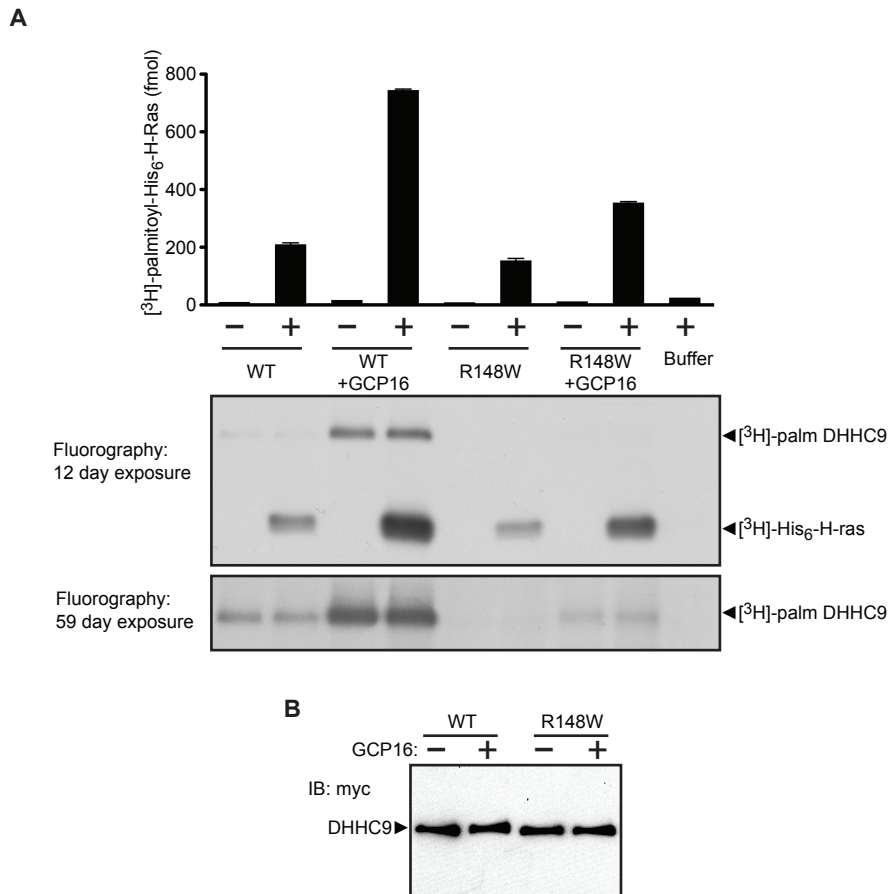


**Figure A.3. DHHC9 R148W displays reduced protein S-acyltransferase activity for H-ras.** *A*, Normalized amounts of partially purified DHHC9-myc-His<sub>6</sub> WT or R148W co-expressed with or without FLAG-GCP16 were incubated with His<sub>6</sub>-H-ras and radiolabeled palmCoA. Fluorography exposures were at -80°C for the indicated time. The longer exposure shows that WT DHHC9 alone and R148W DHHC9 with GCP16 incorporated palmitate, albeit at low levels. *B*, Immunoblot of the reactions in *A* to show that equal amounts of DHHC9 were assayed [PAT ID#785].

## References

1. Nadolski, M. J., and Linder, M. E. 2007. Protein lipidation. *FEBS J.* **274**:5202-5210.
2. Fujita, M., and Kinoshita, T. 2010. Structural remodeling of GPI anchors during biosynthesis and after attachment to proteins. *FEBS Letters.* **584**:1670-1677.
3. Chatterjee, S., and Mayor, S. 2001. The GPI-anchor and protein sorting. *Cell. Mol. Life Sci.* **58**:1969-1987.
4. Takeda, J., and Kinoshita, T. 1995. GPI-anchor biosynthesis. *Trends Biochem. Sci.* **20**:367-371.
5. Chang, S.-C., and Magee, A. I. 2009. Acyltransferases for secreted signalling proteins (Review). *Mol. Membr. Biol.* **26**:104-113.
6. Resh, M. D. 2006. Palmitoylation of ligands, receptors, and intracellular signaling molecules. *Sci. STKE.* **2006**:re14.
7. Miura, G. I., and Treisman, J. E. 2006. Lipid modification of secreted signaling proteins. *Cell Cycle.* **5**:1184-1188.
8. Buglino, J. A., and Resh, M. D. 2008. Hhat is a palmitoylacyltransferase with specificity for N-palmitoylation of Sonic Hedgehog. *J. Biol. Chem.* **283**:22076-22088.
9. Kleuss, C., and Krause, E. 2003. Galpha(s) is palmitoylated at the N-terminal glycine. *EMBO J.* **22**:826-832.
10. Linder, M. E. 2001. Reversible modification of proteins with thioester-linked fatty acids, in *Protein Lipidation*, pp 215-240. Academic Press.
11. Stoffyn, P., and Folch-Pi, J. 1971. On the type of linkage binding fatty acids present in brain white matter proteolipid apoprotein. *Biochemical and Biophysical Research Communications.* **44**:157-161.
12. Gagnon, J., Finch, P. R., Wood, D. D., and Moscarello, M. A. 1971. Isolation of a highly purified myelin protein. *Biochemistry.* **10**:4756-4763.
13. Schmidt, M. F., Bracha, M., and Schlesinger, M. J. 1979. Evidence for covalent attachment of fatty acids to Sindbis virus glycoproteins. *Proc. Natl. Acad. Sci. U.S.A.* **76**:1687-1691.
14. Schlesinger, M. J., Magee, A. I., and Schmidt, M. F. 1980. Fatty acid acylation of proteins in cultured cells. *J. Biol. Chem.* **255**:10021-10024.
15. Wilson, J. P., Raghavan, A. S., Yang, Y.-Y., Charron, G., and Hang, H. C. 2011. Proteomic Analysis of Fatty-acylated Proteins in Mammalian Cells with Chemical Reporters Reveals S-Acylation of Histone H3 Variants. *Molecular & Cellular Proteomics.* **10**.
16. Roth, A. F., Wan, J., Bailey, A. O., Sun, B., Kuchar, J. A., Green, W. N., Phinney, B. S., Yates, J. R., 3rd, and Davis, N. G. 2006. Global analysis of protein palmitoylation in yeast. *Cell.* **125**:1003-1013.
17. Kang, R., Wan, J., Arstikaitis, P., Takahashi, H., Huang, K., Bailey, A. O., Thompson, J. X., Roth, A. F., Drisdell, R. C., Mastro, R., Green, W. N., Yates, J. R., 3rd, Davis, N. G., and El-Husseini, A. 2008. Neural palmitoyl-proteomics reveals dynamic synaptic palmitoylation. *Nature.* **456**:904-909.

18. Forrester, M. T., Hess, D. T., Thompson, J. W., Hultman, R., Moseley, M. A., Stamler, J. S., and Casey, P. J. 2011. Site-specific analysis of protein S-acylation by resin-assisted capture. *J. Lipid Res.* **52**:393-398.
19. Emmer, B. T., Nakayasu, E. S., Souther, C., Choi, H., Sobreira, T. J. P., Epting, C. L., Nesvizhskii, A. I., Almeida, I. C., and Engman, D. M. 2011. Global analysis of protein palmitoylation in African trypanosomes. *Eukaryotic Cell.* **10**:455-463.
20. Yang, W., Di Vizio, D., Kirchner, M., Steen, H., and Freeman, M. R. 2010. Proteome scale characterization of human S-acylated proteins in lipid raft-enriched and non-raft membranes. *Mol. Cell Proteomics.* **9**:54-70.
21. Gutierrez, L., and Magee, A. I. 1991. Characterization of an acyltransferase acting on p21N-ras protein in a cell-free system. *Biochimica et Biophysica Acta (BBA) - Protein Structure and Molecular Enzymology.* **1078**:147-154.
22. Berthiaume, L., and Resh, M. D. 1995. Biochemical characterization of a palmitoyl acyltransferase activity that palmitoylates myristoylated proteins. *J. Biol. Chem.* **270**:22399-22405.
23. Liu, L., Dudler, T., and Gelb, M. H. 1996. Purification of a Protein Palmitoyltransferase that Acts on H-Ras Protein and on a C-terminal N-Ras Peptide. *Journal of Biological Chemistry.* **271**:23269 -23276.
24. Liu, L., Dudler, T., and Gelb, M. H. 1999. Purification of a protein palmitoyltransferase that acts on H-Ras protein and on a C-terminal N-Ras peptide. *Journal of Biological Chemistry.* **274**:3252.
25. Hiol, A., Caron, J. M., Smith, C. D., and Jones, T. L. Z. 2003. Characterization and partial purification of protein fatty acyltransferase activity from rat liver. *Biochimica et Biophysica Acta (BBA) - Molecular and Cell Biology of Lipids.* **1635**:10-19.
26. Dunphy, J. T., Greentree, W. K., Manahan, C. L., and Linder, M. E. 1996. G-protein palmitoyltransferase activity is enriched in plasma membranes. *J. Biol. Chem.* **271**:7154-7159.
27. Ohno, Y., Kihara, A., Sano, T., and Igarashi, Y. 2006. Intracellular localization and tissue-specific distribution of human and yeast DHHC cysteine-rich domain-containing proteins. *Biochim. Biophys. Acta.* **1761**:474-483.
28. Duncan, J. A., and Gilman, A. G. 1996. Autoacylation of G protein alpha subunits. *J. Biol. Chem.* **271**:23594-23600.
29. Bizzozero, O. A., McGarry, J. F., and Lees, M. B. 1987. Autoacylation of myelin proteolipid protein with acyl coenzyme A. *J. Biol. Chem.* **262**:13550-13557.
30. Bharadwaj, M., and Bizzozero, O. A. 1995. Myelin P0 glycoprotein and a synthetic peptide containing the palmitoylation site are both autoacylated. *J. Neurochem.* **65**:1805-1815.
31. O'Brien, P. J., St Jules, R. S., Reddy, T. S., Bazan, N. G., and Zatz, M. 1987. Acylation of disc membrane rhodopsin may be nonenzymatic. *J. Biol. Chem.* **262**:5210-5215.
32. Kümmel, D., Walter, J., Heck, M., Heinemann, U., and Veit, M. 2010. Characterization of the self-palmitoylation activity of the transport protein particle component Bet3. *Cell. Mol. Life Sci.* **67**:2653-2664.

33. Mollner, S., Ferreira, P., Beck, K., and Pfeuffer, T. 1998. Nonenzymatic palmitoylation at Cys 3 causes extra-activation of the alpha-subunit of the stimulatory GTP-binding protein Gs. *Eur. J. Biochem.* **257**:236-241.
34. Scholich, K., Yigzaw, Y., and Patel, T. B. 2000. Cysteine 3 is not the site of in vitro palmitoylation on G(salpa). *Biochem. Biophys. Res. Commun.* **270**:131-136.
35. Zahler, W. L., Barden, R. E., and Cleland, W. W. 1968. Some physical properties of palmityl-coenzyme A micelles. *Biochim. Biophys. Acta.* **164**:1-11.
36. Knudsen, J., Neergaard, T. B., Gaigg, B., Jensen, M. V., and Hansen, J. K. 2000. Role of acyl-CoA binding protein in acyl-CoA metabolism and acyl-CoA-mediated cell signaling. *J. Nutr.* **130**:294S-298S.
37. Leventis, R., Juel, G., Knudsen, J. K., and Silvius, J. R. 1997. Acyl-CoA binding proteins inhibit the nonenzymic S-acylation of cysteinyl-containing peptide sequences by long-chain acyl-CoAs. *Biochemistry.* **36**:5546-5553.
38. Rocks, O., Peyker, A., Kahms, M., Verveer, P. J., Koerner, C., Lumbierres, M., Kuhlmann, J., Waldmann, H., Wittinghofer, A., and Bastiaens, P. I. H. 2005. An acylation cycle regulates localization and activity of palmitoylated Ras isoforms. *Science.* **307**:1746-1752.
39. Dunphy, J. T., Schroeder, H., Leventis, R., Greentree, W. K., Knudsen, J. K., Silvius, J. R., and Linder, M. E. 2000. Differential effects of acyl-CoA binding protein on enzymatic and non-enzymatic thioacylation of protein and peptide substrates. *Biochim. Biophys. Acta.* **1485**:185-198.
40. Bañó, M. C., Jackson, C. S., and Magee, A. I. 1998. Pseudo-enzymatic S-acylation of a myristoylated yes protein tyrosine kinase peptide in vitro may reflect non-enzymatic S-acylation in vivo. *Biochem. J.* **330 ( Pt 2)**:723-731.
41. Quesnel, S., and Silvius, J. R. 1994. Cysteine-containing peptide sequences exhibit facile uncatalyzed transacylation and acyl-CoA-dependent acylation at the lipid bilayer interface. *Biochemistry.* **33**:13340-13348.
42. Xue, Y., Chen, H., Jin, C., Sun, Z., and Yao, X. 2006. NBA-Palm: prediction of palmitoylation site implemented in Naïve Bayes algorithm. *BMC Bioinformatics.* **7**:458.
43. Zhou, F., Xue, Y., Yao, X., and Xu, Y. 2006. CSS-Palm: palmitoylation site prediction with a clustering and scoring strategy (CSS). *Bioinformatics.* **22**:894-896.
44. Ren, J., Wen, L., Gao, X., Jin, C., Xue, Y., and Yao, X. 2008. CSS-Palm 2.0: an updated software for palmitoylation sites prediction. *Protein Eng. Des. Sel.* **21**:639-644.
45. Wang, X.-B., Wu, L.-Y., Wang, Y.-C., and Deng, N.-Y. 2009. Prediction of palmitoylation sites using the composition of k-spaced amino acid pairs. *Protein Eng. Des. Sel.* **22**:707-712.
46. Li, Y.-X., Shao, Y.-H., and Deng, N.-Y. 2011. Improved prediction of palmitoylation sites using PWMs and SVM. *Protein Pept. Lett.* **18**:186-193.
47. Hu, L.-L., Wan, S.-B., Niu, S., Shi, X.-H., Li, H.-P., Cai, Y.-D., and Chou, K.-C. 2011. Prediction and analysis of protein palmitoylation sites. *Biochimie.* **93**:489-496.
48. Peitzsch, R. M., and McLaughlin, S. 1993. Binding of acylated peptides and fatty acids to phospholipid vesicles: pertinence to myristoylated proteins. *Biochemistry.* **32**:10436-10443.

49. Shahinian, S., and Silvius, J. R. 1995. Doubly-lipid-modified protein sequence motifs exhibit long-lived anchorage to lipid bilayer membranes. *Biochemistry*. **34**:3813-3822.
50. Silvius, J. R., and l' Heureux, F. 1994. Fluorimetric evaluation of the affinities of isoprenylated peptides for lipid bilayers. *Biochemistry*. **33**:3014-3022.
51. Resh, M. D. 2006. Trafficking and signaling by fatty-acylated and prenylated proteins. *Nat. Chem. Biol.* **2**:584-590.
52. Aitken, A., Cohen, P., Santikarn, S., Williams, D. H., Calder, A. G., Smith, A., and Klee, C. B. 1982. Identification of the NH<sub>2</sub>-terminal blocking group of calcineurin B as myristic acid. *FEBS Letters*. **150**:314-318.
53. Carr, S. A., Biemann, K., Shoji, S., Parmelee, D. C., and Titani, K. 1982. n-Tetradecanoyl is the NH<sub>2</sub>-terminal blocking group of the catalytic subunit of cyclic AMP-dependent protein kinase from bovine cardiac muscle. *Proceedings of the National Academy of Sciences*. **79**:6128 -6131.
54. Duronio, R. J., Towler, D. A., Heuckeroth, R. O., and Gordon, J. I. 1989. Disruption of the yeast N-myristoyl transferase gene causes recessive lethality. *Science*. **243**:796-800.
55. Ntwasa, M., Aapias, S., Schiffmann, D. A., and Gay, N. J. 2001. Drosophila Embryos Lacking N-Myristoyltransferase Have Multiple Developmental Defects. *Experimental Cell Research*. **262**:134-144.
56. Resh, M. D. 1999. Fatty acylation of proteins: new insights into membrane targeting of myristoylated and palmitoylated proteins. *Biochimica et Biophysica Acta (BBA) - Molecular Cell Research*. **1451**:1-16.
57. Martin, D. D. O., Beauchamp, E., and Berthiaume, L. G. 2011. Post-translational myristoylation: Fat matters in cellular life and death. *Biochimie*. **93**:18-31.
58. Zha, J., Weiler, S., Oh, K. J., Wei, M. C., and Korsmeyer, S. J. 2000. Posttranslational N-myristoylation of BID as a molecular switch for targeting mitochondria and apoptosis. *Science*. **290**:1761-1765.
59. Utsumi, T., Sakurai, N., Nakano, K., and Ishisaka, R. 2003. C-terminal 15 kDa fragment of cytoskeletal actin is posttranslationally N-myristoylated upon caspase-mediated cleavage and targeted to mitochondria. *FEBS Lett.* **539**:37-44.
60. Sakurai, N., and Utsumi, T. 2006. Posttranslational N-myristoylation is required for the anti-apoptotic activity of human tGelsolin, the C-terminal caspase cleavage product of human gelsolin. *J. Biol. Chem.* **281**:14288-14295.
61. Vilas, G. L., Corvi, M. M., Plummer, G. J., Seime, A. M., Lambkin, G. R., and Berthiaume, L. G. 2006. Posttranslational myristoylation of caspase-activated p21-activated protein kinase 2 (PAK2) potentiates late apoptotic events. *Proc. Natl. Acad. Sci. U.S.A.* **103**:6542-6547.
62. Rudnick, D. A., McWherter, C. A., Adams, S. P., Ropson, I. J., Duronio, R. J., and Gordon, J. I. 1990. Structural and functional studies of *Saccharomyces cerevisiae* myristoyl-CoA:protein N-myristoyltransferase produced in *Escherichia coli*. Evidence for an acyl-enzyme intermediate. *J. Biol. Chem.* **265**:13370-13378.

63. Peseckis, S. M., and Resh, M. D. 1994. Fatty acyl transfer by human N-myristyl transferase is dependent upon conserved cysteine and histidine residues. *J. Biol. Chem.* **269**:30888-30892.
64. Rudnick, D. A., McWherter, C. A., Rocque, W. J., Lennon, P. J., Getman, D. P., and Gordon, J. I. 1991. Kinetic and structural evidence for a sequential ordered Bi Bi mechanism of catalysis by *Saccharomyces cerevisiae* myristoyl-CoA:protein N-myristoyltransferase. *J. Biol. Chem.* **266**:9732-9739.
65. Rocque, W. J., McWherter, C. A., Wood, D. C., and Gordon, J. I. 1993. A comparative analysis of the kinetic mechanism and peptide substrate specificity of human and *Saccharomyces cerevisiae* myristoyl-CoA:protein N-myristoyltransferase. *Journal of Biological Chemistry.* **268**:9964 -9971.
66. Weston, S. A., Camble, R., Colls, J., Rosenbrock, G., Taylor, I., Egerton, M., Tucker, A. D., Tunnicliffe, A., Mistry, A., Mancina, F., de la Fortelle, E., Irwin, J., Bricogne, G., and Pauptit, R. A. 1998. Crystal structure of the anti-fungal target N-myristoyl transferase. *Nat. Struct. Biol.* **5**:213-221.
67. Bhatnagar, R. S., Fütterer, K., Farazi, T. A., Korolev, S., Murray, C. L., Jackson-Machelski, E., Gokel, G. W., Gordon, J. I., and Waksman, G. 1998. Structure of N-myristoyltransferase with bound myristoylCoA and peptide substrate analogs. *Nat. Struct. Biol.* **5**:1091-1097.
68. Farazi, T. A., Waksman, G., and Gordon, J. I. 2001. Structures of *Saccharomyces cerevisiae* N-myristoyltransferase with bound myristoylCoA and peptide provide insights about substrate recognition and catalysis. *Biochemistry.* **40**:6335-6343.
69. Farazi, T. A., Waksman, G., and Gordon, J. I. 2001. The biology and enzymology of protein N-myristoylation. *J. Biol. Chem.* **276**:39501-39504.
70. Kamiya, Y., Sakurai, A., Tamura, S., Takahashi, N., Abe, K., Tsuchiya, E., Fukui, S., Kitada, C., and Fujino, M. 1978. Structure of rhodotorucine , a novel lipopeptide, inducing mating tube formation in. *Biochemical and Biophysical Research Communications.* **83**:1077-1083.
71. Casey, P. J., Solski, P. A., Der, C. J., and Buss, J. E. 1989. p21ras is modified by a farnesyl isoprenoid. *Proceedings of the National Academy of Sciences.* **86**:8323 -8327.
72. Reiss, Y., Goldstein, J. L., Seabra, M. C., Casey, P. J., and Brown, M. S. 1990. Inhibition of purified p21ras farnesyl:protein transferase by Cys-AAX tetrapeptides. *Cell.* **62**:81-88.
73. Goodman, L. E., Judd, S. R., Farnsworth, C. C., Powers, S., Gelb, M. H., Glomset, J. A., and Tamanoi, F. 1990. Mutants of *Saccharomyces cerevisiae* defective in the farnesylation of Ras proteins. *Proc. Natl. Acad. Sci. U.S.A.* **87**:9665-9669.
74. He, B., Chen, P., Chen, S. Y., Vancura, K. L., Michaelis, S., and Powers, S. 1991. RAM2, an essential gene of yeast, and RAM1 encode the two polypeptide components of the farnesyltransferase that prenylates a-factor and Ras proteins. *Proc. Natl. Acad. Sci. U.S.A.* **88**:11373-11377.
75. Kohl, N. E., Diehl, R. E., Schaber, M. D., Rands, E., Soderman, D. D., He, B., Moores, S. L., Pompliano, D. L., Ferro-Novick, S., and Powers, S. 1991. Structural homology among mammalian and *Saccharomyces cerevisiae* isoprenyl-protein transferases. *J. Biol. Chem.* **266**:18884-18888.

76. Lane, K. T., and Beese, L. S. 2006. Thematic review series: lipid posttranslational modifications. Structural biology of protein farnesyltransferase and geranylgeranyltransferase type I. *J. Lipid Res.* **47**:681-699.
77. Furfine, E. S., Leban, J. J., Landavazo, A., Moomaw, J. F., and Casey, P. J. 1995. Protein farnesyltransferase: kinetics of farnesyl pyrophosphate binding and product release. *Biochemistry.* **34**:6857-6862.
78. Tschantz, W. R., Furfine, E. S., and Casey, P. J. 1997. Substrate binding is required for release of product from mammalian protein farnesyltransferase. *J. Biol. Chem.* **272**:9989-9993.
79. Bartels, D. J., Mitchell, D. A., Dong, X., and Deschenes, R. J. 1999. Erf2, a novel gene product that affects the localization and palmitoylation of Ras2 in *Saccharomyces cerevisiae*. *Mol. Cell. Biol.* **19**:6775-6787.
80. Zhao, L., Lobo, S., Dong, X., Ault, A. D., and Deschenes, R. J. 2002. Erf4p and Erf2p form an endoplasmic reticulum-associated complex involved in the plasma membrane localization of yeast Ras proteins. *J. Biol. Chem.* **277**:49352-49359.
81. Lobo, S., Greentree, W. K., Linder, M. E., and Deschenes, R. J. 2002. Identification of a Ras palmitoyltransferase in *Saccharomyces cerevisiae*. *J. Biol. Chem.* **277**:41268-41273.
82. Roth, A. F., Feng, Y., Chen, L., and Davis, N. G. 2002. The yeast DHHC cysteine-rich domain protein Akr1p is a palmitoyl transferase. *J. Cell Biol.* **159**:23-28.
83. Mitchell, D. A., Vasudevan, A., Linder, M. E., and Deschenes, R. J. 2006. Protein palmitoylation by a family of DHHC protein S-acyltransferases. *J. Lipid Res.* **47**:1118-1127.
84. Bannan, B. A., Van Etten, J., Kohler, J. A., Tsoi, Y., Hansen, N. M., Sigmon, S., Fowler, E., Buff, H., Williams, T. S., Ault, J. G., Glaser, R. L., and Korey, C. A. 2008. The *Drosophila* protein palmitoylome: characterizing palmitoyl-thioesterases and DHHC palmitoyl-transferases. *Fly (Austin).* **2**:198-214.
85. Hemsley, P. A., and Grierson, C. S. 2008. Multiple roles for protein palmitoylation in plants. *Trends Plant Sci.* **13**:295-302.
86. Greaves, J., and Chamberlain, L. H. 2011. DHHC palmitoyl transferases: substrate interactions and (patho)physiology. *Trends Biochem. Sci.* **36**:245-253.
87. Putilina, T., Wong, P., and Gentleman, S. 1999. The DHHC domain: a new highly conserved cysteine-rich motif. *Mol. Cell. Biochem.* **195**:219-226.
88. Politis, E. G., Roth, A. F., and Davis, N. G. 2005. Transmembrane topology of the protein palmitoyl transferase Akr1. *J. Biol. Chem.* **280**:10156-10163.
89. González Montoro, A., Quiroga, R., Maccioni, H. J. F., and Valdez Taubas, J. 2009. A novel motif at the C-terminus of palmitoyltransferases is essential for Swf1 and Pfa3 function in vivo. *Biochem. J.* **419**:301-308.
90. Faergeman, N. J., and Knudsen, J. 1997. Role of long-chain fatty acyl-CoA esters in the regulation of metabolism and in cell signalling. *Biochem. J.* **323 ( Pt 1)**:1-12.
91. Smotrys, J. E., Schoenfish, M. J., Stutz, M. A., and Linder, M. E. 2005. The vacuolar DHHC-CRD protein Pfa3p is a protein acyltransferase for Vac8p. *J. Cell Biol.* **170**:1091-1099.

92. Oyama, T., Miyoshi, Y., Koyama, K., Nakagawa, H., Yamori, T., Ito, T., Matsuda, H., Arakawa, H., and Nakamura, Y. 2000. Isolation of a novel gene on 8p21.3-22 whose expression is reduced significantly in human colorectal cancers with liver metastasis. *Genes Chromosomes Cancer*. **29**:9-15.
93. Noritake, J., Fukata, Y., Iwanaga, T., Hosomi, N., Tsutsumi, R., Matsuda, N., Tani, H., Iwanari, H., Mochizuki, Y., Kodama, T., Matsuura, Y., Bredt, D. S., Hamakubo, T., and Fukata, M. 2009. Mobile DHHC palmitoylating enzyme mediates activity-sensitive synaptic targeting of PSD-95. *J. Cell Biol.* **186**:147-160.
94. Greaves, J., Carmichael, J. A., and Chamberlain, L. H. 2011. The palmitoyl transferase DHHC2 targets a dynamic membrane cycling pathway: regulation by a C-terminal domain. *Mol. Biol. Cell.* **22**:1887-1895.
95. Greaves, J., Gorleku, O. A., Salaun, C., and Chamberlain, L. H. 2010. Palmitoylation of the SNAP25 protein family: specificity and regulation by DHHC palmitoyl transferases. *J. Biol. Chem.* **285**:24629-24638.
96. Jia, L., Linder, M. E., and Blumer, K. J. 2011. Gi/o signaling and the palmitoyltransferase DHHC2 regulate palmitate cycling and shuttling of RGS7 family-binding protein. *J. Biol. Chem.* **286**:13695-13703.
97. Dighe, S. A., and Kozminski, K. G. 2008. Swf1p, a member of the DHHC-CRD family of palmitoyltransferases, regulates the actin cytoskeleton and polarized secretion independently of its DHHC motif. *Mol. Biol. Cell.* **19**:4454-4468.
98. Kraft, B., Johswich, A., Kauczor, G., Scharenberg, M., Gerardy-Schahn, R., and Bakker, H. 2011. "Add-on" domains of Drosophila  $\beta$ 1,4-N-acetylgalactosaminyltransferase B in the stem region and its pilot protein. *Cell Mol Life Sci.*
99. Goytain, A., Hines, R. M., and Quamme, G. A. 2008. Huntingtin-interacting proteins, HIP14 and HIP14L, mediate dual functions, palmitoyl acyltransferase and Mg<sup>2+</sup> transport. *J. Biol. Chem.* **283**:33365-33374.
100. Hines, R. M., Kang, R., Goytain, A., and Quamme, G. A. 2010. Golgi-specific DHHC zinc finger protein GODZ mediates membrane Ca<sup>2+</sup> transport. *J. Biol. Chem.* **285**:4621-4628.
101. Roy, S., Plowman, S., Rotblat, B., Prior, I. A., Muncke, C., Grainger, S., Parton, R. G., Henis, Y. I., Kloog, Y., and Hancock, J. F. 2005. Individual palmitoyl residues serve distinct roles in H-ras trafficking, microlocalization, and signaling. *Mol. Cell. Biol.* **25**:6722-6733.
102. Henis, Y. I., Rotblat, B., and Kloog, Y. 2006. FRAP beam-size analysis to measure palmitoylation-dependent membrane association dynamics and microdomain partitioning of Ras proteins. *Methods*. **40**:183-190.
103. Singaraja, R. R., Kang, M. H., Vaid, K., Sanders, S. S., Vilas, G. L., Arstikaitis, P., Coutinho, J., Drisdell, R. C., El-Husseini, A. E. D., Green, W. N., Berthiaume, L., and Hayden, M. R. 2009. Palmitoylation of ATP-binding cassette transporter A1 is essential for its trafficking and function. *Circ. Res.* **105**:138-147.
104. Delint-Martinez, I., Willoughby, D., Hammond, G. V. R., Ayling, L. J., and Cooper, D. M. F. 2011. Palmitoylation targets AKAP79 to lipid rafts and promotes its regulation of the calcium sensitive adenylyl cyclase type 8. *J Biol Chem.*

105. Chakrabandhu, K., Hérincs, Z., Huault, S., Dost, B., Peng, L., Conchonaud, F., Marguet, D., He, H.-T., and Hueber, A.-O. 2007. Palmitoylation is required for efficient Fas cell death signaling. *EMBO J.* **26**:209-220.
106. Guardiola-Serrano, F., Rossin, A., Cahuzac, N., Luckeath, K., Melzer, I., Mailfert, S., Marguet, D., Zornig, M., and Hueber, A.-O. 2010. Palmitoylation of human FasL modulates its cell death-inducing function. *Cell Death and Dis.* **1**:e88.
107. Levental, I., Lingwood, D., Grzybek, M., Coskun, U., and Simons, K. 2010. Palmitoylation regulates raft affinity for the majority of integral raft proteins. *Proc. Natl. Acad. Sci. U.S.A.* **107**:22050-22054.
108. Harder, T., Scheiffele, P., Verkade, P., and Simons, K. 1998. Lipid domain structure of the plasma membrane revealed by patching of membrane components. *J. Cell Biol.* **141**:929-942.
109. Abrami, L., Leppla, S. H., and van der Goot, F. G. 2006. Receptor palmitoylation and ubiquitination regulate anthrax toxin endocytosis. *J. Cell Biol.* **172**:309-320.
110. Yang, H., Qu, L., Ni, J., Wang, M., and Huang, Y. 2008. Palmitoylation participates in G protein coupled signal transduction by affecting its oligomerization. *Mol. Membr. Biol.* **25**:58-71.
111. Yanai, A., Huang, K., Kang, R., Singaraja, R. R., Arstikaitis, P., Gan, L., Orban, P. C., Mullard, A., Cowan, C. M., Raymond, L. A., Drisdell, R. C., Green, W. N., Ravikumar, B., Rubinsztein, D. C., El-Husseini, A., and Hayden, M. R. 2006. Palmitoylation of huntingtin by HIP14 is essential for its trafficking and function. *Nat. Neurosci.* **9**:824-831.
112. Stoffel, R. H., Inglese, J., Macrae, A. D., Lefkowitz, R. J., and Premont, R. T. 1998. Palmitoylation increases the kinase activity of the G protein-coupled receptor kinase, GRK6. *Biochemistry.* **37**:16053-16059.
113. Mueller, G. M., Maarouf, A. B., Kinlough, C. L., Sheng, N., Kashlan, O. B., Okumura, S., Luthy, S., Kleyman, T. R., and Hughey, R. P. 2010. Cys palmitoylation of the beta subunit modulates gating of the epithelial sodium channel. *J. Biol. Chem.* **285**:30453-30462.
114. Swarthout, J. T., Lobo, S., Farh, L., Croke, M. R., Greentree, W. K., Deschenes, R. J., and Linder, M. E. 2005. DHHC9 and GCP16 constitute a human protein fatty acyltransferase with specificity for H- and N-Ras. *J. Biol. Chem.* **280**:31141-31148.
115. Huang, K., Sanders, S. S., Kang, R., Carroll, J. B., Sutton, L., Wan, J., Singaraja, R., Young, F. B., Liu, L., El-Husseini, A., Davis, N. G., and Hayden, M. R. 2011. Wild-type HTT modulates the enzymatic activity of the neuronal palmitoyl transferase HIP14. *Hum Mol Genet.*
116. Charych, E. I., Jiang, L.-X., Lo, F., Sullivan, K., and Brandon, N. J. 2010. Interplay of palmitoylation and phosphorylation in the trafficking and localization of phosphodiesterase 10A: implications for the treatment of schizophrenia. *J. Neurosci.* **30**:9027-9037.
117. Ho, G. P. H., Selvakumar, B., Mukai, J., Hester, L. D., Wang, Y., Gogos, J. A., and Snyder, S. H. 2011. S-Nitrosylation and S-Palmitoylation Reciprocally Regulate Synaptic Targeting of PSD-95. *Neuron.* **71**:131-141.

118. Veit, M., and Schmidt, M. F. G. 2006. Palmitoylation of influenza virus proteins. *Berl. Munch. Tierarztl. Wochenschr.* **119**:112-122.
119. Corvi, M. M., Berthiaume, L. G., and De Napoli, M. G. 2011. Protein palmitoylation in protozoan parasites. *Front Biosci (Schol Ed)*. **3**:1067-1079.
120. Majeau, N., Fromentin, R., Savard, C., Duval, M., Tremblay, M. J., and Leclerc, D. 2009. Palmitoylation of hepatitis C virus core protein is important for virion production. *J. Biol. Chem.* **284**:33915-33925.
121. Huang, K., Yanai, A., Kang, R., Arstikaitis, P., Singaraja, R. R., Metzler, M., Mullard, A., Haigh, B., Gauthier-Campbell, C., Gutekunst, C.-A., Hayden, M. R., and El-Husseini, A. 2004. Huntingtin-interacting protein HIP14 is a palmitoyl transferase involved in palmitoylation and trafficking of multiple neuronal proteins. *Neuron*. **44**:977-986.
122. Ducker, C. E., Stettler, E. M., French, K. J., Upson, J. J., and Smith, C. D. 2004. Huntingtin interacting protein 14 is an oncogenic human protein: palmitoyl acyltransferase. *Oncogene*. **23**:9230-9237.
123. Fukata, M., Fukata, Y., Adesnik, H., Nicoll, R. A., and Brecht, D. S. 2004. Identification of PSD-95 palmitoylating enzymes. *Neuron*. **44**:987-996.
124. Okubo, K., Hamasaki, N., Hara, K., and Kageura, M. 1991. Palmitoylation of cysteine 69 from the COOH-terminal of band 3 protein in the human erythrocyte membrane. Acylation occurs in the middle of the consensus sequence of F--I-IICLAVL found in band 3 protein and G2 protein of Rift Valley fever virus. *J. Biol. Chem.* **266**:16420-16424.
125. Casey, W. M., Gibson, K. J., and Parks, L. W. 1994. Covalent attachment of palmitoleic acid (C16:1 delta 9) to proteins in *Saccharomyces cerevisiae*. Evidence for a third class of acylated proteins. *J. Biol. Chem.* **269**:2082-2085.
126. Fujimoto, T., Stroud, E., Whatley, R. E., Prescott, S. M., Muszbek, L., Laposata, M., and McEver, R. P. 1993. P-selectin is acylated with palmitic acid and stearic acid at cysteine 766 through a thioester linkage. *J. Biol. Chem.* **268**:11394-11400.
127. Veit, M., Reverey, H., and Schmidt, M. F. 1996. Cytoplasmic tail length influences fatty acid selection for acylation of viral glycoproteins. *Biochem. J.* **318 ( Pt 1)**:163-172.
128. Hallak, H., Muszbek, L., Laposata, M., Belmonte, E., Brass, L. F., and Manning, D. R. 1994. Covalent binding of arachidonate to G protein alpha subunits of human platelets. *J. Biol. Chem.* **269**:4713-4716.
129. Muszbek, L., and Laposata, M. 1993. Covalent modification of proteins by arachidonate and eicosapentaenoate in platelets. *J. Biol. Chem.* **268**:18243-18248.
130. Choi, Y.-W., Bae, S. M., Kim, Y.-W., Lee, H. N., Kim, Y. W., Park, T. C., Ro, D. Y., Shin, J. C., Shin, S. J., Seo, J.-S., and Ahn, W. S. 2007. Gene expression profiles in squamous cell cervical carcinoma using array-based comparative genomic hybridization analysis. *Int. J. Gynecol. Cancer*. **17**:687-696.
131. Brunner, R. M., Srikanthai, T., Murani, E., Wimmers, K., and Ponsuksili, S. 2011. Genes with expression levels correlating to drip loss prove association of their polymorphism with water holding capacity of pork. *Mol Biol Rep*.

132. Hungermann, D., Schmidt, H., Natrajan, R., Tidow, N., Poos, K., Reis-Filho, J. S., Brandt, B., Buerger, H., and Korsching, E. 2011. Influence of whole arm loss of chromosome 16q on gene expression patterns in oestrogen receptor-positive, invasive breast cancer. *J. Pathol.* **224**:517-528.
133. Sudo, H., Tsuji, A. B., Sugyo, A., Imai, T., Saga, T., and Harada, Y.-nobu. 2007. A loss of function screen identifies nine new radiation susceptibility genes. *Biochem. Biophys. Res. Commun.* **364**:695-701.
134. Mukai, J., Liu, H., Burt, R. A., Swor, D. E., Lai, W.-S., Karayiorgou, M., and Gogos, J. A. 2004. Evidence that the gene encoding ZDHHC8 contributes to the risk of schizophrenia. *Nat. Genet.* **36**:725-731.
135. Chen, W.-Y., Shi, Y.-Y., Zheng, Y.-L., Zhao, X.-Z., Zhang, G.-J., Chen, S.-Q., Yang, P.-D., and He, L. 2004. Case-control study and transmission disequilibrium test provide consistent evidence for association between schizophrenia and genetic variation in the 22q11 gene ZDHHC8. *Hum. Mol. Genet.* **13**:2991-2995.
136. Shin, H. D., Park, B. L., Bae, J. S., Park, T. J., Chun, J. Y., Park, C. S., Sohn, J.-W., Kim, B.-J., Kang, Y.-H., Kim, J. W., Kim, K.-H., Shin, T.-M., and Woo, S.-I. 2010. Association of ZDHHC8 polymorphisms with smooth pursuit eye movement abnormality. *Am. J. Med. Genet. B Neuropsychiatr. Genet.* **153B**:1167-1172.
137. Mukai, J., Dhillia, A., Drew, L. J., Stark, K. L., Cao, L., MacDermott, A. B., Karayiorgou, M., and Gogos, J. A. 2008. Palmitoylation-dependent neurodevelopmental deficits in a mouse model of 22q11 microdeletion. *Nat. Neurosci.* **11**:1302-1310.
138. Maynard, T. M., Meechan, D. W., Dudevoir, M. L., Gopalakrishna, D., Peters, A. Z., Heindel, C. C., Sugimoto, T. J., Wu, Y., Lieberman, J. A., and Lamantia, A.-S. 2008. Mitochondrial localization and function of a subset of 22q11 deletion syndrome candidate genes. *Mol. Cell. Neurosci.* **39**:439-451.
139. Raymond, F. L., Tarpey, P. S., Edkins, S., Tofts, C., O'Meara, S., Teague, J., Butler, A., Stevens, C., Barthorpe, S., Buck, G., Cole, J., Dicks, E., Gray, K., Halliday, K., Hills, K., Hinton, J., Jones, D., Menzies, A., Perry, J., Raine, K., Shepherd, R., Small, A., Varian, J., Widaa, S., Mallya, U., Moon, J., Luo, Y., Shaw, M., Boyle, J., Kerr, B., Turner, G., Quarrell, O., Cole, T., Easton, D. F., Wooster, R., Bobrow, M., Schwartz, C. E., Gecz, J., Stratton, M. R., and Futreal, P. A. 2007. Mutations in ZDHHC9, which encodes a palmitoyltransferase of NRAS and HRAS, cause X-linked mental retardation associated with a Marfanoid habitus. *Am. J. Hum. Genet.* **80**:982-987.
140. Mansilla, F., Birkenkamp-Demtroder, K., Kruhøffer, M., Sørensen, F. B., Andersen, C. L., Laiho, P., Aaltonen, L. A., Verspaget, H. W., and Orntoft, T. F. 2007. Differential expression of DHH9 in microsatellite stable and instable human colorectal cancer subgroups. *Br. J. Cancer.* **96**:1896-1903.
141. Maak, S., Boettcher, D., Tetens, J., Swalve, H. H., Wimmers, K., and Thaller, G. 2010. Expression of microRNAs is not related to increased expression of ZDHHC9 in hind leg muscles of splay leg piglets. *Mol. Cell. Probes.* **24**:32-37.
142. Birkenkamp-Demtroder, K., Christensen, L. L., Olesen, S. H., Frederiksen, C. M., Laiho, P., Aaltonen, L. A., Laurberg, S., Sørensen, F. B., Hagemann, R., and ØRntoft, T. F. 2002. Gene expression in colorectal cancer. *Cancer Res.* **62**:4352-4363.

143. Yamamoto, Y., Chochi, Y., Matsuyama, H., Eguchi, S., Kawauchi, S., Furuya, T., Oga, A., Kang, J. J., Naito, K., and Sasaki, K. 2007. Gain of 5p15.33 is associated with progression of bladder cancer. *Oncology*. **72**:132-138.
144. Kang, J. U., Koo, S. H., Kwon, K. C., Park, J. W., and Kim, J. M. 2008. Gain at chromosomal region 5p15.33, containing TERT, is the most frequent genetic event in early stages of non-small cell lung cancer. *Cancer Genet. Cytogenet.* **182**:1-11.
145. Saleem, A. N., Chen, Y.-H., Baek, H. J., Hsiao, Y.-W., Huang, H.-W., Kao, H.-J., Liu, K.-M., Shen, L.-F., Song, I.-W., Tu, C.-P. D., Wu, J.-Y., Kikuchi, T., Justice, M. J., Yen, J. J. Y., and Chen, Y.-T. 2010. Mice with alopecia, osteoporosis, and systemic amyloidosis due to mutation in *Zdhhc13*, a gene coding for palmitoyl acyltransferase. *PLoS Genet.* **6**:e1000985.
146. Rinaldi, A., Kwee, I., Poretti, G., Mensah, A., Pruneri, G., Capello, D., Rossi, D., Zucca, E., Ponzoni, M., Catapano, C., Tibiletti, M. G., Paulli, M., Gaidano, G., and Bertoni, F. 2006. Comparative genome-wide profiling of post-transplant lymphoproliferative disorders and diffuse large B-cell lymphomas. *Br. J. Haematol.* **134**:27-36.
147. Anami, K., Oue, N., Noguchi, T., Sakamoto, N., Sentani, K., Hayashi, T., Hinoi, T., Okajima, M., Graff, J. M., and Yasui, W. 2010. Search for transmembrane protein in gastric cancer by the *Escherichia coli* ampicillin secretion trap: expression of DSC2 in gastric cancer with intestinal phenotype. *J. Pathol.* **221**:275-284.
148. Yu, L., Reader, J. C., Chen, C., Zhao, X. F., Ha, J. S., Lee, C., York, T., Gojo, I., Baer, M. R., and Ning, Y. 2011. Activation of a novel palmitoyltransferase ZDHHC14 in acute biphenotypic leukemia and subsets of acute myeloid leukemia. *Leukemia*. **25**:367-371.
149. Mansouri, M. R., Marklund, L., Gustavsson, P., Davey, E., Carlsson, B., Larsson, C., White, I., Gustavson, K.-H., and Dahl, N. 2005. Loss of ZDHHC15 expression in a woman with a balanced translocation t(X;15)(q13.3;cen) and severe mental retardation. *Eur. J. Hum. Genet.* **13**:970-977.
150. Metzger, S., Bauer, P., Tomiuk, J., Laccone, F., Didonato, S., Gellera, C., Mariotti, C., Lange, H. W., Weirich-Schwaiger, H., Wenning, G. K., Seppi, K., Meleggh, B., Havasi, V., Balikó, L., Wiczorek, S., Zaremba, J., Hoffman-Zacharska, D., Sulek, A., Basak, A. N., Soydan, E., Zidovska, J., Kebrdlova, V., Pandolfo, M., Ribaï, P., Kadasi, L., Kvasnicova, M., Weber, B. H. F., Kreuz, F., Dose, M., Stuhmann, M., and Riess, O. 2006. Genetic analysis of candidate genes modifying the age-at-onset in Huntington's disease. *Hum. Genet.* **120**:285-292.
151. Berchtold, L. A., Størling, Z. M., Ortis, F., Lage, K., Bang-Berthelsen, C., Bergholdt, R., Hald, J., Brorsson, C. A., Eizirik, D. L., Pociot, F., Brunak, S., and Størling, J. 2011. Huntingtin-interacting protein 14 is a type 1 diabetes candidate protein regulating insulin secretion and  $\beta$ -cell apoptosis. *Proc Natl Acad Sci U S A*.
152. Ducker, C. E., Griffel, L. K., Smith, R. A., Keller, S. N., Zhuang, Y., Xia, Z., Diller, J. D., and Smith, C. D. 2006. Discovery and characterization of inhibitors of human palmitoyl acyltransferases. *Mol. Cancer Ther.* **5**:1647-1659.
153. Jacobsen, M., Kracht, S. S., Estes, G., Cirera, S., Edfors, I., Archibald, A. L., Bendixen, C., Andersson, L., Fredholm, M., and Jørgensen, C. B. 2010. Refined

- candidate region specified by haplotype sharing for Escherichia coli F4ab/F4ac susceptibility alleles in pigs. *Anim. Genet.* **41**:21-25.
154. Draper, J. M., and Smith, C. D. 2010. DHHC20: a human palmitoyl acyltransferase that causes cellular transformation. *Mol. Membr. Biol.* **27**:123-136.
155. Mill, P., Lee, A. W. S., Fukata, Y., Tsutsumi, R., Fukata, M., Keighren, M., Porter, R. M., McKie, L., Smyth, I., and Jackson, I. J. 2009. Palmitoylation regulates epidermal homeostasis and hair follicle differentiation. *PLoS Genet.* **5**:e1000748.
156. Honey, S., Schneider, B. L., Schieltz, D. M., Yates, J. R., and Futcher, B. 2001. A novel multiple affinity purification tag and its use in identification of proteins associated with a cyclin-CDK complex. *Nucleic Acids Research.* **29**:e24.
157. Li, Y. 2010. Commonly used tag combinations for tandem affinity purification. *Biotechnology and Applied Biochemistry.* **55**:73-83.
158. Infed, N., Hanekop, N., Driessen, A. J. M., Smits, S. H. J., and Schmitt, L. 2011. Influence of detergents on the activity of the ABC transporter LmrA. *Biochimica et Biophysica Acta (BBA) - Biomembranes.* **1808**:2313-2321.
159. Vergis, J. M., Purdy, M. D., and Wiener, M. C. 2010. A high-throughput differential filtration assay to screen and select detergents for membrane proteins. *Anal. Biochem.* **407**:1-11.
160. Anderson, J. L., Frase, H., Michaelis, S., and Hrycyna, C. A. 2005. Purification, functional reconstitution, and characterization of the Saccharomyces cerevisiae isoprenylcysteine carboxymethyltransferase Ste14p. *J. Biol. Chem.* **280**:7336-7345.
161. Romir, J., Lilie, H., Egerer-Sieber, C., Bauer, F., Sticht, H., and Muller, Y. A. 2007. Crystal structure analysis and solution studies of human Lck-SH3; zinc-induced homodimerization competes with the binding of proline-rich motifs. *J. Mol. Biol.* **365**:1417-1428.
162. Getz, E. B., Xiao, M., Chakrabarty, T., Cooke, R., and Selvin, P. R. 1999. A comparison between the sulfhydryl reductants tris(2-carboxyethyl)phosphine and dithiothreitol for use in protein biochemistry. *Anal. Biochem.* **273**:73-80.
163. Hallak, H., and Rubin, R. 2004. Ethanol inhibits palmitoylation of G protein G alpha(s). *J. Neurochem.* **89**:919-927.
164. De Vos, M. L., Lawrence, D. S., and Smith, C. D. 2001. Cellular pharmacology of cerulenin analogs that inhibit protein palmitoylation. *Biochem. Pharmacol.* **62**:985-995.
165. DeJesus, G., and Bizzozero, O. A. 2002. Effect of 2-fluoropalmitate, cerulenin and tunicamycin on the palmitoylation and intracellular translocation of myelin proteolipid protein. *Neurochem. Res.* **27**:1669-1675.
166. Lawrence, D. S., Zilfou, J. T., and Smith, C. D. 1999. Structure-activity studies of cerulenin analogues as protein palmitoylation inhibitors. *J. Med. Chem.* **42**:4932-4941.
167. Patterson, S. I., and Skene, J. H. 1995. Inhibition of dynamic protein palmitoylation in intact cells with tunicamycin. *Meth. Enzymol.* **250**:284-300.
168. Grosenbach, D. W., Hansen, S. G., and Hruby, D. E. 2000. Identification and analysis of vaccinia virus palmitoylproteins. *Virology.* **275**:193-206.

169. Duraffour, S., Vigne, S., Vermeire, K., Garcel, A., Vanstreels, E., Daelemans, D., Yang, G., Jordan, R., Hruby, D. E., Crance, J.-M., Garin, D., Andrei, G., and Snoeck, R. 2008. Specific targeting of the F13L protein by ST-246 affects orthopoxvirus production differently. *Antivir. Ther. (Lond.)*. **13**:977-990.
170. Marciano, D., Ben-Baruch, G., Marom, M., Egozi, Y., Haklai, R., and Kloog, Y. 1995. Farnesyl derivatives of rigid carboxylic acids-inhibitors of ras-dependent cell growth. *J. Med. Chem.* **38**:1267-1272.
171. Marom, M., Haklai, R., Ben-Baruch, G., Marciano, D., Egozi, Y., and Kloog, Y. 1995. Selective inhibition of Ras-dependent cell growth by farnesylthiosalicylic acid. *J. Biol. Chem.* **270**:22263-22270.
172. Bhat, B. G., Wang, P., and Coleman, R. A. 1994. Hepatic monoacylglycerol acyltransferase is regulated by sn-1,2-diacylglycerol and by specific lipids in Triton X-100/phospholipid-mixed micelles. *J. Biol. Chem.* **269**:13172-13178.
173. Bayburt, T. H., and Sligar, S. G. 2010. Membrane protein assembly into Nanodiscs. *FEBS Letters*. **584**:1721-1727.
174. Sando, J. J., Maurer, M. C., Bolen, E. J., and Grisham, C. M. 1992. Role of cofactors in protein kinase C activation. *Cell. Signal.* **4**:595-609.
175. Mitchell, D. A., Mitchell, G., Ling, Y., Budde, C., and Deschenes, R. J. 2010. Mutational analysis of *Saccharomyces cerevisiae* Erf2 reveals a two-step reaction mechanism for protein palmitoylation by DHHC enzymes. *J. Biol. Chem.* **285**:38104-38114.
176. Goodwin, J. S., Drake, K. R., Rogers, C., Wright, L., Lippincott-Schwartz, J., Philips, M. R., and Kenworthy, A. K. 2005. Depalmitoylated Ras traffics to and from the Golgi complex via a nonvesicular pathway. *J. Cell Biol.* **170**:261-272.
177. Lorentzen, A., Kinkhabwala, A., Rocks, O., Vartak, N., and Bastiaens, P. I. H. 2010. Regulation of Ras localization by acylation enables a mode of intracellular signal propagation. *Sci Signal.* **3**:ra68.
178. Marrari, Y., Crouthamel, M., Irannejad, R., and Wedegaertner, P. B. 2007. Assembly and trafficking of heterotrimeric G proteins. *Biochemistry*. **46**:7665-7677.
179. Fernández-Hernando, C., Fukata, M., Bernatchez, P. N., Fukata, Y., Lin, M. I., Brecht, D. S., and Sessa, W. C. 2006. Identification of Golgi-localized acyl transferases that palmitoylate and regulate endothelial nitric oxide synthase. *J. Cell Biol.* **174**:369-377.
180. Shipston, M. J. 2011. Ion channel regulation by protein palmitoylation. *J. Biol. Chem.* **286**:8709-8716.
181. Jennings, B. C., Nadolski, M. J., Ling, Y., Baker, M. B., Harrison, M. L., Deschenes, R. J., and Linder, M. E. 2009. 2-Bromopalmitate and 2-(2-hydroxy-5-nitrobenzylidene)-benzo[b]thiophen-3-one inhibit DHHC-mediated palmitoylation in vitro. *J. Lipid Res.* **50**:233-242.
182. Fery-Forgues, S., Fayet, J.-P., and Lopez, A. 1993. Drastic changes in the fluorescence properties of NBD probes with the polarity of the medium: involvement of a TICT state? *Journal of Photochemistry and Photobiology A: Chemistry*. **70**:229-243.

183. Varner, A. S., De Vos, M. L., Creaser, S. P., Peterson, B. R., and Smith, C. D. 2002. A fluorescence-based high performance liquid chromatographic method for the characterization of palmitoyl acyl transferase activity. *Anal. Biochem.* **308**:160-167.
184. Mumby, S. M., and Linder, M. E. 1994. Myristoylation of G-protein alpha subunits. *Meth. Enzymol.* **237**:254-268.
185. Schroeder, H., Leventis, R., Shahinian, S., Walton, P. A., and Silviu, J. R. 1996. Lipid-modified, cysteinyl-containing peptides of diverse structures are efficiently S-acylated at the plasma membrane of mammalian cells. *J. Cell Biol.* **134**:647-660.
186. Cook, P. F., and Cleland, W. W. 2007. *Enzyme Kinetics and Mechanism* 1st ed. Garland Science.
187. Tsutsumi, R., Fukata, Y., Noritake, J., Iwanaga, T., Perez, F., and Fukata, M. 2009. Identification of G protein alpha subunit-palmitoylating enzyme. *Mol. Cell. Biol.* **29**:435-447.
188. Hou, H., John Peter, A. T., Meiringer, C., Subramanian, K., and Ungermann, C. 2009. Analysis of DHHC acyltransferases implies overlapping substrate specificity and a two-step reaction mechanism. *Traffic.* **10**:1061-1073.
189. Carman, G. M., Deems, R. A., and Dennis, E. A. 1995. Lipid signaling enzymes and surface dilution kinetics. *J. Biol. Chem.* **270**:18711-18714.
190. Denic, V., and Weissman, J. S. 2007. A molecular caliper mechanism for determining very long-chain fatty acid length. *Cell.* **130**:663-677.
191. Linder, M. E., and Deschenes, R. J. 2007. Palmitoylation: policing protein stability and traffic. *Nat. Rev. Mol. Cell Biol.* **8**:74-84.
192. el-Husseini, A. el-D., and Brecht, D. S. 2002. Protein palmitoylation: a regulator of neuronal development and function. *Nat. Rev. Neurosci.* **3**:791-802.
193. Singaraja, R. R., Hadano, S., Metzler, M., Givan, S., Wellington, C. L., Warby, S., Yanai, A., Gutekunst, C.-A., Leavitt, B. R., Yi, H., Fichter, K., Gan, L., McCutcheon, K., Chopra, V., Michel, J., Hersch, S. M., Ikeda, J.-E., and Hayden, M. R. 2002. HIP14, a novel ankyrin domain-containing protein, links huntingtin to intracellular trafficking and endocytosis. *Hum. Mol. Genet.* **11**:2815-2828.
194. Stowers, R. S., and Isacoff, E. Y. 2007. Drosophila huntingtin-interacting protein 14 is a presynaptic protein required for photoreceptor synaptic transmission and expression of the palmitoylated proteins synaptosome-associated protein 25 and cysteine string protein. *J. Neurosci.* **27**:12874-12883.
195. Ohshima, T., Verstreken, P., Ly, C. V., Rosenmund, T., Rajan, A., Tien, A.-C., Hauer, C., Schulze, K. L., and Bellen, H. J. 2007. Huntingtin-interacting protein 14, a palmitoyl transferase required for exocytosis and targeting of CSP to synaptic vesicles. *J. Cell Biol.* **179**:1481-1496.
196. Willumsen, B. M., Cox, A. D., Solski, P. A., Der, C. J., and Buss, J. E. 1996. Novel determinants of H-Ras plasma membrane localization and transformation. *Oncogene.* **13**:1901-1909.
197. Webb, Y., Hermida-Matsumoto, L., and Resh, M. D. 2000. Inhibition of protein palmitoylation, raft localization, and T cell signaling by 2-bromopalmitate and polyunsaturated fatty acids. *J. Biol. Chem.* **275**:261-270.

198. Chase, J. F., and Tubbs, P. K. 1972. Specific inhibition of mitochondrial fatty acid oxidation by 2-bromopalmitate and its coenzyme A and carnitine esters. *Biochem. J.* **129**:55-65.
199. Coleman, R. A., Rao, P., Fogelson, R. J., and Bardes, E. S. 1992. 2-Bromopalmitoyl-CoA and 2-bromopalmitate: promiscuous inhibitors of membrane-bound enzymes. *Biochim. Biophys. Acta.* **1125**:203-209.
200. Omura, S. 1976. The antibiotic cerulenin, a novel tool for biochemistry as an inhibitor of fatty acid synthesis. *Bacteriol Rev.* **40**:681-697.
201. Duronio, R. J., Jackson-Machelski, E., Heuckeroth, R. O., Olins, P. O., Devine, C. S., Yonemoto, W., Slice, L. W., Taylor, S. S., and Gordon, J. I. 1990. Protein N-myristoylation in *Escherichia coli*: reconstitution of a eukaryotic protein modification in bacteria. *Proc. Natl. Acad. Sci. U.S.A.* **87**:1506-1510.
202. Duronio, R. J., Reed, S. I., and Gordon, J. I. 1992. Mutations of human myristoyl-CoA:protein N-myristoyltransferase cause temperature-sensitive myristic acid auxotrophy in *Saccharomyces cerevisiae*. *Proc. Natl. Acad. Sci. U.S.A.* **89**:4129-4133.
203. Budde, C., Schoenfish, M. J., Linder, M. E., and Deschenes, R. J. 2006. Purification and characterization of recombinant protein acyltransferases. *Methods.* **40**:143-150.
204. Osanai, K., Takahashi, K., Nakamura, K., Takahashi, M., Ishigaki, M., Sakuma, T., Toga, H., Suzuki, T., and Voelker, D. R. 2005. Expression and characterization of Rab38, a new member of the Rab small G protein family. *Biol. Chem.* **386**:143-153.
205. Bijlmakers, M. J., Isobe-Nakamura, M., Ruddock, L. J., and Marsh, M. 1997. Intrinsic signals in the unique domain target p56(lck) to the plasma membrane independently of CD4. *J. Cell Biol.* **137**:1029-1040.
206. Turner, J. M., Brodsky, M. H., Irving, B. A., Levin, S. D., Perlmutter, R. M., and Littman, D. R. 1990. Interaction of the unique N-terminal region of tyrosine kinase p56lck with cytoplasmic domains of CD4 and CD8 is mediated by cysteine motifs. *Cell.* **60**:755-765.
207. Resh, M. D. 1994. Myristylation and palmitylation of Src family members: the fats of the matter. *Cell.* **76**:411-413.
208. Sharma, C., Yang, X. H., and Hemler, M. E. 2008. DHHC2 affects palmitoylation, stability, and functions of tetraspanins CD9 and CD151. *Mol. Biol. Cell.* **19**:3415-3425.
209. el-Aleem, S. A., and Schulz, H. 1987. Evaluation of inhibitors of fatty acid oxidation in rat myocytes. *Biochem. Pharmacol.* **36**:4307-4312.
210. Fong, J. C., Leu, S. J., and Chai, S. P. 1997. Differential inhibition of lipolysis by 2-bromopalmitic acid and 4-bromocrotonic acid in 3T3-L1 adipocytes. *Biochim. Biophys. Acta.* **1344**:65-73.
211. Raaka, B. M., and Lowenstein, J. M. 1979. Inhibition of fatty acid oxidation by 2-bromooctanoate. Evidence for the enzymatic formation of 2-bromo-3-ketooctanoyl coenzyme A and the inhibition of 3-ketothiolase. *J. Biol. Chem.* **254**:6755-6762.
212. Mikic, I., Planey, S., Zhang, J., Ceballos, C., Seron, T., von Massenbach, B., Watson, R., Callaway, S., McDonough, P. M., Price, J. H., Hunter, E., and Zacharias, D.

2006. A live cell, image-based approach to understanding the enzymology and pharmacology of 2-bromopalmitate and palmitoylation. *Meth. Enzymol.* **414**:150-187.
213. Baron, R. A., Peterson, Y. K., Otto, J. C., Rudolph, J., and Casey, P. J. 2007. Time-dependent inhibition of isoprenylcysteine carboxyl methyltransferase by indole-based small molecules. *Biochemistry.* **46**:554-560.
214. Hou, H., Subramanian, K., LaGrassa, T. J., Markgraf, D., Dietrich, L. E. P., Urban, J., Decker, N., and Ungermann, C. 2005. The DHHC protein Pfa3 affects vacuole-associated palmitoylation of the fusion factor Vac8. *Proc. Natl. Acad. Sci. U.S.A.* **102**:17366-17371.
215. Yang, J., Brown, M. S., Liang, G., Grishin, N. V., and Goldstein, J. L. 2008. Identification of the acyltransferase that octanoylates ghrelin, an appetite-stimulating peptide hormone. *Cell.* **132**:387-396.
216. Chisari, M., Saini, D. K., Kalyanaraman, V., and Gautam, N. 2007. Shuttling of G protein subunits between the plasma membrane and intracellular membranes. *J. Biol. Chem.* **282**:24092-24098.
217. Fyrst, H., Knudsen, J., Schott, M. A., Lubin, B. H., and Kuypers, F. A. 1995. Detection of acyl-CoA-binding protein in human red blood cells and investigation of its role in membrane phospholipid renewal. *Biochem. J.* **306 ( Pt 3)**:793-799.
218. Wan, J., Roth, A. F., Bailey, A. O., and Davis, N. G. 2007. Palmitoylated proteins: purification and identification. *Nat Protoc.* **2**:1573-1584.
219. Fang, C., Deng, L., Keller, C. A., Fukata, M., Fukata, Y., Chen, G., and Lüscher, B. 2006. GODZ-mediated palmitoylation of GABA(A) receptors is required for normal assembly and function of GABAergic inhibitory synapses. *J. Neurosci.* **26**:12758-12768.
220. Yuan, C., Rieke, C. J., Rimon, G., Wingerd, B. A., and Smith, W. L. 2006. Partnering between monomers of cyclooxygenase-2 homodimers. *Proc. Natl. Acad. Sci. U.S.A.* **103**:6142-6147.
221. Ubarretxena-Belandia, I., Cox, R. C., Dijkman, R., Egmond, M. R., Verheij, H. M., and Dekker, N. 1999. Half-of-the-sites reactivity of outer-membrane phospholipase A against an active-site-directed inhibitor. *Eur. J. Biochem.* **260**:794-800.
222. Planey, S. L., and Zacharias, D. A. 2010. Identification of targets and inhibitors of protein palmitoylation. *Expert Opin. Drug Discov.* **5**:155-164.
223. Chung, C. C., Ohwaki, K., Schneeweis, J. E., Stec, E., Varnerin, J. P., Goudreau, P. N., Chang, A., Cassaday, J., Yang, L., Yamakawa, T., Kornienko, O., Hodder, P., Inglese, J., Ferrer, M., Strulovici, B., Kusunoki, J., Tota, M. R., and Takagi, T. 2008. A fluorescence-based thiol quantification assay for ultra-high-throughput screening for inhibitors of coenzyme A production. *Assay Drug Dev Technol.* **6**:361-374.
224. Liu, J. O., Titov, D. V., Dang, Y., and He, Q. 2011. Regulator of Ras depalmitoylation and retrograde trafficking: a new hat for FKBP. *Mol. Cell.* **41**:131-133.
225. Zhang, J., Planey, S. L., Ceballos, C., Stevens, S. M., Jr, Keay, S. K., and Zacharias, D. A. 2008. Identification of CKAP4/p63 as a major substrate of the palmitoyl acyltransferase DHHC2, a putative tumor suppressor, using a novel proteomics method. *Mol. Cell Proteomics.* **7**:1378-1388.

# Benjamin C Jennings

Department of Molecular Medicine  
C3-177 Veterinary Medical Center  
College of Veterinary Medicine  
Cornell University  
Ithaca, New York 14853 USA

Lab Phone: 607-253-3252  
Mobile Phone: 314-853-575  
E-mail: bcj29@cornell.edu

## PERSONAL INFORMATION

Date of Birth: November 28, 1981  
Place of Birth: Green Bay, Wisconsin, USA  
Citizenship: U.S. Citizen

## EDUCATION

*Washington University in St. Louis* August 2004 – August 2011  
St. Louis, Missouri  
Graduate Program in Biochemistry

*University of Wisconsin-Madison* August 2000 - August 2004  
Madison, Wisconsin  
Degree: B.S. in Biochemistry with Honors & Distinction  
GPA: 3.83/4.00

## AWARDS and HONORS

American Society for Biochemistry and Molecular Biology – Member Jan 2010 - present  
ASBMB Travel Grant Award April 2010  
American Heart Association Predoctoral Fellowship Jan 2008 - Dec 2009  
David F. Silbert Outstanding Teaching Assistant Award Oct 2006  
UW-Madison Graduate with Honors and Distinction in Biochemistry Aug 2004  
University of Wisconsin-Madison Dean's List Aug 2000-Aug 2004  
and Honors Program  
Wisconsin Agriculture and Life Science Alumni Association May 2004  
Senior Activity and Leadership Award  
Mary Shine Peterson Scholarship for Biochemistry Research, Fall 2003, Spring 2004  
UW-Madison  
Gamma Sigma Delta, Honorary Life Science Society April 2003

## RESEARCH EXPERIENCE

### *Doctoral Thesis:*

**Enzymology of DHHC-mediated protein S-acylation**  
Dr. Maurine Linder, Ph.D. June 2005 - Present  
Department of Cell Biology and Physiology, Washington University in St. Louis  
Department of Molecular Medicine, Cornell University

### *Doctoral Rotations at Washington University in St. Louis:*

**Detection and purification of human von Willebrand factor fragments**  
Dr. J. Evan Sadler, M.D., Ph.D. April 2005 - June 2005  
Howard Hughes Medical Institute  
Internal Medicine: Division of Hematology and Oncology

**Characterizing the pH-dependency of substrate specificity of the *Plasmodium falciparum* metalloprotease falcilysin.**

Dr. Daniel E. Goldberg, M.D., Ph.D.

January 2005 - April 2005

Howard Hughes Medical Institute

Departments of Medicine and Molecular Microbiology

**Transcriptional control of connexin43 expression: insights from Naxos Disease**

Dr. Jeffrey E. Saffitz, M.D., Ph.D.

August 2004 - December 2004

Departments of Pathology and Cardiology

*Undergraduate Research at University of Wisconsin-Madison:*

**Monitoring phosphorylation of mutant cardiac troponin I with MALDI-TOF mass spectrometry**

Dr. Jeffery W. Walker, Ph.D.

May 2003- August 2004

Department of Physiology

**Development of a strategy for mitochondrially transforming cucumber pollen**

Dr. Michael J. Havey, Ph.D.

August 2001- December 2001

Department of Horticulture and USDA-Agriculture Research Station

TEACHING EXPERIENCE

Teaching Assistant

August 2005- December 2005

Molecular Foundations of Medicine, course master Dr. Linda J. Pike

Washington University in St. Louis, MO

Peer Mentor Tutor

August 2003-May 2004

Introductory and Intermediate Biochemistry Courses

Chemistry Learning Center

University of Wisconsin-Madison

LEADERSHIP AND ACTIVITIES

More Than Carpentry, Project Leader and Advisory Committee,  
Wellston, MO

April 2006-August 2009

Firm Foundations Tutoring (Reading, Math, Science)  
Division of Restore St. Louis, MO

October 2005-August 2009

Mentor for BiomedRAP: Biomedical Research Apprenticeship Program  
Washington University in St. Louis, MO

June 2006-August 2006

Mentor for MARC (Minority Access to Research Careers) Program  
University of Wisconsin-Madison

May 2003-August 2003

PUBLICATIONS

*Primary Research:*

**Jennings BC** and Linder ME. DHHC protein S-acyltransferases use a similar ping-pong kinetic mechanism but display different acyl-CoA specificities. *J Biol. Chem.* Accepted pending revisions.

Ahearn IM, Tsai FD, Court H, Zhou M, **Jennings BC**, Ahmed M, Fehrenbacher N, Linder ME, Philips MR. FKBP12 binds to acylated H-ras and promotes depalmitoylation. *Mol. Cell.* **41**(2):173-85. 2011.

**Jennings BC**, Nadolski MJ, Ling Y, Baker MB, Harrison ME, Deschenes RJ, Linder ME. 2-Bromopalmitate and 2-(2-hydroxy-5-nitro-benzylidene)-benzo[b]thiophen-3-one inhibit DHHC-mediated palmitoylation in vitro. *J. Lipid Res.* **50**(2):233-42. 2009.

*Reviews:*

**Jennings BC and Linder ME.** Regulation of G-proteins by covalent modification. Chapter 200 in *Handbook of Cellular Signaling*. 2<sup>nd</sup> Edition. Bradshaw and Dennis. 2009.

**Jennings BC** and Linder ME. DHHC2. UCSD-Nature Molecule Pages published online: 13 Mar 2008. doi:10.1038/mp.a003731.01

**Jennings BC** and Linder ME. DHHC7. UCSD-Nature Molecule Pages published online: 28 Feb 2008. doi:10.1038/mp.a003724.01

**Jennings BC** and Linder ME. DHHC8. UCSD-Nature Molecule Pages published online: 13 Mar 2008. doi:10.1038/mp.a003723.01

**Jennings BC** and Linder ME. DHHC21. UCSD-Nature Molecule Pages published online: 13 Mar 2008. doi:10.1038/mp.a003729.01

ABSTRACTS AND PRESENTATIONS

**Jennings BC** and Linder ME. Enzymology of DHHC-mediated protein palmitoylation. Poster presented at Experimental Biology 2010 conference and ASBMB annual meeting in Anaheim, CA. April 2010.

**Jennings BC** and Linder ME. Enzymatic characterization of DHHC-mediated protein palmitoylation. Poster presented at FASEB Protein Lipidation, Signaling, and Membrane Domains conference in Saxtons River, VT. July 2009.

**Jennings BC**, He Y, and Linder ME. Characterization of human palmitoyltransferase DHHC2. Poster presented at FASEB Protein Lipidation, Signaling, and Membrane Domains conference in Palm Springs, CA. July 2006.

**Jennings BC**, Jacobson RM, and Walker JW. Alteration of phosphorylation in mutated cardiac troponin I. 9<sup>th</sup> Annual Scientific Poster Fair held by the UW Cardiovascular Research Center, Madison, WI. December 2003.

Rivera-Santiago VJ, **Jennings BC**, and Walker JW. Interaction of FHC mutations and phosphorylation of troponin I. Poster presented at the Annual Biomedical Research Conference for Minority Students in San Diego, CA. October 2003.